Measurement of Freeway Traffic Flow Quality Using GPS-Equipped Vehicles

A Dissertation
Presented to
The Academic Faculty

By

Joonho Ko

In Partial Fulfillment
Of the Requirement for the Degree
Doctor of Philosophy in Civil Engineering

Georgia Institute of Technology

August 2006

Measurement of Freeway Traffic Flow Quality
Using GPS-Equipped Vehicles

Approved by:

Dr. Randall Guensler, Advisor
School of Civil and Environmental Engineering
Georgia Institute of Technology

Dr. Michael Hunter, Co-Advisor
School of Civil and Environmental Engineering
Georgia Institute of Technology

Dr. Michael Meyer
School of Civil and Environmental Engineering
Georgia Institute of Technology

Dr. Michael Rodgers
School of Civil and Environmental Engineering
Georgia Institute of Technology

Dr. Jennifer Ogle
Department of Civil Engineering
Clemson University

Date Approved: June 23, 2006

ACKNOWLEDGEMENTS

I would like to thank many people who helped me complete this doctoral thesis. Above all, my advisor, Dr. Randall Guensler, provided invaluable guidance and suggestions. In addition, he has been a good mentor since he accepted me as a graduate student five years ago. Without his help and encouragement, this work could not have been successfully completed. As a co-advisor, Dr. Michael Hunter also provided greatly helpful guidance throughout this research work. He has taught me how to face problems to effectively and efficiently solve them. Through conversations with him, I learned many things. Dr. Michael Meyer, serving as a member of my doctoral committee, also provided me with great insights into various aspects easily missed to my less-experienced eyes. Dr. Michael Rodgers also contributed to the achievement of this research work by pinpointing errors and mistakes that I made. Dr. Jennifer Ogle was a kind advisor as both a committee member and a colleague. Her advice guided me in the right direction during this research work.

In addition to my committee members, my gratitude should be given to my colleagues in Drivelab, Dr. Hainan Li, Vetri Elango, Jungwook Jun, Jaesup Lee, and Kai Zuehlke. As project team members, they greatly affected my work and even my school life. Finally, I would like to express my deepest gratitude to my family. My wife, Mina, has supported me in every aspect, and my lovely children, Emily and Justin, have always encouraged me by showing their smiles. Without their support and patience, I could not have done this work.

TABLE OF CONTENTS

LIST OF TABLES

LIST OF FIGURES

LIST OF ABBREVIATIONS

CV	Coefficient of Variation
DEM	Digital Elevation Model
FHWA	Federal Highway Administration
GDOT	Georgia Department of Transportation
GIS	Geographic Information System
GPS	Global Positioning System
GT	Georgia Institute of Technology
HCM	Highway Capacity Manual
HOV	High Occupancy Vehicle
HPMS	Highway Performance Monitoring System
KS Test	Kolmogorov-Smirnov Test
LOS	Level of Service
LSI	Level of Traffic Service Index
MAE	Mean Absolute Error
ML	Maximum Likelihood
MVG	Mean Velocity Gradient
OBD	On-board Diagnostic
pdf	Probability Density Function
PDOP	Positional Dilution of Precision
PKE	Positive Kinetic Energy
RC	Roadway Characteristics

REML	Restricted Maximum Likelihood
RMS	Root Mean Square
SA	Selective Availability
SD	Standard Deviation
SMS	Short Message Service
SUV	Sport Utility Vehicle
TAD	Total Absolute Speed Difference
TDC	Trip Data Collector
TMC	Transportation Management Center
USGS	United States Geological Survey
VDS	Video Detection System
VE	Variance of Error
VSS	Vehicle Speed Sensor

Summary

The evaluation of freeway service quality is crucial work, and thus, transportation professionals have developed numerous measures including traffic volume, speed, and density. However, recent research efforts have indicated that such traditional measures may not fully reflect the quality of roadway service from the perspective of individual drivers, necessitating the development of alternative approaches that complement or replace the current service quality measures. As an alternative approach, the speed variation of a vehicle has been suggested as a promising indicator of traffic flow quality perceived by individual drivers. In particular, acceleration noise, defined by the standard deviation of the acceleration of a vehicle, has been often studied as a measure of the degree of speed variation. However, previous studies have been limited to the experimental level due to the difficulty in collecting high-resolution vehicle speed profiles for computing acceleration noise.

In this dissertation, the characteristics of speed variation, measured by acceleration noise, are investigated using the rich set of GPS data collected from the instrumented vehicles driven by the participants of the Commute Atlanta research program. The employment of the real-world vehicle activity data, composed of every second of vehicle operation, renders this research effort unique and provides an opportunity to investigate the various aspects of acceleration noise in the real-world context. The investigation is performed by relating acceleration noise to its three influential factors: traffic conditions, roadway, and driver/vehicles. In addition, a fuzzy inference system-based methodology, combining vehicle speed and acceleration noise

from instrumented vehicles, is proposed as an approach to evaluating traffic flow quality.

As a result, this research effort found that acceleration noise is affected by traffic conditions, roadway characteristics, and driver/vehicle characteristics. In general, the worse traffic congestion or poor roadway conditions increase acceleration noise. In addition, the various aspects of interactions between roadway characteristics and traffic conditions were also found, which has not yet been examined in the previous studies. By comparing with vehicle speed, this research effort found that under free-flow conditions (LOS A-to-C ranges), acceleration noise is more sensitive to traffic than speed, indicating the usefulness of acceleration noise for evaluating traffic flow quality under these ranges. Finally, the application of the fuzzy inference system-based approach successfully demonstrated its potential capability to evaluate traffic flow quality using GPS-equipped instrumented vehicles.

Chapter 1
Introduction

Background

Effective and efficient planning and operation of freeway systems should be based on the adequate evaluation of roadway service quality. For such an evaluation, transportation professionals have used numerous measures including traffic volume, travel time, speed, and density. In particular, density, measured by the number of vehicles per mile per lane, is the primary measure for evaluating the level of service of freeway systems. However, recent studies have indicated that such traditional measures might not fully represent the level of service perceived by drivers (Choocharukul et al. 2004; Flannery et al. 2006). Along with this study, factors affecting the perceptions of the quality of service are being actively studied (Hostovsky and Hall 2003; Hostovsky et al. 2004; Pecheux et al. 2004; Pfefer 1999; Washburn et al. 2004). A common claim of these studies is that the quality of service should be determined by incorporating the perspective of road-users, not relying solely on effectiveness measures developed by system managers or experts. The incorporation of road-user perception requires the development of alternative approaches that supplement or replace the current service quality measures.

An example of the alternative measures is the degree of speed variation, which describes the degree of speed changes of a vehicle and the smoothness of traffic flow over a roadway segment. A proposal of this measure for the quality of service was based on the notion that drivers tend to maintain their desired speeds unless traffic or

roadway conditions restrict their maneuverability. In general, the higher degree of speed variation indicates poorer quality of service, and thus, driver discomfort. Recognition of the importance of speed variation is found in the following statement: *"...motion in the form of speed and the magnitude and frequency of speed changes is an important measure of level of service from the point of view of the individual driver"* (Drew and Keese 1965). This statement suggests that the degree of speed variation can be effectively linked to road-user-oriented service measures.

As suggested in the Highway Capacity Manual (HCM), a good service measure should encompass various aspects of service quality such as travel time and speed, freedom to maneuver, traffic interruptions, and comfort and convenience. In this sense, the use of speed variation seems to have merit because it includes additional elements of service quality perceived by drivers. In addition, speed variation is associated with the values of system managers. In fact, the degree of speed variation is directly or indirectly related to driver satisfaction, safety, traffic conditions, vehicle operation cost, emissions (Eisele et al. 1996; Yoon et al. 2005), and fuel consumption (Chang and Morlok 2005), as depicted in Figure 1. This characteristic, a multi-variable capturing capability, was the reason for the proposal of the service indices incorporating the degree of speed variation (Platt 1963).

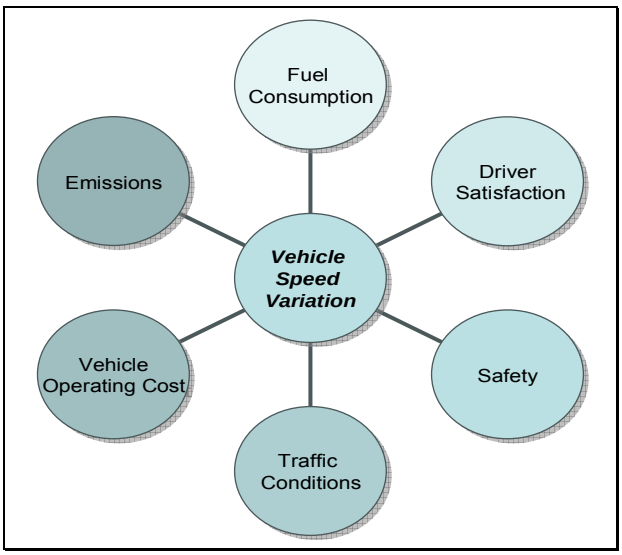

Figure 1: Speed Variation and Related Factors

Another reason for the proposal of speed variation as a service measure is that a mere examination of speed cannot fully reveal the quality of service over a roadway segment. Figure 2 provides an example, in which two freeway speed profiles with the same average speed of 65mph were plotted with corresponding second-by-second acceleration profiles. The speed profiles, obtained from two different vehicles which traveled on a 0.5-mile freeway segment with a speed limit of 65 mph, indicate that the driver of Vehicle A drove smoothly around the speed limit (65mph) while the driver of Vehicle B attempted to drive at a higher speed. As suggested by the acceleration profiles, the speed variation of Vehicle B seems higher than that of Vehicle A. In fact, the standard deviations of acceleration are 0.20 and 1.29 mph/s for Vehicle A and Vehicle B, respectively, implying a smoother and more comfortable traffic flow for Vehicle A. Consequently, this example demonstrates that roadway service quality should not be represented by speed alone. Another example can be found in a speed-

density curve, in which speed decreases only marginally until traffic conditions reach the capacity (i.e., LOS E) of the road (TRB 2000).

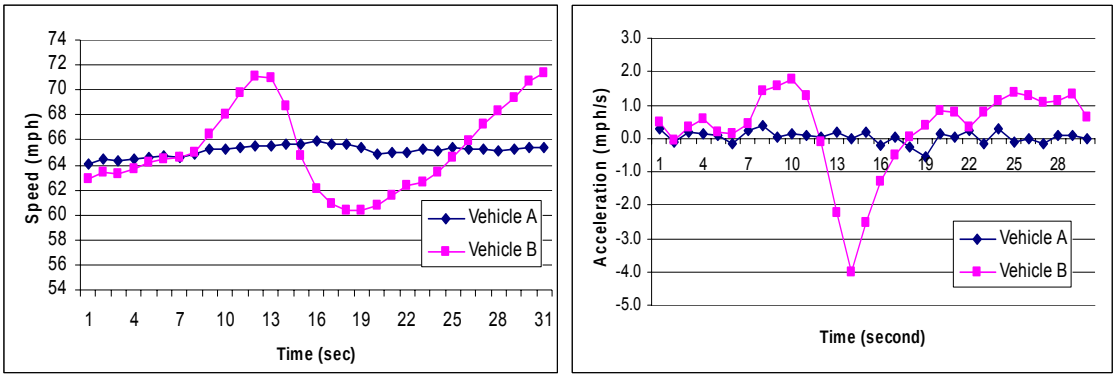

Figure 2: Vehicle Speed and Acceleration Profiles Obtained from Trips with the Same Average Speed

As a measure of speed variation, the standard deviation of acceleration, known as acceleration noise, was proposed nearly a half century ago (Herman et al. 1959) and applied to measuring traffic flow quality for two basic reasons: 1) its dependency on the three basic elements of the traffic stream: driver, road, and traffic conditions and 2) its capability to measure the smoothness of traffic flow (Drew 1968; Herman et al. 1959). Attempting to prove these characteristics, researchers have found that acceleration noise indeed depends on various traffic and roadway conditions. In addition, their findings suggest that driver behavior could affect the values of acceleration noise. However, previous research efforts have been limited to the experimental level, and thus, more extensive studies are needed to be carried out so that the understanding of acceleration noise can be enhanced. Without a proper understanding of acceleration noise, its applications will be limited.

The application of any performance measure should be supported by proper data, and data availability may determine the degree of the applicability of the measure.

Unfortunately, acceleration noise requires high resolution speed profiles such as a second-by-second level, for which data collection has proven difficult, particularly in the past, when only vehicles instrumented with special equipment could provide speed profiles. However, the recent advancement of global positioning system (GPS) technology has significantly facilitated speed profile data collection, rendering the application of acceleration noise more practical. In addition, given the rapid integration of GPS and communication systems into new vehicles, speed profile data will become much more readily available in the near future. These developments provide an opportunity for more active research efforts on acceleration noise, particularly those using the speed profiles from GPS devices. Ultimately, such research efforts should contribute to the improvement of freeway operations by helping transportation engineers appropriately measure the quality of service.

Research Objectives

This research effort is motivated by the finding that little research has been conducted on the characteristics of speed variation, in particular acceleration noise, and the measurement of traffic flow quality using instrumented vehicle data. Instrumented vehicle data will be much more available in the near future due to the advancement of technology. Above all, this research effort is motivated by the opportunity provided by the rich set of GPS data obtained from the Commute Atlanta project, an instrumented vehicle research program deployed in the metro Atlanta region. The research program has monitored more than 1.5 million vehicle trips (as of May 2006) on a second-by-second basis.

Thus, this research effort aims to investigate acceleration noise as one speed variation measure. In particular, the relationships between acceleration noise and traffic conditions, roadway characteristics, and driver/vehicle characteristics were closely examined using the data from the Commute Atlanta project. This examination is expected to enhance the understanding of acceleration noise characteristics and complement the findings obtained from previous research efforts. In addition, a methodology for measuring traffic flow quality using GPS-equipped vehicles is proposed. Along with these main research objectives, the sensitivities of the values of acceleration noise to computation approaches and data frequencies are also examined. In summary, major research objectives of this research effort are as follows:

- An investigation of the relationships between acceleration noise and traffic conditions,
- An investigation of the relationships between acceleration noise and roadway characteristics,
- An investigation of the relationships between acceleration noise and driver/vehicle characteristics, and
- The development of a methodology for measuring the quality of traffic flow using instrumented vehicles

Research Methods

Data

Unlike previous research efforts which have relied primarily on experiments employing a small number of vehicles under controlled conditions, this study utilizes the GPS data

obtained from the instrumented vehicles employed in the metro Atlanta region. The vehicle activity data cover the whole metro Atlanta region and a long time period more than two years, indicating a huge amount of accumulated data (more than 1.5 million vehicle trips over the period of October 2003 and May 2006). The use of the whole data set is impractical in terms of data management and analysis. Based on this notion, this study utilizes only a subset of the instrumented vehicle data limited to a specific corridor and a time period. In addition to the instrumented vehicle data, Georgia Department of Transportation (GDOT) Transportation Management Center (TMC) data are utilized to capture parallel macroscopic freeway traffic conditions under which the instrumented vehicles traveled. Finally, roadway characteristics data, obtained from several sources such as GDOT Roadway Characteristics database, Digital Elevation Model (DEM), and high-resolution aerial photos, are also utilized.

Statistical Methods

This study utilizes various statistical methods, including the Gaussian kernel density estimation technique, Kolmogorov-Smirnov (KS) test, and random coefficient models. In particular, random coefficient models are used as a key statistical tool to evaluate the effects of roadway conditions and drivers/vehicles characteristics on acceleration noise, reflecting the feature of the instrumented vehicle data, repeated measurements. In addition, a fuzzy inference system is applied to generate indices of traffic flow quality incorporating both acceleration noise and speed.

Research Contributions

This research effort is expected to contribute to the field of traffic operations in several ways. First, this study uses the largest data set to date to understand the characteristics of speed variation, measured by acceleration noise, of a vehicle. In particular, this study is the first study to be able to investigate the potential effects of roadway conditions and drivers/vehicles on acceleration noise. Ultimately, the results of this study are expected to provide numerous insights into the application of the speed variation measures to measuring traffic flow quality. Second, this study begins to reveal the characteristics of freeway traffic flow interacting with roadway conditions and drivers/vehicles, which cannot be captured without the help of the instrumented vehicle data and corresponding traffic data (TMC data) accumulated over a long time period and a freeway corridor. Third, this study provides the framework for the evaluation of traffic flow quality measured by both acceleration noise and speed. The framework may result in a significant contribution in that it utilizes multiple measures that complement each other, rather than relying on a single measure. The use of the multiple measures is attractive since it is generally regarded as a better approach to reflecting various users' perceptions. Fourth, this study demonstrates methods and procedures for the data collection and management of second-by-second vehicle activity data for use in roadway performance evaluation and illustrates the useful characteristics of the GPS data. This demonstration provides researchers who plan to perform studies utilizing GPS technologies with helpful guidelines.

Dissertation Outline

Following this introductory chapter, Chapter 2 reviews the existing research efforts on roadway service quality measures incorporating the degree of speed variation. In addition, a comprehensive literature review focuses on acceleration noise. Chapter 3 discusses the data set and study site employed in this study. Chapter 4 evaluates the quality of GPS data employed in this study and reports procedures for the data management. Chapter 5 analyzes the sensitivity of acceleration noise values to its computation approaches and data sampling rates with an aim to better understand acceleration noise. Chapters 6, 7 and 8 analyze how acceleration noise is influenced by traffic, roadway, and drivers/vehicles, respectively. Chapter 9 proposes a methodology for evaluating traffic flow quality by incorporating both acceleration noise and vehicle speed. Finally, Chapter 10 summarizes the findings from this research effort and suggests future research directions.

Chapter 2

Literature Review

Roadway Service Quality and Speed Variation

Several research efforts have attempted to measure roadway service quality that reflects the degree of speed variation. One example is the "Quality index" of traffic flow (Greenshields 1961). The quality index was formulated as a function of speed, speed changes per mile, and expressed as follows:

$$Q = \frac{KS}{\Delta S\sqrt{f}},$$

where Q = quality index

S = average speed in miles per hour

ΔS = absolute sum of speed changes per mile

f = number of speed changes per mile

K = 1000, a constant.

As can be seen in this equation, the quality index increases as travel speed increases, and it decreases as the amount of speed changes increases. The terms ΔS and f were introduced to reflect the "frustration" factors experienced by individual drivers. The research effort suggested that the proposed index could be applied to the development of cost factors for vehicle operation.

In another research effort, which incorporated various driver inputs such as speed change rate, steering wheel reversal rate, accelerator reversal rate, and brake

application rate, the "Level of Traffic Service Index (LSI)" was proposed (Platt 1963). The index was conceptualized in human factors as follows:

$$LSI = Quality\ of\ Traffic\ Flow + \frac{Driver\ Satisfaction}{Driver\ Effort} - Driver\ Annoyance\ Due\ to\ Delay.$$

This concept was then formulated using the relevant variables that could be obtained from the special devices developed by the author and his colleagues. The formulation follows:

$$LSI = C_2\left[\frac{\overline{S}}{(SCR + C_1)(GYR + 0.1)}\right] + C_3\left[\frac{\overline{S}}{SCR[SRR + ARR + 2BAR]}\right] - C_4\left[\left(\frac{TT}{RT}\right)^3 - 1\right],$$

where S = Average speed in miles per hour

SCR = Speed change rate

GYR = Gyroscopic rate

SRR = Steering reversal rate

ARR = Accelerator reversal rate

BAR = Brake application rate

TT = Travel time

RT = Running time (time the vehicle is in motion)

C_1, C_2, C_3, C_4 = Constants.

In this equation, the speed change rate (SCR) is the absolute sum of vehicle acceleration and deceleration and aimed to measure the degree of the smoothness of motion. In addition, the gyroscopic rate (GR) represents the radius of vehicle turns per minute due to lane changes, curves, and turns.

These research efforts are some of the first to introduce methodologies for incorporating the degree of speed variation into a traffic flow quality measure in a

quantitative manner. In addition, they provided the relationships between the proposed indices and conventional traffic parameters, suggesting the effectiveness of the speed variation-based measures.

Measures of Speed Variation

A literature review revealed that existing studies have used various measures to quantify speed variation, depending on their applications, such as vehicle emissions analysis, safety analysis, and congestion index development. For example, Babu and Pattnaik (1997) investigated the relationship between traffic congestion and several speed variation measures including acceleration noise, the standard deviation of speed, and the coefficient of variation of speed. The standard deviation of speed (σ_v) for a single vehicle can be formulated as follows:

$$\sigma_v = \sqrt{\frac{\sum_{i=1}^{n}(v_i - \bar{v})^2}{n-1}},$$

where v_i is the second-by-second speed at time *i*, *n* is the number of observations, and $\bar{v}$ is the average speed for the given link or segment. The coefficient of variation (CV) is defined by the normalized standard deviation by the average speed and expressed as follows:

$$\text{CV} = \frac{\sigma_v}{\bar{v}}.$$

Positive kinetic energy (PKE) is a measure of acceleration kinetic energy per unit distance and defined as

$$\text{PKE} = \frac{\sum_{i=1}^{n-1} pos(v_{i+1}^2 - v_i^2)}{d},$$

where the function *pos* returns only the positive values of its result, and *d* is the distance traveled along the given roadway segment. This parameter was incorporated in an urban fuel consumption model as a predictor variable (TRB 1975). In addition, Barth et al. (1996) investigated the relationship between PKE and macroscopic traffic parameters by collecting GPS second-by-second speed data using a test vehicle. Total absolute second-by-second speed differences divided by travel distance (TAD) was also used as a speed variation measure (Barth et al. 1996). This statistic increases whenever speed changes, regardless of positive or negative changes in a given speed profile. Its mathematical expression follows:

$$\text{TAD} = \frac{\sum_{i=1}^{n-1} | v_{i+1} - v_i |}{d}.$$

In addition to these measures, acceleration noise, which will be discussed in detail in the next section, and mean velocity gradient (MVG), normalized acceleration noise by average speed, were also adopted as speed variation measures (D'Este et al. 1999; Underwood 1968). The mathematical definition of MVG follows:

$$\text{MVG} = \frac{\sigma}{\bar{v}},$$

where σ indicates acceleration noise. Among other measures, acceleration noise has been the most often studied and suggested as a traffic parameter capable of representing traffic flow quality from a microscopic perspective.

Acceleration Noise

Acceleration noise was proposed nearly a half century ago as a parameter that might be employed to characterize the driver-car-road complex under various conditions (Herman et al. 1959). In the proposal of acceleration noise, it was defined as "the root-mean-square deviation of the acceleration of the car." The definition can be formulated as follows (Jones and Potts 1962):

$$\sigma^2 = \frac{1}{T}\int_0^T [a(t) - a_{av}]^2 dt = \frac{1}{T}\int_0^T a(t)^2 dt - (a_{av})^2,$$

$$\text{where } a_{av} = \frac{1}{T}\int_0^T a(t)dt = \frac{1}{T}[v(T) - v(0)].$$

In the equations above, σ indicates acceleration noise, and *v(t)* and *a(t)* are the speed and acceleration of a car at time *t*. In addition, *T* is the total time spent moving. This definition was simplified by assuming *v(T)* and *v(0)* are equal (i.e., the starting speed = ending speed), and thus, the second term in the first equation above was set to zero (Jones and Potts 1962). The simplified approach measures the fluctuation of acceleration around origin while the original definition measures it around the mean acceleration. These two different approaches may produce different acceleration noise values because the starting and ending speeds are not always the same. However, researchers have used acceleration noise in both ways without noting the potential difference.

Researchers in the 1960's asserted that acceleration noise could be influenced by traffic and roadway conditions, and vehicle/driver behavior. To demonstrate these aspects, researchers implemented experiments and found that speeding behavior

increased acceleration noise (Herman et al. 1959; Jones and Potts 1962). In addition, acceleration noise measured on roadways with worse geometric conditions tends to increase (Drew et al. 1967; Jones and Potts 1962). The effects of roadway grade and trucks, on urban freeway, were also investigated, resulting in increasing acceleration noise on a grade and inadequacy of acceleration noise for evaluating the effects of trucks on the level of service (Humphreys 1969). Upon examining the relationship between acceleration noise and vehicle position in a queue (Herman and Rothery 1962), acceleration noise of following cars was found to be larger than that of the freely-moving lead car, as shown in Figure 3.

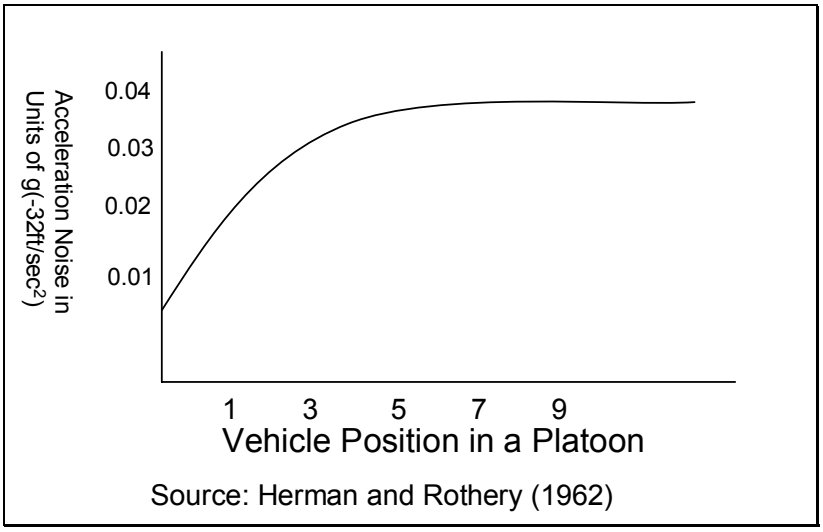

Figure 3: Relationship between Acceleration Noise and Vehicle Position

More importantly, numerous research efforts, attempting to identify the relationship between acceleration noise and traffic conditions (or level of service), concluded that acceleration noise, in general, increases with traffic congestion (Babu and Pattnaik 1997; Croft and Clark 1985; Jones and Potts 1962; Kim et al. 2003). Based on this conclusion, researchers suggested that acceleration noise could be a

potential traffic parameter reflecting traffic flow quality or level of service. Associated with the level of service, acceleration noise was theoretically related to the freeway level of service using the energy-momentum theory (Drew 1968; Drew et al. 1967). In the research effort, acceleration noise was theoretically linked to macroscopic traffic parameters: speed, volume, and density. By assuming that the energy for the traffic stream over a section of road is conserved, Drew and his colleagues established a relationship, total energy (T) = kinetic energy (E) + internal energy (I), formulated as follows:

$$T = \alpha k u^2 + \sigma,$$

where α, k, and u represent parameter, density, and speed of the traffic stream, respectively, and σ indicates acceleration noise. The parameter α serves to adjust kinetic energy (E) and internal energy (I) so that their sum is equal to total energy T. The equation suggests that internal energy (I) is represented by acceleration noise. By combining this relationship and the well-known linear relationships among macroscopic traffic flow parameters (speed (u), volume (q), and density (k)), the researchers (Capelle 1966; Drew et al. 1967) suggested the following theoretical relationships linking acceleration noise to traffic flow parameters (see Appendix A for details):

- Acceleration noise as a function of speed

$$\sigma = \sigma_{\max} - \frac{27\sigma_{\max}}{4}\left[\left(\frac{u}{u_f}\right)^2 - \left(\frac{u}{u_f}\right)^3\right]$$

- Acceleration noise as a function of density

$$\sigma = \sigma_{\max} - \frac{27\sigma_{\max}}{4}\left[\frac{k}{k_j} - 2\left(\frac{k}{k_j}\right)^2 + \left(\frac{k}{k_j}\right)^3\right]$$

- Acceleration noise as a function of flow

$$\sigma = \sigma_{\max} - \frac{27\sigma_{\max}}{32} \cdot \frac{q}{q_m} \pm \frac{27}{32}\sigma_{\max} \frac{q}{q_m} \sqrt{1 - \frac{q}{q_m}} .$$

In the equations above, $\sigma_{\max}$ indicates the maximum acceleration noise observed when kinetic energy (E) is zero, and u_f, k_j, and q_m represent free-flow speed, jam concentration, and the maximum flow, respectively. These relationships are graphically illustrated in Figure 4, which indicates that acceleration noise generally increases as speed decreases or density increases although such a trend does not continue under high speed or low density.

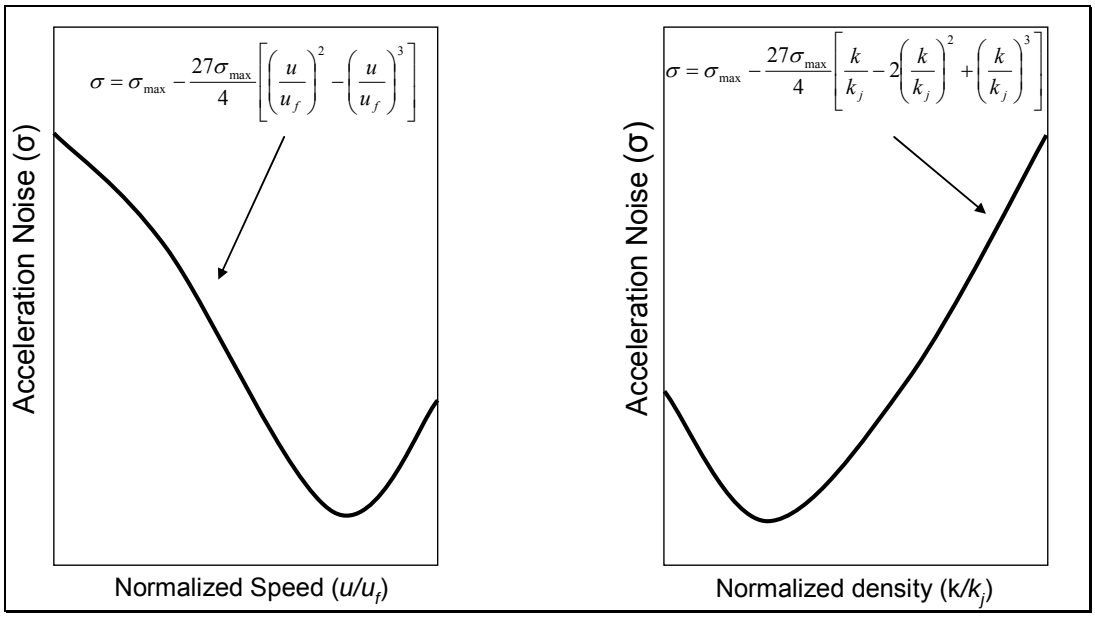

Figure 4: Relationships between Acceleration Noise and Speed and Density

An important feature of the energy model developed by Drew is that the model has the capability of quantifying roadway level of service from the perspective of acceleration noise. His concept can be visualized using Figure 5, which compares the typical flow-speed relationship with the energy-speed relationship. The figure suggests

that the maximum satisfaction of drivers can be achieved at a speed of $2/3u_f$, whereas the optimum speed from the maximization of flow is 1/2 u_f. Hence, the maximization of driver satisfaction occurs at speeds higher than those observed at the maximum flow rate. Although the relationship between drivers' maximum satisfaction and flow smoothness (lower acceleration noise) should be established in a further research effort, the model throws insights into the concept of level of service that should be interpreted from the perspective of roadway users, drivers.

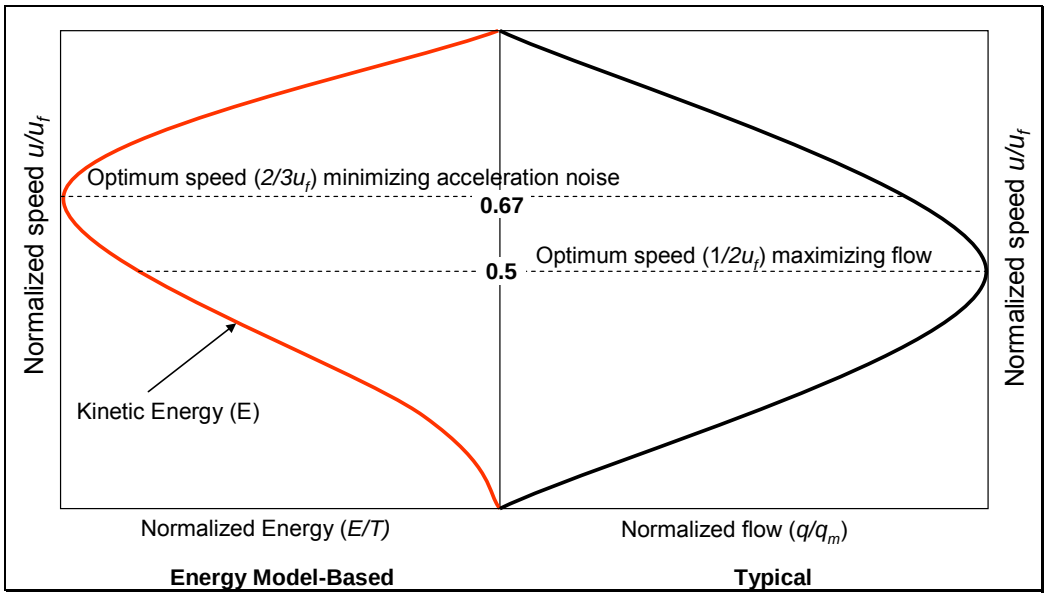

Figure 5: Quantitative Approach to Level of Service Using Acceleration Noise

After the concept of the energy model was published, research on acceleration noise continued on, and several researchers attempted to apply acceleration noise to measure roadway level of service (Croft and Clark 1985; Ryden 1976; Torres 1969). Some researchers pointed out that Drew's energy model had a weakness, that is, it could not explain boundary conditions and that acceleration noise might not represent a good indication of internal energy (Lee and Yu 1973; Winzer 1981). Another research effort

indicated that acceleration noise might not be a good measure of congestion because of its non-linear relationship with travel time and suggested that MVG might be a better indicator of traffic congestion (Underwood 1968). In addition, some researchers pointed out that the relationship between acceleration noise and traffic conditions was not as pronounced on urban arterials as on freeways (Rowan 1967; Ryden 1976). This situation may provide a reason why most research efforts on acceleration noise have focused on freeway traffic.

The literature review revealed that studies on acceleration noise did not actively continue in spite of the numerous initial research efforts in the late 1950's and 1960's, probably due to the difficulty of speed profile data collection. In fact, most of these studies relied upon vehicle speed monitored by special devices; in some cases, speed profile data were obtained from aerial photos taken from an aircraft (Humphreys 1969; Lee and Yu 1973). However, the difficulty of data collection has been alleviated with GPS devices, which are easy to install and provide accurate speed profiles. Recent research efforts that have deployed instrumented vehicles equipped with GPS devices for collecting speed profile data have concluded that acceleration noise could be more usefully utilized for traffic studies with GPS technology (D'Este et al. 1999; Taylor et al. 2000).

Research efforts on acceleration noise were chronologically summarized in Table 1, which contains such information as topics of research, methods of data collection, and the definition of acceleration noise for each study. The summary covers the years when acceleration noise was first proposed to those when a simulation study (Kim et al. 2003) that evaluates several roadway service measures including

acceleration noise on rural freeways was implemented. As suggested in the table, the previous studies employed only a small number of test vehicles at an experimental level, implying limitations in reflecting real-world vehicle activities. In particular, the use of a computer simulation model may be problematic since the acceleration behavior embedded in the simulation model is likely to fail to represent drivers' accelerating behavior observed in the real-world context (Hallmark and Guensler 1999).

Table 1: Summary of Research on Acceleration Noise

Year	Authors	Facility Type	Location	Research Topic	Data Collection Method	Equipment	Acceleration Noise Definition
1959	Herman, et al	Research Laboratory	Detroit	Proposal of Acceleration noise	Experimental measurements	Accelerometer	Standard deviation of acceleration
1962	Jones and Potts	Urban/suburban Roads	Adelaid Hills, Australia	Effects of road, driver, and traffic	Experimental measurements	Tachograph	Root-mean-square of acceleration
1962	Herman and Rothery	Research Laboratory	Detroit	Relationship with vehicle position in a platoon	Experimental mesurement	Instrumented Vehicle	Not clear
1965	Drew and Keese	Urban Freeway	NA	Introduction of energy-momentum theory	NA	NA	NA
1966	Capelle	Urban Freeway	Chicago, Illinoise	Relationship with traffic praramters	Average car method	Tachograph	Root-mean-square of acceleration
1967	Drew, et al	Urban Freeway	Houston, Texas	Relationship with LOS	Floating car by a single driver	Speed recorder	Root-mean-square of acceleration
1968	Underwood	Urban Streets	Victoria, Austrailia	Acceleration Noise, Mean velocity gradient, and congestion	Test car	Speedometer reading	Root-mean-square of acceleration
1969	Humphreys	Urban Freeway	Houston, Texas	Effects of trucks on grade	Aerial photo	35-mm aerial films	Root-mean-square of acceleration
1969	Torres	Urban Freeway	Ventura Freeway (CA)	Relationship with traffic parameter	One test car by six drivers	Accelerometer	Standard deviation of acceleration
1969	Rowan	Arterial	College Station, Texas	Energy model for major streets	Average car method	Speed recorder	Root-mean-square of acceleration
1973	Lee and Yu	unknown	unknown	Acceptable parameters for the internal energy of traffic flow	Aerial photo	Not clear	Not clear
1976	Ryden	Urban Streets	St. Louis, Missouri	Application of energy-momentum techniques to city street	Test car	Traffic analyzer	Root-mean-square of acceleration
1981	Winzer	Suburban Freeway (Autobahn)	Germany	Relationship with traffic parameters	Test car	electronic speedometer, tachograph, accelerometer	Standard deviation of acceleration
1985	Croft and Clark	Urban Freeway	Louisville, Kentucky	Relationship with traffic parameters	Floating car by a single driver	Traffic analyzer	Standard deviation of acceleration
1997	Babu and Pattnaik	Urban Streets	Madras, India	Various speed variation measures and LOS	Test car	Manual recording of speed at an interval of 30 seconds	Not clear
1999	D'Este, et al	Urban Streets	Adelaid, Australia	GPS technology and traffic parameters	Test car	GPS	Root-mean-square of acceleration
2000	Taylor, et al	Expressway /City street	Adelaid, Australia	GPS and congestion index	One probe vehicle	GPS	Root-mean-square of acceleration
2003	Kim, et al	Rural Freeway	Hypothetical	Acceleration noise and LOS of rural freeway	Simulation (CORSIM)	NA	Standard deviation of acceleration

Chapter 3

Data

Instrumented Vehicle Data

Commute Atlanta Project

Instrumented vehicle data obtained from the Commute Atlanta project, a research program undertaken by the researchers of the Georgia Institute of Technology, are the main data source for this research. The purpose of the Commute Atlanta project, funded by the Federal Highway Administration (FHWA) Office of Value Pricing Programs and the Georgia Department of Transportation (GDOT), is to assess the effects of converting fixed automotive insurance costs into variable driving costs. To this end, the research team recruited 275 households in the metro Atlanta, Georgia, based on the random stratified sampling approach considering household income, size, and vehicle ownership (Ogle 2005; Ogle et al. 2005). The spatial distribution of the recruited households is illustrated in Figure 6. Then, the research team instrumented 485 vehicles from the households with the GT Trip Data Collectors (GT-TDC) to monitor the second-by-second speed and positions of the vehicles. Currently, the research team is assessing the impacts of mileage-based incentives based on variable cent/mile rates, from 5 cents/mile up to 15 cents/mile. In the research effort, the households reducing their miles of travel relative to the baseline year mileage will receive credits based on the cent/mile rate. In the next stage, the research team will investigate the impacts of real-time congestion pricing strategies by communicating prices into the participating vehicles through onboard equipment.

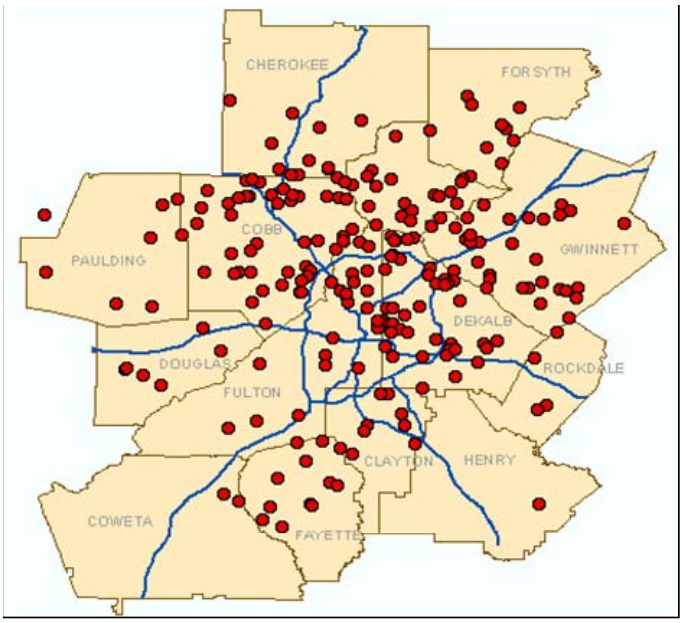

Figure 6: Location of the Commute Atlanta Project Participating Households

Vehicle Instrumentation

The vehicles participating in the Commute Atlanta project were equipped with GT-TDC shown in Figure 7. The instrumentation package includes:

- 386 Linux computer
- 12V Power, 3mA draw
- Ignition Sensor
- Vehicle Speed Sensor
- Global Positioning System (GPS) receiver (SirfStarIIe/LP)
- Onboard Diagnostics (OBD) Connection
- Cellular Transceiver
- 6 on/off sensors
- 1 open serial port for optional systems

For each engine ignition, the equipment starts and records a trip file until the vehicle stops and the driver shuts off the engine. The trip file records second-by-second vehicle operations including speed, heading, and vehicle position (latitude and longitude) provided by the GPS system. Then, the trip file is transmitted to Georgia Tech sever via short message service (SMS) provided by a cellular system. The data collection system deployed in the Commute Atlanta project is illustrated in Figure 8.

Figure 7: GT Trip Data Collector and Wiring Harnesses and Antennas

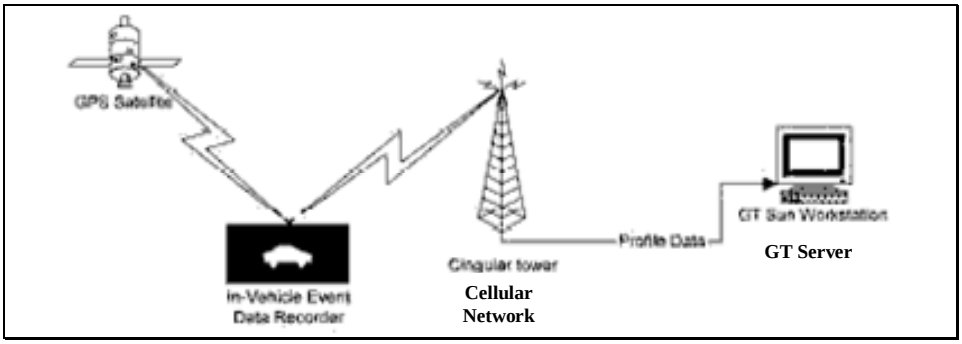

Figure 8: Data Collection System for the Commute Atlanta Project

Study Area

The Commute Atlanta project provides instrumented vehicle data for the whole metro Atlanta area and provides an opportunity to investigate the characteristics of acceleration noise under various roadway conditions. However, this research focuses on only a single freeway corridor as a test case. The main reason for the use of a single corridor is to facilitate the data collection efforts, in particular for roadway geometric data such as grade and curvature, for which no available and reliable data source was found. Some factors were considered to select the study corridor as follows:

- Availability of traffic data,
- The amount of instrumented vehicle data,
- The presence of various traffic conditions,
- The presence of various roadway geometrics,
- The non-presence of HOV lane, and
- Low truck traffic.

The traffic data are indispensable for this study since they provide the information on the general traffic conditions that the instrumented vehicles experienced. Thus, the study corridor should be under TMC coverage, for which traffic data are available. In addition, the study objectives require that the instrumented vehicle trips be obtained from various drivers/vehicles and from roadways with various characteristics. Also, various traffic conditions should be observed for the trips. These conditions will provide more meaningful results from the analyses planned in this study. In addition, the presence of HOV lanes should be considered since the operational characteristics of HOV lanes are likely to be considerably different from the regular lanes, in particular

during congested time periods. Thus, the selection of a corridor without HOV lanes may remove the complexity of data interpretations. Finally, truck traffic was considered since the presence of trucks can significantly influence the speed profiles (Grant 1998). Thus, the selection of a corridor with significant truck traffic would require an additional data collection effort for the truck traffic, rendering data collection and analysis more complicated. In this situation, the selection of a corridor with a minimum amount of truck traffic would be desirable for ease of analysis.

Considering these factors, this study selected the 12-mile GA400 corridor outside interstate 285, as shown in Figure 9. For this corridor, TMC data aggregated in 20 seconds were available, and a considerable amount of the instrumented vehicle data could be observed under various traffic conditions, due to its serving as a major commute corridor. In addition, various roadway conditions—two speed limits (55mph and 65mph); and two-, three-, and four-lane roadways—can be observed over the corridor, allowing an opportunity to more effectively investigate the effects of roadway characteristics. The absence of HOV lanes and low truck traffic on this corridor also provided reasons for the selection. The truck traffic on this corridor is relatively low, as shown in Figure 9. In fact, the data from the Highway Performance Monitoring System (HPMS) indicate that the truck percentage of this corridor ranges between 3 and 6%.

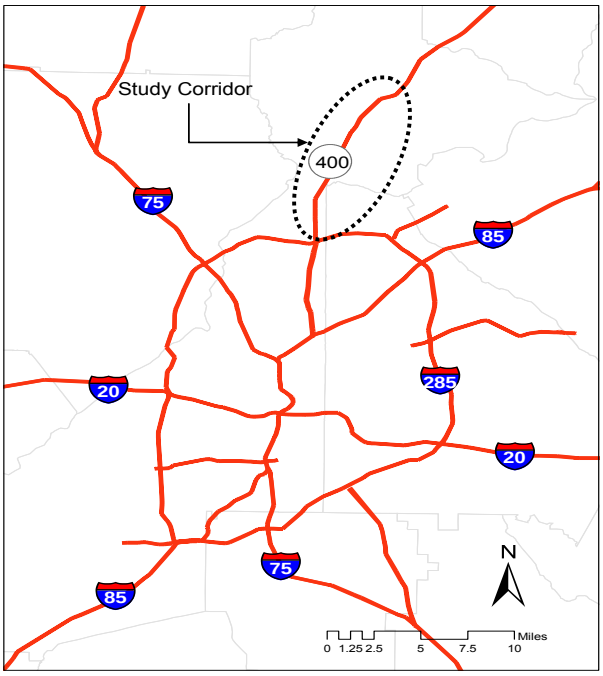

Figure 9: Study Area

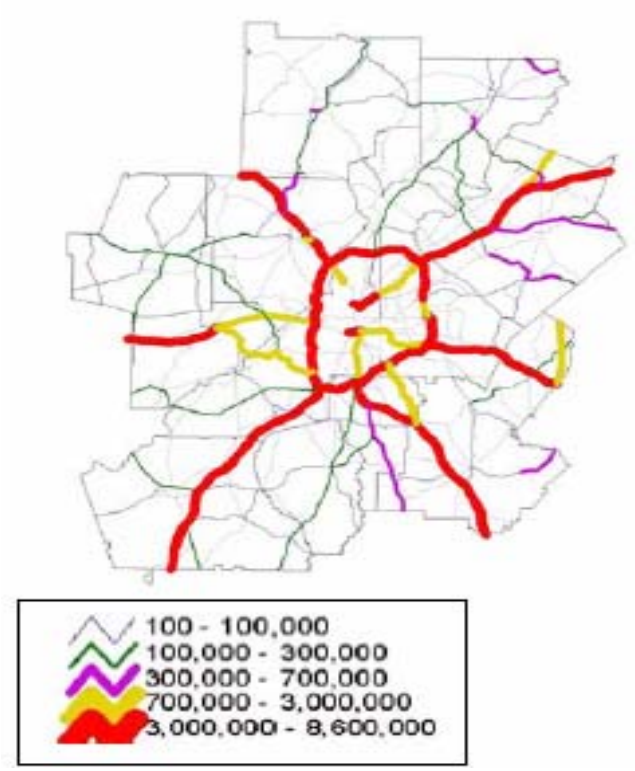

Source: Atlanta Regional Commission, Mobility 2030, Regional Transportation Plan, 2004.

Figure 10: Annual Truck Loads in the Atlanta Region

Study Time Frame

The study time frame for this research is between October 2003 and August 2004 (eleven months). The starting point of the time period is when the full instrumentation was completed, as shown in Figure 11. The figure shows that it took several months to install the GT-TDCs for the Commute Atlanta project and that the number of installed GT-TDCs stabilized after September 2003. Meanwhile, the ending point of the study period was decided based on the time period of a road construction project performed in the study corridor beginning in September 2004, as the roadwork was likely to affect the vehicle activity. Consequently, August 2004 was decided as the ending point of the study time period, which prevents the complexity of data analysis.

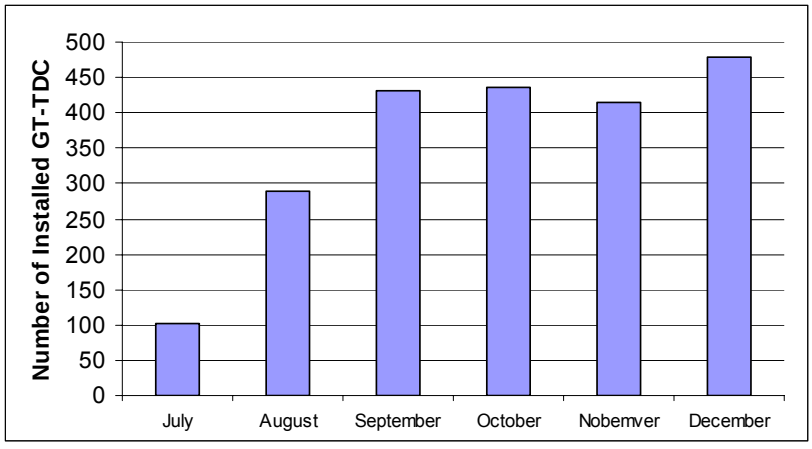

Figure 11: Number of Installed GT-Trip Data Collectors during 2003

Macroscopic Traffic Data

In addition to the instrumented vehicle data, TMC data, collected from video detection system (VDS) cameras on GA400, were employed to capture macroscopic traffic conditions associated with the instrumented vehicle trips. For the mainline (excluding ramps) of the GA400 corridor, 77 VDS stations, 39 stations for southbound and 38

stations for northbound, provide lane-by-lane traffic data, including traffic speed, volume, and density, in 20-second intervals (http://www.georgianavigator.com). For this study, these traffic data were aggregated into one-minute intervals on a station-by-station basis. Thus, the lane-by-lane data were combined into the station level data, and three 20-second observations were aggregated into one observation.

Roadway Characteristics Data

The study corridor was segmented into smaller sections, minimizing the occurrence of composite roadway characteristics. The roadway characteristics considered were the number of lanes, speed limit, grade, facility type, and curvature, all of which are likely to affect the speed profiles of a vehicle. Data sources used for determining the roadway characteristics are summarized in Figure 12, indicating that three major data sources—Roadway Characteristics (RC) table, Digital Elevation Model (DEM), and U.S. Geological Survey (USGS) aerial photo—were utilized for the determination. Detailed explanations about the geometric data collection processes will be provided in the following sections. As a result of the segmentation, 89 segments (42 for northbound and 47 for southbound) were obtained (Figure 14). The average, minimum, and maximum lengths of the segments are 0.28, 0.20, and 0.39 miles, respectively. Figure 13 illustrates the distribution of segment lengths, indicating that a majority of segments are between 0.25 and 0.3 miles.

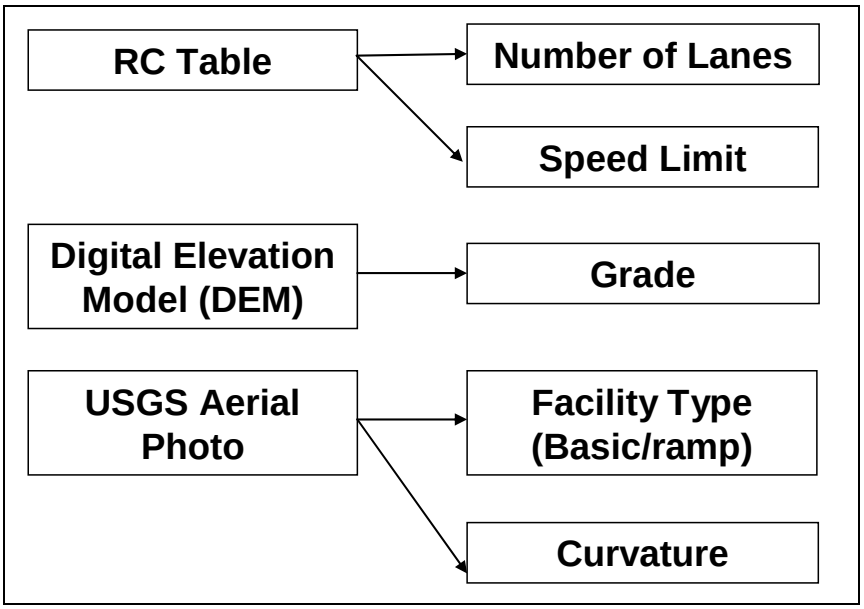

Figure 12: Factors for Roadway Segmentation

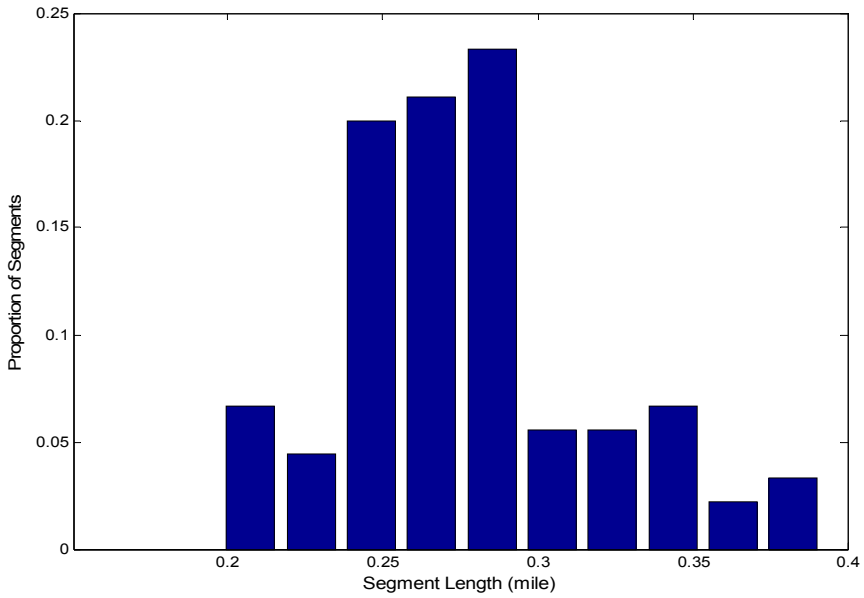

Figure 13: Distribution of Segment Lengths

Number of Lanes and Speed Limit

The number of lanes and speed limit information were obtained from the GDOT RC file, which contains roadway characteristics for all roadways in the state. The RC file indicated that the study corridor is composed of roadway segments with 2, 3, and 4

lanes and 55 and 65mph speed limits. Figure 14 indicates that 65mph and four lanes are the prevailing speed limit and the number of lanes in this corridor, respectively. In fact, the segments with a speed limit of 65mph occupy 79% of the study corridor, and 61% of the corridor contains four lanes. The speed limit of the segments with two or three lanes is only 65mph while four-lane segments have a speed limit of 55mph or 65mph, depending on the locations.

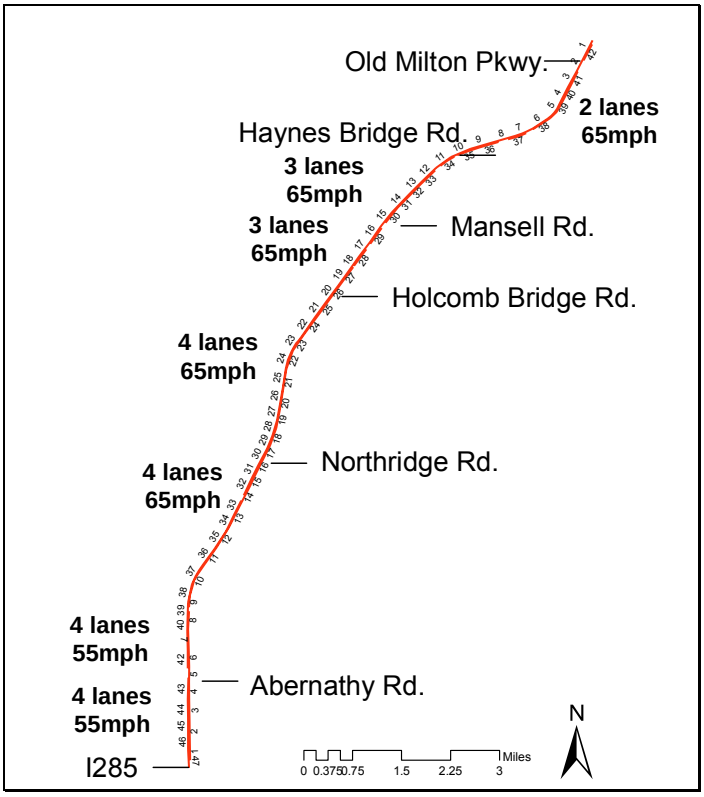

Figure 14: Number of Lanes and Speed Limit

Grade

The grade of roadway segments was measured using USGS 7.5-minute DEM data, which contain arrays of regularly-spaced elevation values. According to the USGS, 90% of the 7.5-minute DEM data have a vertical accuracy of 7-meter root-mean-square error or better, and 10% are in the 8- to 15-meter range

(http://erg.usgs.gov/isb/pubs/factsheets/fs04000.html). In the process of the grade calculation, the DEM data file (an image file) was converted to a polygon feature using the tool of the spatial analyst in ArcGIS. The generated polygons were then overlaid on the roadway network, resulting in an identification of polygons that the study corridor passes through. Figure 15 illustrates the DEM data and converted polygons for a small segment of the study corridor. The elevation difference between two end points of a segment and the segment length were used for the grade estimation (i.e., grade (%) = elevation difference/segment length×100). The resulting grade ranges from -3.7 to +3.4% for the 89 segments (for both directions), and among them, 74 segments have a grade within a ±3% range.

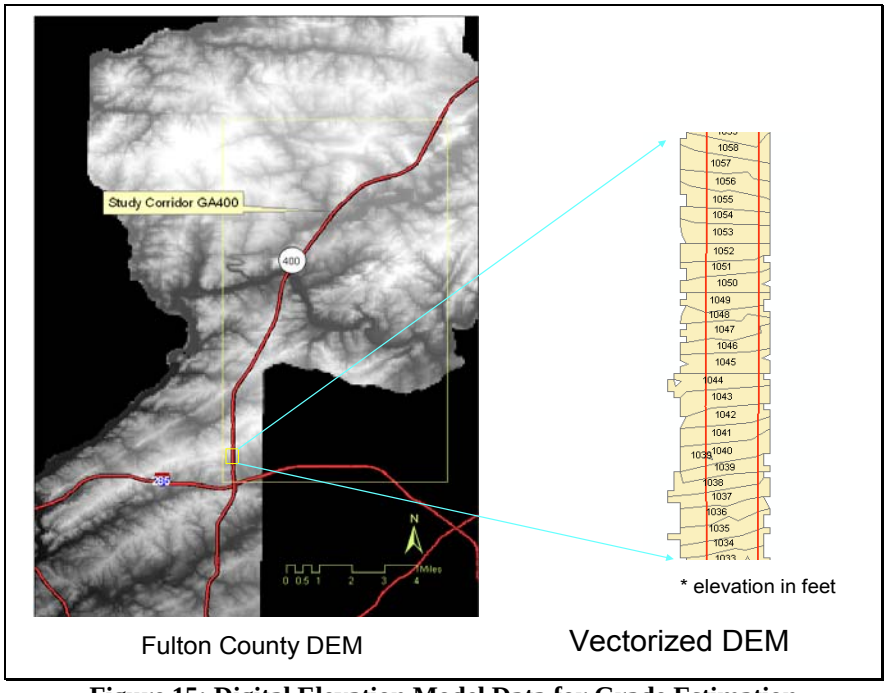

Figure 15: Digital Elevation Model Data for Grade Estimation

In the calculation of roadway grade using DEM, care was taken near the bridge sections since the altitude obtained from DEM is based on the surface of the water, if

the bridge is over a river. As an illustration, Figure 16 shows DEM, aerial photo, and vectorized DEM near Chattahoochee River, indicating the DEM-based altitude of the bridge is the same with that of the river. Thus, the use of the altitude for the grids where a bridge is located may exaggerate the slope. Based on this notion, the grade near the bridge was computed using the altitudes at the ends of the bridge.

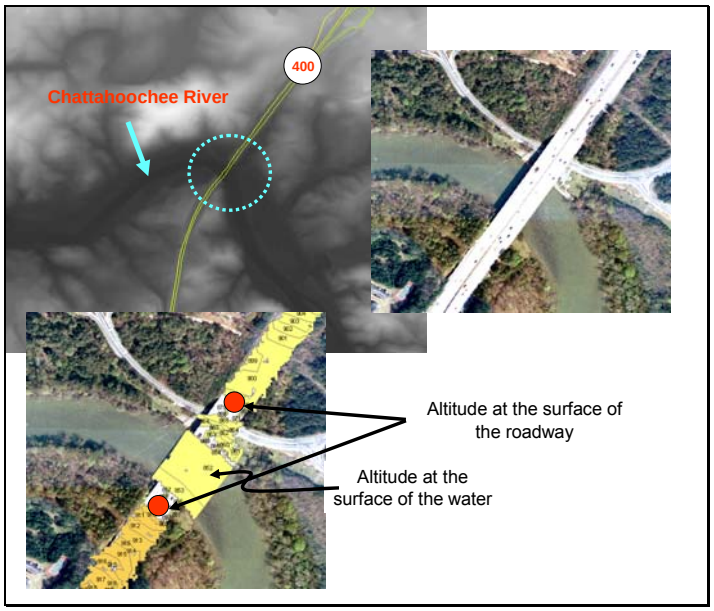

Figure 16: DEM, Aerial Photo, and Vectorized DEM near Chattahoochee River

Curvature

The degree of curvature was measured based on the radius of the circle which fits the segment. The radius of curvature was then calculated using the relationships among radius, chord, and arc in the circle. A graphic illustration of these elements is shown in Figure 17 in which the region (a-b-c-a) is a segment of a circle and no larger than a semi-circle. Using the notations in the figure, their relationship can be formulated as follows:

$$R^2 = (R - H)^2 + (\frac{X}{2})^2 \ ,$$

where R, X, and H are the radius, the chord length, and the height, respectively. Thus, the radius of a circle can be computed using

$$R = \frac{(X/2)^2 + H^2}{2H}.$$

An application of this equation requires accurate information about the shape of the roadways, which can be observed in the high-resolution USGS aerial photos. Under the GIS framework, points were superimposed on the aerial photo along the middle lane of the study corridor for each direction, and these points were used for measuring the chord length (X) and the height (H). Based on the chord length and the height, the radius of a curve were computed using the equation above. The resulting radii of curves were large numbers for most freeway segments, and the minimum radius (2,515 feet) was found at southbound Segment 5 between Old Milton Parkway and Haynes Bridge Road.

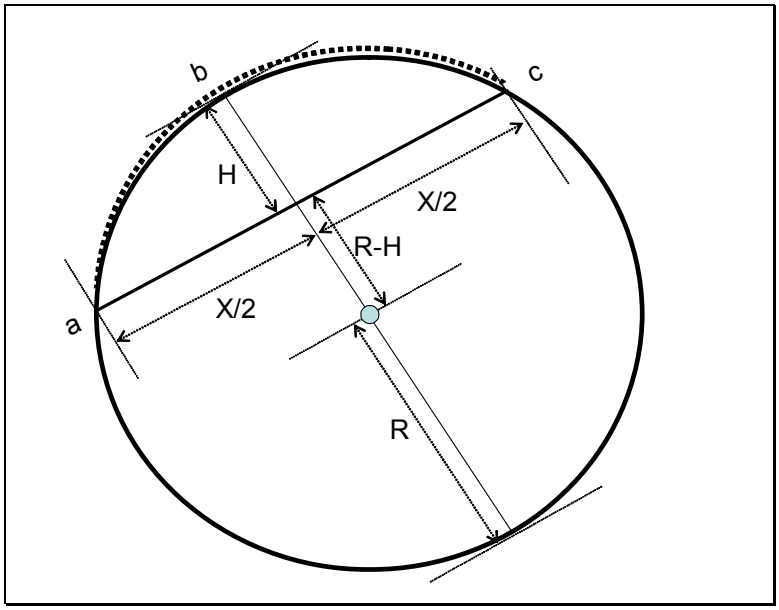

Figure 17: Relationships Among Radius, Arc, and Chord in a Circle

Facility Type

Freeway facilities can be classified into three types: basic, on/off ramp, and weaving segments. These three types have different operational characteristics, and thus, the HCM suggests different analysis approaches for each type. Figure 18 illustrates the facility type and indicates that ramp influence areas extend to 1,500 feet upstream from a physical diverge point and to 1,500 feet downstream from a physical merge point. In particular, lanes 1 and 2 (from the right-most lane), including acceleration and deceleration lanes, are the areas most significantly affected by the entering or exiting vehicles. Based on this situation, this study classified the segments of the study corridor into basic, on-ramp, and off-ramp segments. Note that the study corridor does not contain weaving sections. In the classification effort, USGS aerial photos were utilized to locate merge or diverge points.

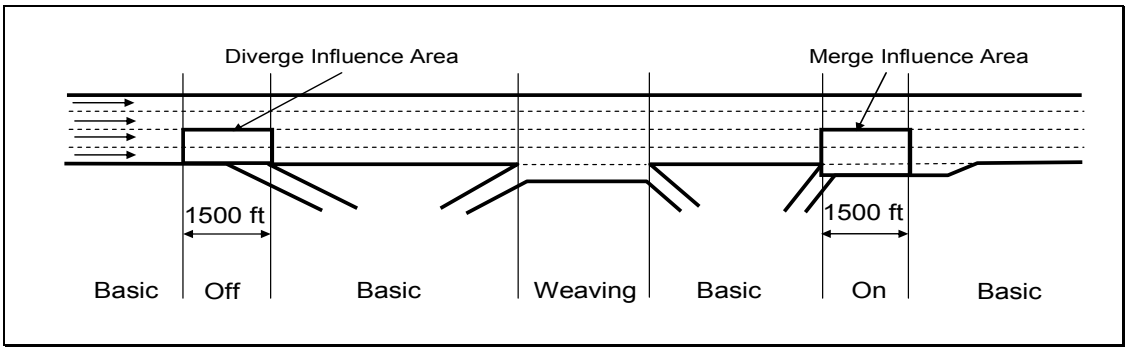

Figure 18: Freeway Facility Types

Relationship Among Roadway Characteristics

The relationships among the roadway characteristics, which can be easily correlated due to roadway design guidelines, were examined, and the scatter plots revealing potential

relationships were illustrated in Figure 19. The figure compares grade and the degree of curvature (represented by 10,000 divided by the radius of the curve in feet) with the number of lanes, speed limit, and facility type, indicating weak correlations among the grade and the roadway characteristics. However, the higher degrees of curvature were found in the segments with two lanes or a 65mph speed limit. In fact, the average degrees of curvature are 0.93, 0.54, and 0.52 for segments with two, three, and four lanes, respectively. For facility types, segments affected by on-ramps tend to have a lower degree of curvature. The average degrees of curvature are 0.67, 0.30, and 0.54 for basic, on-ramp, and off-ramp segments, respectively. As a whole, however, significant correlations were not found among the roadway characteristics. In addition, the correlation between the grade and the degree of curvature were examined, as shown in Figure 20, indicating a weak correlation between the two geometric variables.

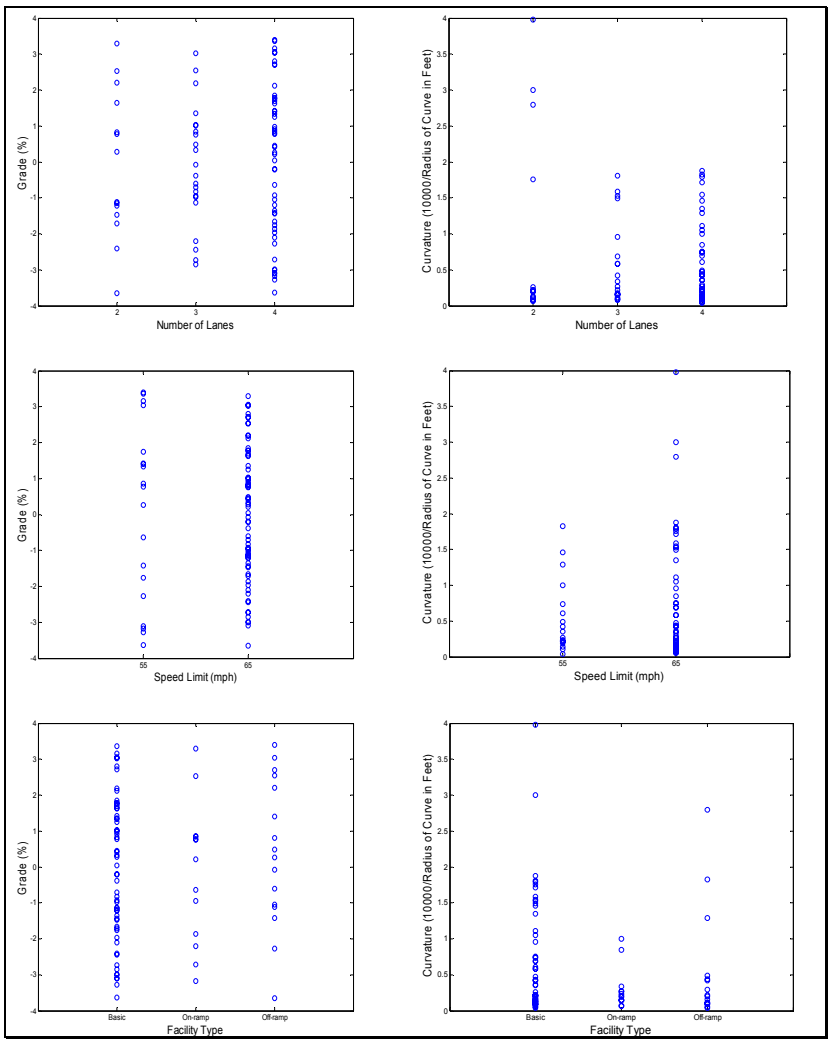

Figure 19: Relationships among Roadway Characteristics

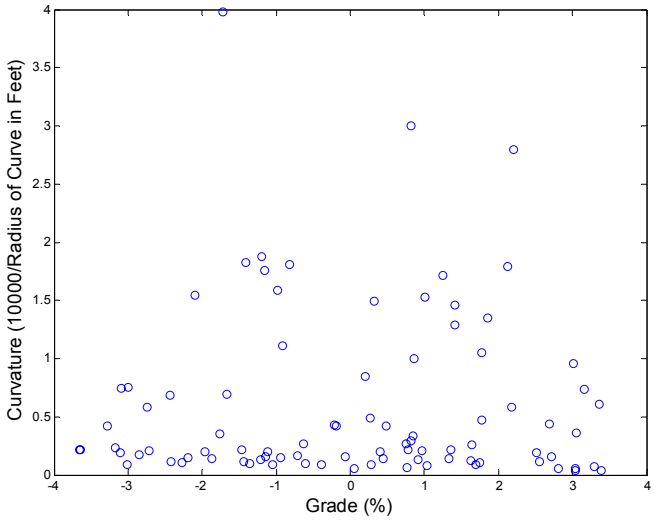

Figure 20: Scatter Plot of Grade and Curvature

Chapter 4

GPS Data Quality and Processing

GPS Data

Background

The main data source for this research effort is GPS devices which provide second-by-second vehicle speed and position. GPS was originally developed for military purposes, but it is now being expanded to numerous civilian applications including vehicle navigation systems. In particular, in 2000, the removal of Selective Availability (SA), an intentional degradation of the GPS signal, significantly improved the accuracy of GPS data. The determination of the position of GPS receivers follows the principle of trigonometry which requires at least four of the 24 satellites in six orbital paths circle the earth twice a day. This constellation of satellites continuously transmits signals containing positional and timing information at high frequencies (approximately 1,500MHz). These signals are picked up by GPS receivers with an antenna, and they are utilized for computing the coordinates of antenna positions and speed. For the speed calculation, GPS receivers use the Doppler shift of the GPS signals, independent of the position calculation (Czerniak and Reilly 1998; Hofmann-Wellenhof et al. 1994; Zito et al. 1995).

Since the calculations of position and speed rely on signals from the satellites, the reliability of the GPS data can be affected by factors obstructing or reflecting the signals in the urban environment (e.g., building and tunnel), rural environment (e.g., trees) and weather. The reliability of GPS data is usually measured by the number of satellites and the positional dilution of precision (PDOP). In general, reliable GPS data

points can be obtained when at least four satellites are in view and the PDOP value lies between 1 and 8 (Ogle 2005). Although these parameters provide a good guidance for the identification of reliable GPS data points, random errors imbedded in the GPS outputs still require additional data processing that minimizes the errors.

Quality of Study Data

The quality of GPS data used in this study was examined using 264,973 segmented trips collected over the study corridor during the study period (October 2003 to August 2004). For the examination, potentially bad one-second GPS data points were identified based on two criteria: the number of satellites in view and PDOP. If a GPS data point (second-by-second speed) does not satisfy both the criteria (i.e., at least four satellites and a PDOP value between 1 and 8), the data point was regarded as a bad data point. Based on this rule, a bad data rate for a segmented trip was computed from dividing the number of bad data points by the total number of data points for the trip. The distribution of the bad data rates for the instrumented vehicle trips (n = 264,973) were obtained as shown in Figure 21. The figure indicates that 70% of the trips do not have even a single bad data point and that 5% of the trips have bad data rates larger than 0.5. Note that the data quality of the trips is expected to be much better than any other trips since the trips were obtained from only freeway segments where obstructed GPS signals are less likely to occur. In addition, during the freeway operation, the chances of cold (or warm) starts of GPS receivers may be significantly low. In case of cold (receivers were off for several days) or warm (receivers were off for less than a day) starts, it takes time for receivers to acquire satellites signals, and thus, the GPS data during the time

period are subject to be unreliable. However, in spite of the good circumstances on freeways, the occurrence of bad GPS data points still requires additional data smoothing or filtering processes.

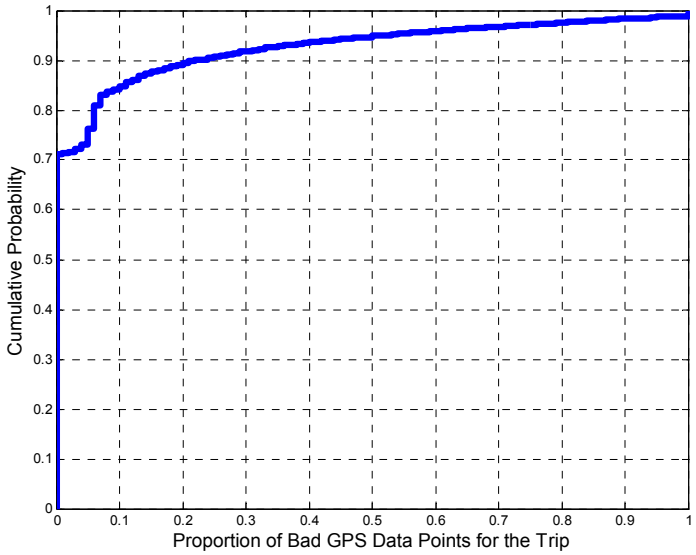

Figure 21: Cumulative Distribution of Bad Data Ratio for a Trip (n = 264,973)

GPS Data Smoothing Using the Kalman Filter

Associated with GPS data smoothing approaches, a research effort reported that GPS random errors could be effectively mitigated using the Kalman filter (Jun et al. 2006). In particular, the research effort showed that the performance of the filtering process could be improved using the GPS data quality parameters: the number of satellites and PDOP. These two parameters are the indicators of GPS signal qulaity, and thus, they could help the researchers effectively adjust the amount of error variances in the Kalman filter processes. The Kalman filter process is composed of two recursive processes: prediction and correction steps. In the prediction step, the next value is estimated based only on the past measurements, and then, the correction step refines the

value of the estimate using the current value. Based on these processes, the GPS speed data used in this study were filtered as an attempt to reduce the random errors.

Quality of Filtered GPS Data

Vehicle Speed Sensor Data

The data quality of filtered GPS-based acceleration profiles was examined using the vehicle speed sensor (VSS) included in the GT Trip Data Collector (GT-TDC). The VSS measures the number of revolutions of the transmission using magnetic sensors and updates the number every ¼ seconds. Using this number, vehicle speeds can be estimated by multiplying appropriate factors, for which vehicle manufacturers use standard revolution counts such as 2,000, 4,000, or 8,000 wheel-tick/mile, depending on sensor spacing (Ogle 2005). However, the factors may not reflect the true activity of a vehicle since tire sizes and pressures can vary depending on vehicles and driving conditions. For example, a vehicle may not be equipped with standard tires for the vehicle, and surrounding temperatures can change the pressure of tires. In spite of these uncertainties imbedded in VSS speeds, acceleration profiles obtained from VSS were assumed to be reliable, and they were compared with the speed profiles from GPS devices.

Accuracy of Acceleration from Vehicle Speed Sensor

The accuracy of speed and acceleration from the VSS can be identified based on standard revolution counts and data frequency. The characteristics of the VSS data employed in this study dictated that the standard revolution count is generally 8,000

wheel-tick/mile and that the data frequency is 4 Hz (i.e., wheel-tick count is updated every quarter second). These 4 Hz data were aggregated on a second-by-second basis to match with the GPS data stream, resulting in a data frequency of 1 Hz. Thus, the travel distance for one wheel-tick during one second becomes 1/8,000 miles. Then, the speed for one wheel-tick over a second can be calculated as follows:

$$\text{Speed/wheel-tick} = \frac{1/8000\ mile}{1/3600\ hour} = 0.45 \text{ mph.}$$

Technically, the wheel-tick number is counted only when the transmission shaft finishes revolving, meaning that incomplete revolutions during a specific time interval are not reflected in the number of wheel-ticks. This situation incurs an error for the measured number of wheel-ticks, and the true value lies between the measured number and the measured number+1. In particular, when the aggregation process is considered, the error occurs only at the boundaries of the aggregation time interval. This concept was represented in Figure 22, in which 4Hz speed data are aggregated into 1Hz data. As suggested in the figure, the range of true value (W) becomes $w \le W \le w + 2$, in which w is the aggregated wheel-tick number on a second-by-second basis. As a result, the accuracy of an acceleration rate obtained from speed differences becomes ±2 wheel-tick numbers as follows:

$$w_1 \le W_1 \le w_1 + 2,$$

$$w_2 \le W_2 \le w_2 + 2,$$

$$\text{and } w_2 - w_1 - 2 \le W_2 - W_1 \le w_2 - w_1 + 2,$$

in which the subscripts 1 and 2 indicate the time when the values are measured. The ±2 wheel-tick numbers can be converted into ±0.90 mph by applying the rate of

0.45mph/wheel-tick. Thus, based on the conditions stated earlier, the accuracy of VSS-based acceleration is equivalent to ±0.90 mph/s (the upper and lower bounds of the errors). A notable aspect of this accuracy is that it is directly affected by the standard revolution count and the aggregation time interval. In other words, as the standard revolution count becomes lower and/or the aggregation time interval shorter, the measurement error becomes greater. Again, the specific number ±0.90 mph/s is founded on a mathematical ground, and thus, it should be carefully interpreted and applied.

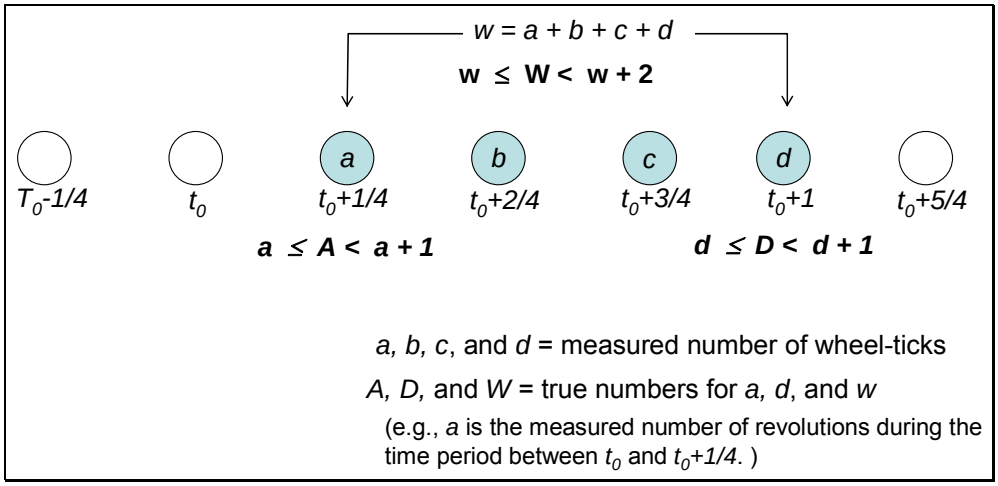

Figure 22: Illustration of Potential Errors from Vehicle Speed Sensor

Speed Profile Comparisons

Speed profiles from GPS devices and VSS were compared using the data obtained from six VSS-equipped instrumented vehicles which traveled on the study corridor GA400 during March 2004. Not all the vehicles participated in the Commute Atlanta project were equipped with VSS, and only the six VSS-equipped vehicles were observed to travel the study corridor during the time period. The comparisons made in this study

focused on only freeway trips, which have more chances to contain reliable GPS data because obstructed satellite signals and the cold/warm starts of GPS receivers are less likely to occur, as mentioned before.

As an example, Figure 23 illustrates three speed profiles—raw GPS, Kalman filtered GPS, and VSS speed profiles—from the same vehicle over a 60-second period. As can be expected, the three speed profiles follow the same trend. In fact, the average speeds of the three speed profiles are 70.8, 70.9, and 70.8 mph, indicating little difference in average speeds. The figure indicates that some peaks found in the raw GPS speed profile were smoothed after the Kalman filtering. For more objective comparisons, two metrics—the mean of the absolute errors (MAE) and the variance of the errors (VE)—were calculated for the speed profiles in Figure 23 in the following ways:

$$MAE = \frac{\sum_{i}^{n} abs(Y_i - \hat{Y}_i)}{n}$$

$$VE = Var(Y_i - \hat{Y}_i),$$

where n, Y_i, and $\hat{Y}_i$ represent sample size, true value, and estimated value, respectively. By taking the VSS-based speeds as true values, MAE and VE for the raw GPS profile were computed, resulting in 0.66 for MAE and 0.34 for VE. Meanwhile, for the filtered GPS profile, MAE and VE are 0.65 and 0.32, respectively, indicating the speeds from

the filtered GPS data are slightly closer to those of the VSS data with less variance.

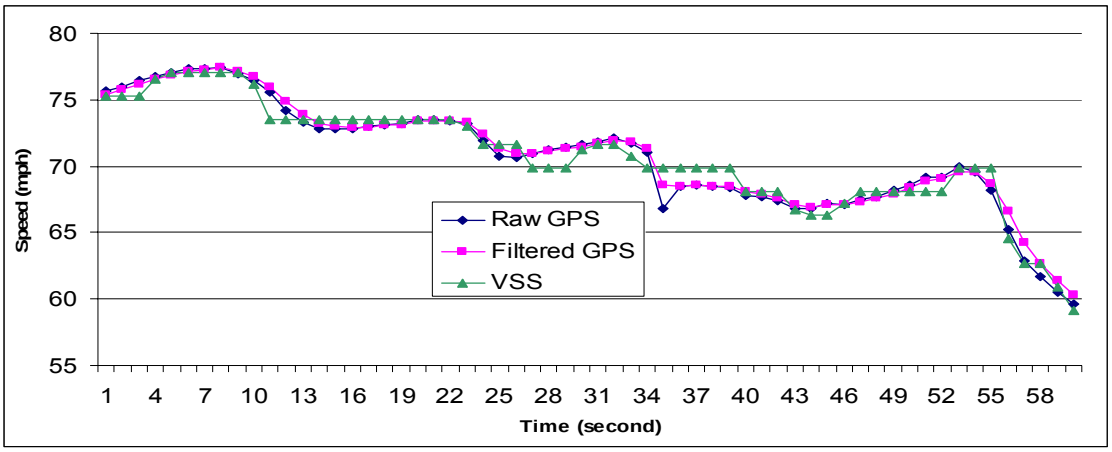

Figure 23: Comparison of Speed Profiles (Raw GPS, Kalman Filtered GPS, and VSS)

In addition, MAE and VE were computed for a larger data set composed of 13,865 second-by-second speeds obtained from the trips over GA400 study corridor. As a result, the raw GPS data exhibited 1.28 and 2.99 for MAE and VE, respectively, while those are 1.29 and 3.03 for filtered GPS data. Although the raw GPS second-by-second speeds are slightly closer to VSS second-by-second speed with less variance, the result indicated little difference between the raw and filtered GPS speeds.

Acceleration Profile Comparisons

Using the same speed profile data in Figure 23, acceleration profiles were obtained based on the backward difference approach (subtraction of the previous speed from the current speed). The comparison of the acceleration profiles indicates that GPS-based accelerations are smoother than VSS-based accelerations. Note that the VSS-based acceleration rates change at a constant rate such as 0.45 mph/s because of its data characteristics, as previously described. This feature might contribute to the bumpy

speed changes in the VSS-based acceleration profile. By taking the VSS-based accelerations as true values, MAE and VE for the raw GPS profiles were computed, resulting in 0.61 for MAE and 0.53 for VE. Meanwhile, for the filtered GPS profiles, MAE and VE are 0.58 and 0.43, respectively, indicating the values of acceleration from the filtered GPS data reflect the VSS-acceleration profile more closely with less variance.

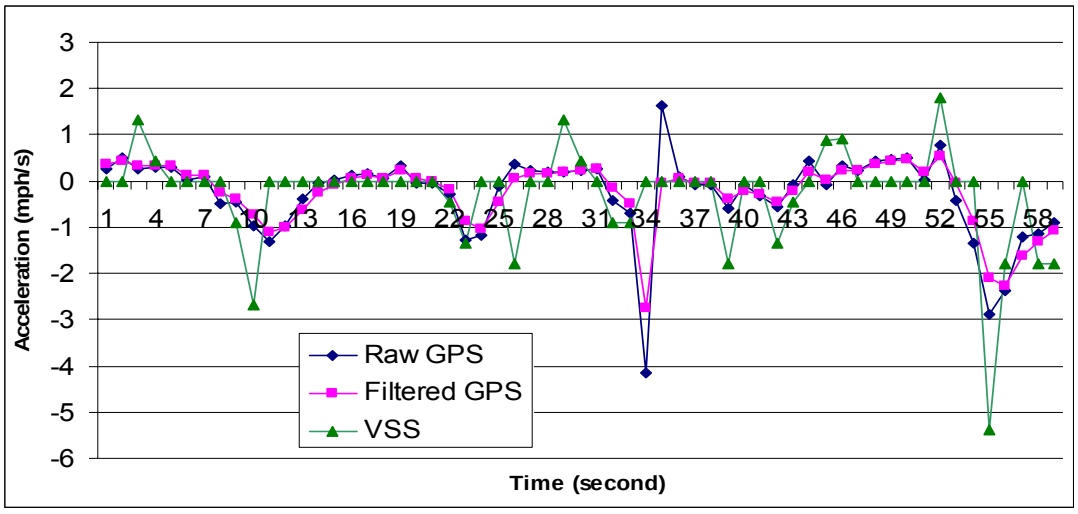

Figure 24: Comparison of Acceleration Profiles (Raw GPS, Kalman Filtered GPS, and VSS)

In addition, MAE and VE were computed for a larger data set composed of 12,834 acceleration values obtained from the trips over GA400 study corridor. The results coincided with the example case above. Raw GPS data produced 0.92 and 2.02 for MAE and VE, respectively, while the values are 0.83 and 1.77 for the filtered GPS data. Again, the filtering of GPS data showed smaller errors with less variance, supporting the use of GPS speed data smoothing.

Average Speed Comparisons

The average speeds for segmented trips were compared for the three different speed profiles. In this effort, speed profiles were obtained over quarter-mile segments, consistent with the length of the roadway segments (average segment length = 0.28 miles) used in this study. Thus, the trip length for each speed profile used in this comparison is 0.25 miles. In total, 1,031 segmented trips, composed of 13,865 second-by-second speeds (equivalent to a driving distance of 258 miles), were obtained.

Based on the trips, scatter plots showing the relationships between the average speeds from the three different speed profiles were obtained, as shown in Figure 25. The figure exhibits little difference between them, implying that the filtering process has little effect on speed profiles. This result may be reasonable since the GPS second-by-second speeds from freeway trips are generally reliable, and thus, the filtering process tends to be implemented at a minimum level.

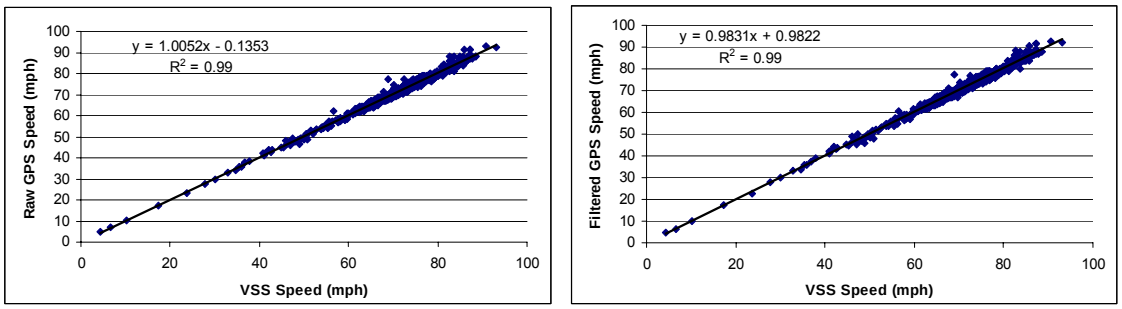

Figure 25: Comparisons of Average Speeds from Raw GPS, Filtered GPS, and VSS (n=1,031)

Acceleration Noise Comparisons

Using the 1,031 segmented trips, a comparison of acceleration noise from raw and filtered GPS data was performed, as shown in Figure 26. The figure indicates that

acceleration noise from the raw GPS data is greater than that from the filtered GPS data. In addition, the figure implies that the values of acceleration noise from the filtered data are reduced by approximately 25%, as indicated by the estimated slope of the regression line. In addition, the figure indicates that the variance of the differences of acceleration noise values from the two different data sets increases as acceleration noise increases.

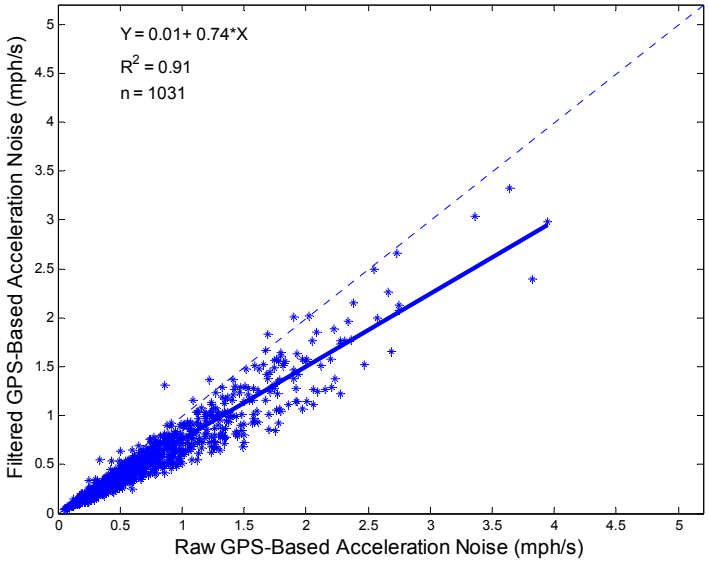

Figure 26: Comparison of Acceleration Noise from Raw and Filtered GPS Data

In addition, acceleration noise was computed using the VSS-based data. One notable phenomenon in the computation results is zero acceleration noise, not observed in the calculations of GPS-based acceleration noise. The VSS-based zero acceleration noise was found for 108 trips (10.5% of the sampled trips), and their corresponding GPS-based acceleration noise was always greater than zero. The distributions of the GPS-based acceleration noise values for the trips with the VSS-based zero acceleration noise were obtained, as shown in Figure 27. The figures indicate that the raw GPS-based acceleration noise has a larger variance, as suggested by the long tail of the histogram and that the variance was mitigated after the filtering process. This

phenomenon can also be illustrated by cumulative distributions, which suggest that 90% of the trips with VSS-based zero acceleration noise have the values of acceleration noise less than 0.8 for the filtered GPS data, however the 90% acceleration noise value becomes 1.3 for the raw GPS data.

A formal test can be simply carried out using the VSS-based acceleration accuracy, ±0.9 mph/s, implying that the true acceleration noise values for the zero VSS-based acceleration noise lie between 0 and 0.9 mph/s. The zero lower bound can be observed when speeds do not change at all. Meanwhile, the upper bound (0.9 mph/s) can be observed when two distinct extreme acceleration rates, +0.9 mph/s and -0.9mph/s are recorded the same number of times. For this situation, acceleration noise, calculated from the population standard deviation, becomes exactly 0.9 mph/s. When the number of acceleration observations is an odd number, acceleration noise becomes slightly smaller than 0.9, however, it is still very close to 0.9 mph/s. For example, given eleven acceleration observations, the upper bound becomes 0.896 mph/s. The application of the range with 0 and 0.9 mph/s for lower and upper bounds resulted that 20% of the trips with zero VSS-based acceleration noise have implausible acceleration noise values for the raw GPS data. However, the implausible trip rate was reduced to 6% for the filtered GPS data, which can be illustrated using the cumulative distribution function in Figure 27. As a result, the filtering process contributed to reducing the occurrences of unreliable acceleration noise values.

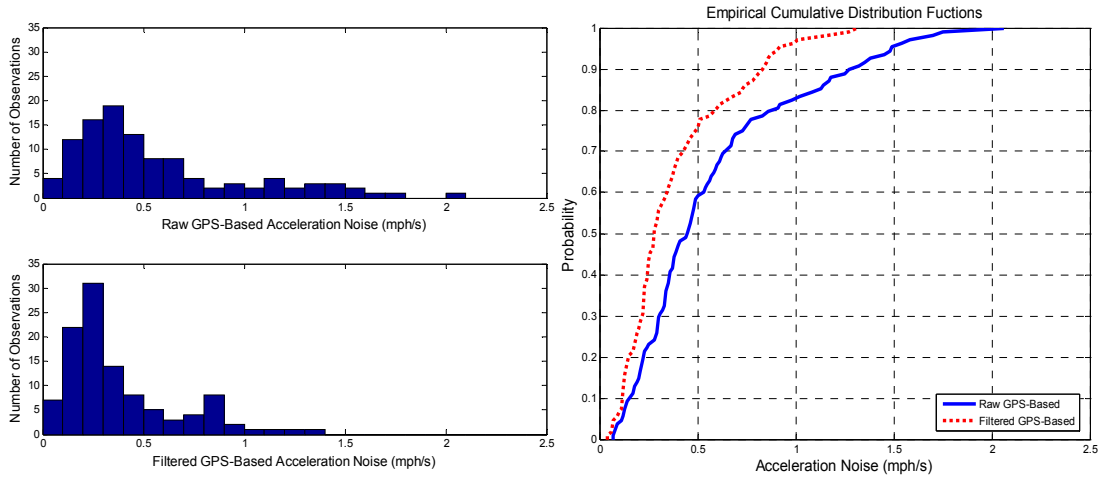

Figure 27: Distributions of GPS-Based Acceleration Noise Values for the Trips with Zero Acceleration Noise

Summary

The comparison results indicate that the Kalman-filtered GPS speed profiles have more preferable characteristics than the raw GPS speed profiles since the acceleration values from the filtered data are closer to the VSS-based ones assumed to be more accurate with less error variance. In addition, the filtering process seemingly prevents the occurrence of unreliable acceleration noise values, as illustrated in the analysis of the VSS-based zero acceleration noise. However, note that the filtering process has no capability to discern the abrupt speed changes due to unreliable GPS signals from those due to real situations. In other words, the filtering process may introduce a drawback which incurs a lost of information associated with a higher degree of speed changes, as the process eliminates even the real high acceleration rates. Meanwhile, second-by-second speeds are not significantly affected by the filtering process, at least for the data set obtained from the freeway trips.

Map-Matching Process

The selection of instrumented vehicle trips which passed through the roadway segments of interest requires a map-matching process. For this process, this study applied the point-in-polygon approach, in which all the GPS data points within a specified polygon were captured and processed for further analyses. This approach was relatively easy to apply compared to other map-matching algorithms such as route-based approaches since its decision-making process is simple. However, the point-in-polygon approach has a disadvantage that it is not practical for the areas where roadway networks are dense. In these areas, the creation of a polygon which does not overlap with other polygons is difficult since the roadway network is likely to be too close. However, this issue was not critical for this study since the study area is a freeway corridor which generally has a sufficient distance from other roadways. The captured freeway GPS data points based on the point-in-polygon approach are illustrated in Figure 28, which shows only southbound vehicle movements. The differentiation of the moving direction was possible by examining the coordinate changes. Alternatively, the moving direction can be identified through the values of heading provided by GPS receivers.

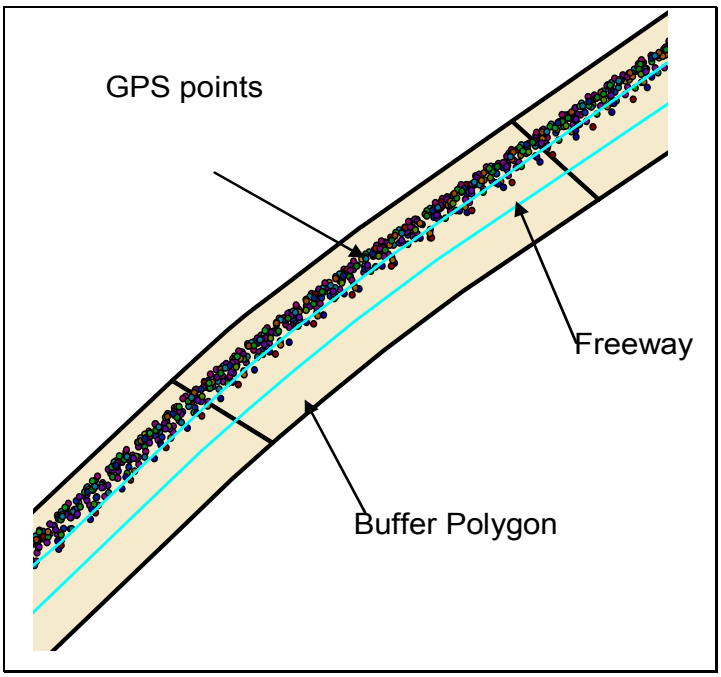

Figure 28: Illustration of Selected GPS Data Points within Freeway Polygons

Based on the captured GPS data from the point-in-polygon approach, additional data processing steps were implemented to obtain average speed and acceleration noise values. The values were calculated for each segment and incorporated in a database with trip time information, the degree of data reliability (represented by the bad data ratio), weather information and so on. Trip-by-trip speed profiles and vehicle trajectories are illustrated in Figure 29, for which trips made over a GA400 NB segment during March 2004 were utilized. The figure indicates that the segment have experienced various traffic conditions, from congested conditions to free-flow conditions, during the data collection time period.

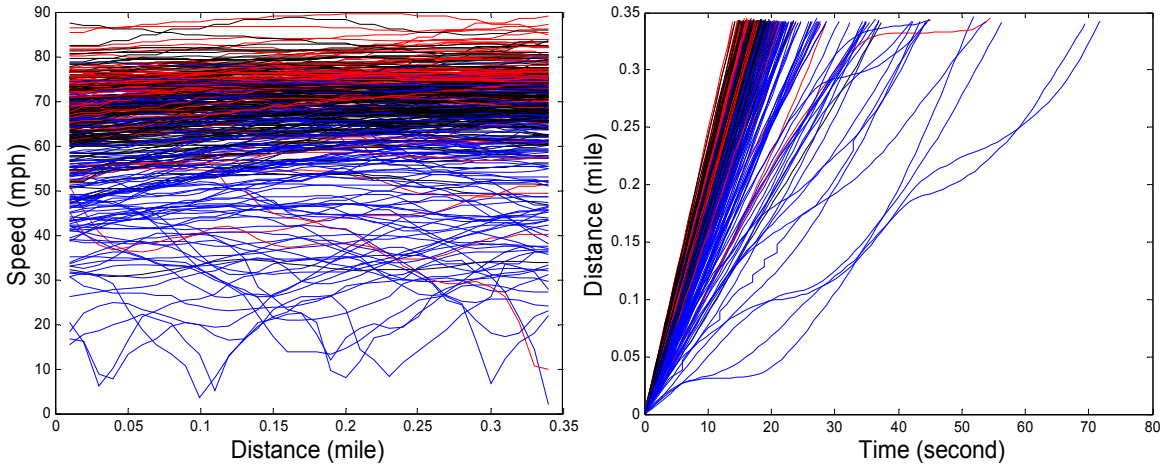

Figure 29: Speed Profiles from Instrumented Vehicles over a Segment (NB12, March 2004)

Combination of GPS and TMC Data

Method

The GPS trip database was combined with TMC data to acquire the information about the macro-level traffic conditions that instrumented vehicles experienced. The data combining process was implemented spatially and temporally. For the spatial combination, appropriate VDS cameras for each roadway segment were identified using the camera coverage map (in GIS format) provided by the GDOT. When a roadway segment straddles two neighboring VDS cameras, combined traffic data from the two cameras were utilized for the roadway segment. For the temporal combination, the midpoint of instrumented vehicle trips over a segment was designated as the reference time, and the reference time was compared with the data collection time period of the TMC data aggregated in one-minute intervals. If the reference time is contained in the traffic data collection time period, the two data sources were considered to be matched.

Combined Data Size

The data combining process was implemented for the instrumented vehicle trips collected over the time period between October 2003 and August 2004 (eleven months), during which 264,973 segmented trips (SB - 139,099 trips over 47 segments; NB - 125,874 trips over 42 segments) were collected. The total travel distance for the whole initial trips is 73,995 miles, which is equivalent to 1,374 hours of driving. Of these trips, 205,505 trips (77.6% of total initial trips) could be matched the TMC data. The remaining trips could not be matched due to temporary TMC data outages. In an extreme case, for northbound Segment 23, TMC traffic data were not available for seven months. The instrumented vehicle trip data sizes before and after the matching are illustrated in Figure 30, in which a cell contains the information for both a month and a segment. The figure indicates that the number of trips is relatively smaller for the northern part of the study corridor.

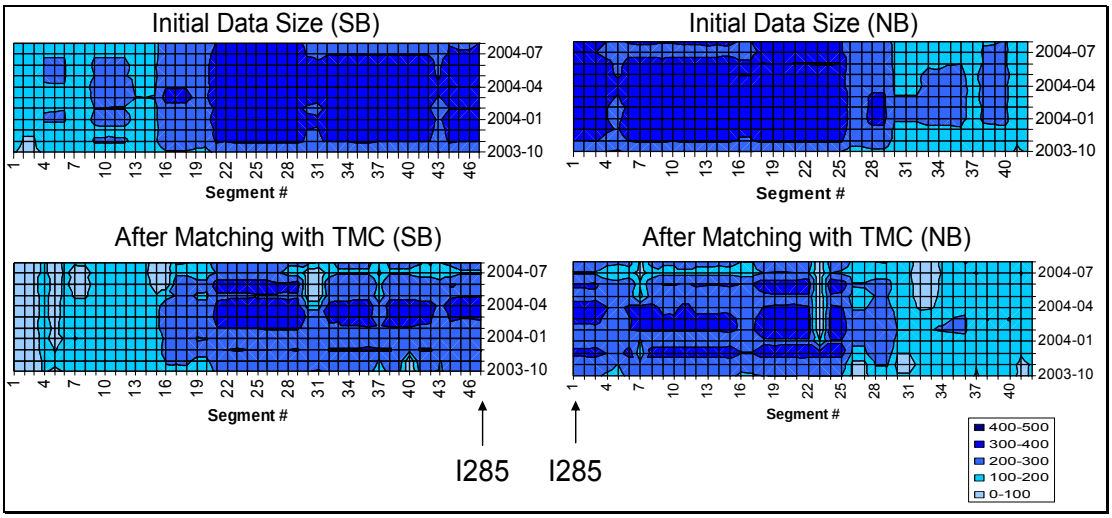

Figure 30: Instrumented Vehicle Trip Data Size Before and After the Matching with TMC Data

Comparison of Instrumented Vehicle and TMC Data

After the process for data joining was completed, the TMC data and the matched instrumented vehicle data were compared using a subset of the combined data. The subset data were extracted from the instrumented vehicle trips traveled northbound during March 2004. For the initially selected 12,525 segmented trips (equivalently, 3,619 vehicle-miles), GPS data quality in terms of the number of satellites and PDOP was examined. In the examination, bad data points were identified if the number of satellites was less than four, or PDOP was outside a range of one to eight (Ogle 2005). Based on the bad data points, segmented trips with a bad data rate (number of bad data points/total number of data points) of 0.5 or greater were discarded from the data set because such trip data were likely to be collected from the vehicles with a bad GPS unit and antenna. Since the original speed data were filtered using Kalman filters, and thus, major data errors had been fixed, this approach should be reasonable (Jun et al. 2006). Consequently, 10,465 trips (84% of initial data size; 3,037 vehicle-miles and equivalently 60.7 vehicle-hours) from 112 vehicles were used in this comparison.

Figure 31 illustrates the comparison results, indicating that speeds from the two data sources match with the R^2 value of 0.75 (for a linear equation, *instrumented vehicle speed = 0.81×TMC speed + 2.92*) and that instrumented vehicle speed decreases as density increases. This situation indicates that the data combining process was properly implemented although some outliers and scatters are found. Note that the variation found in Figure 31 is likely to be larger than those in other research efforts in which drivers were trained or directed to follow the general traffic stream. In addition, the data shown in the figure were obtained from various locations (41 segments), and thus,

they may contain wider variability due to localized traffic conditions. Note that the variability may be more pronounced to some degree due to traffic monitoring sensors. A research effort showed that the quality of TMC data depends on the measurement locations, as some traffic monitoring sensors seem to require site-oriented calibrations (Lee et al. 2006).

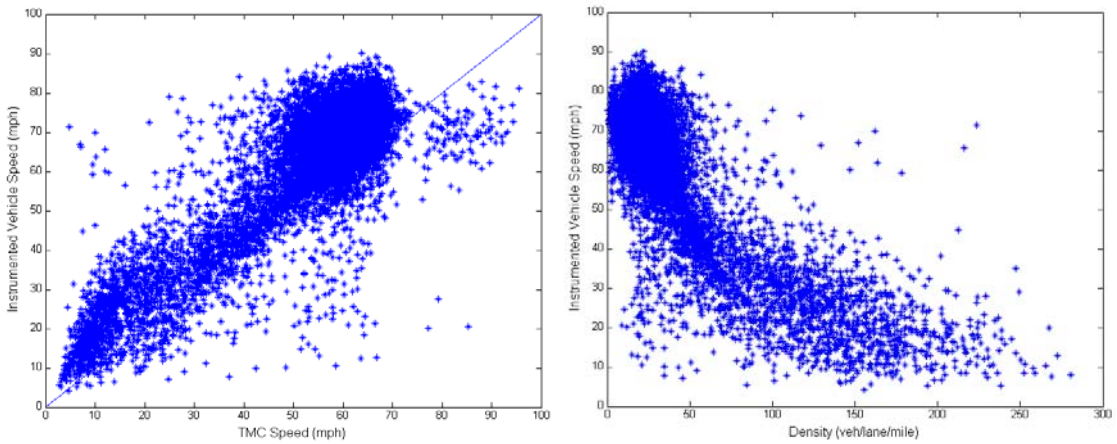

Figure 31: Comparison of Instrumented Vehicle Speeds and Macroscopic Traffic Parameters (N = 10,465)

Chapter 5

Sensitivity of Acceleration Noise

Sensitivity to Computation Approaches

Background

Acceleration noise, originally proposed as a potential measure to characterize the driver-car-road complex under various conditions, is defined as the root-mean-square deviation of the acceleration (Herman et al. 1959). In practice, acceleration noise has been computed from the population standard deviation (the original definition of acceleration noise) or the root-mean-square of acceleration. These approaches can be simply represented using the following equations, in which acceleration noise is denoted by σ, and T is the total time spent moving. In addition, $a(t)$ and $\bar{a}$ represent the acceleration of a car at time t and average acceleration for the trip, respectively.

$$\sigma_{SD}{}^2 = \frac{1}{T}\sum_{1}^{T}(a(t)-\bar{a})^2 \text{ : Population standard deviation of acceleration}$$

$$\sigma_{RMS}{}^2 = \frac{1}{T}\sum_{1}^{T}a(t)^2 \text{ : Root-mean-square of acceleration}$$

As suggested by the equations, the two approaches can produce the same results when $\bar{a}$ is zero, which can be observed when the initial and final speeds of the trip are the same. Based on this fact, researchers have used either definition with little regard for the potential differences induced by the different approaches, simply assuming that the

amount of $\bar{a}$ should be small and can be neglected in most cases (Jones and Potts 1962).

Note that the assumption that acceleration noise computed from the two approaches should be approximately the same is likely to be violated on a real-world road segment, in particular, when gradual speed changes occur at a constant rate of acceleration. In this case, the standard deviation of acceleration is zero while the root-mean-square of acceleration is equal to the constant acceleration rate. Not realizing this situation, researchers may fail to adequately compare various research results in establishing acceleration noise-based criteria for evaluating traffic flow quality.

Unfortunately, this issue has seldom been addressed in the research even though researchers assert the value of acceleration noise as a potential traffic parameter with the advancement of in-vehicle data collection technology such as GPS. This study analyzed the differences between the results from the two different approaches—root-mean-square (RMS)-based and population standard deviation (SD)-based approaches—by comparing their resulting distribution characteristics. The analysis also considers the effects of traffic conditions using traffic density data obtained from traffic surveillance cameras installed along the study corridor. The consideration of traffic conditions is meaningful becasue acceleration noise has been related to traffic congestion, and thus, such consideration can provide insights for researchers to properly interpret research outcomes obtained from various sources.

Data

For this sensitivity analysis, northbound instrumented vehicle trips obtained during March 2004 were utilized. Unreliable trip data, in terms of the number of satellites and PDOP, were screened out from the data set (refer to Chapter 4), and 10,465 trips were finally selected for this analysis. The segment-by-segment distributions of numbers of trips and vehicles are shown in Figure 32.

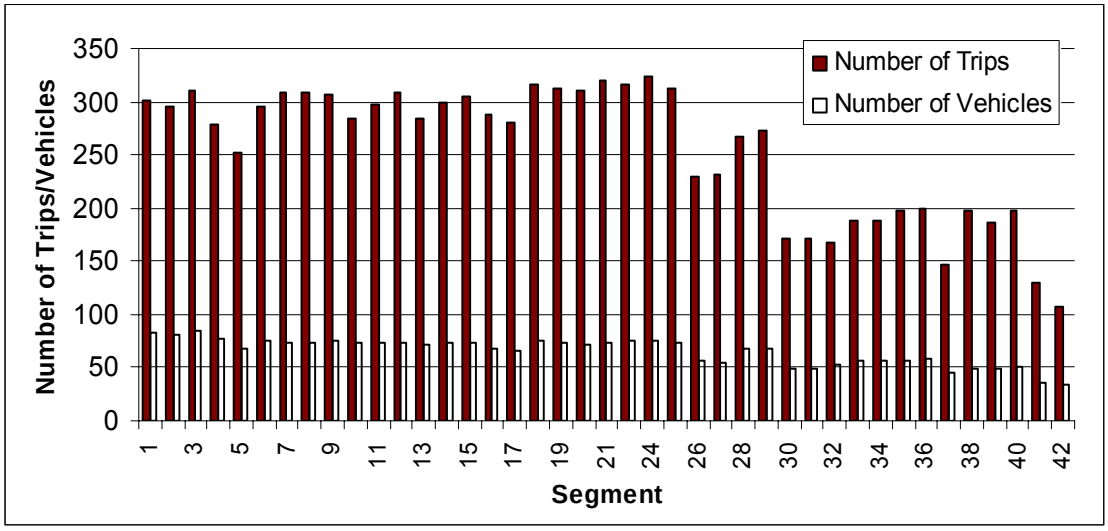

Figure 32: Segment-by-Segment Distributions of Numbers of Trips and Vehicles (N = 10,465)

Analytical Methods

As mentioned before, this study investigates the differences between the results from the RMS- and SD-based acceleration noise computation approaches in terms of their distribution characteristics. The differences between distributions were investigated using two nonparametric statistical techniques, the Gaussian kernel density estimation and the Kolmogorov-Smirnov (KS) two-sample test. These nonparametric techniques have an advantage in that researchers do not need to impose assumptions about the

distributions inherent in the data set. Brief descriptions of these statistical techniques follow.

Gaussian Kernel Density Estimation: A convenient way to examine the form of distributions is to use histograms. However, irregular and bumpy patterns in the histograms may introduce difficulties in judging the shape of the distributions. The difficulties can be addressed by applying the kernel density estimation technique (Hastie et al. 2001). Let's suppose that N samples $x_1, \ldots, x_N$, are drawn from a probability density $f_x(x)$, and f_x is to be estimated at point x_0. Then, density estimate $\hat{f}_X$ can be obtained using the following equation:

$$\hat{f}_X(x_0) = \frac{1}{N(2\lambda^2\pi)^{\frac{p}{2}}} \sum_{i=1}^{N} e^{-\frac{1}{2}(\|x_i - x_0\|/\lambda)^2},$$

where λ is the bandwidth, and p is the dimension of the data. In the equation above, the kernel function takes the form of the Gaussian function which is the most popularly used kernel function. In the kernel density estimation, the selection of a bandwidth is critical since too narrow a bandwidth can result in spurious details while too wide a bandwidth can be less sensitive to the curvature of the true density. An optimal bandwidth was suggested and successfully applied to real-world data as follows (Kharoufeh and Goulias 2002):

$$\lambda = 0.9 \cdot min(s, \text{interquartile range}/1.34) \cdot N^{-1/5},$$

where *s* is the sample standard deviation. This study used this optimal bandwidth when estimating the probability density functions (pdf) of acceleration noise.

Kolmogorov-Smirnov (KS) Two-Sample Test: The Kolmogorov-Smirnov (KS) two-sample test performs the hypothesis test whether two independent samples may have been drawn from the same population (Conover 1980). The two-tailed test statistic for the KS test is given by

$$T = Max_{x \in Q} \left| S_1(x) - S_2(x) \right|,$$

where $S_1(x)$ and $S_2(x)$ are the empirical cumulative distribution functions for the two independent samples, and Q is the set of points at which the distribution functions are evaluated. T is the maximum difference over all x values, and thus, the larger T indicates that the two samples compared are less likely to be drawn from the same population. For larger sample sizes m, n, the critical values for two-sided tests can be approximately computed by $1.36\sqrt{\frac{m+n}{mn}}$ at a significance level of 0.05. Alternatively, p-values can be used to draw conclusions for the test and approximated in a recursive manner for larger samples (Gibbons and Chakraborti 2003).

Preliminary Analysis

A preliminary analysis was conducted by comparing the RMS- and SD-based acceleration noise without considering the effects of traffic conditions. Figure 33 illustrates a scatter plot and an empirical cumulative distribution function for the acceleration noise differences, which indicate that the RMS-based acceleration noise is

always equal to or larger than the SD-based acceleration noise. This phenomenon is intuitively reasonable since the RMS-based acceleration noise is the degree of deviation from zero while in the SD-based acceleration noise, the deviation is measured from the mean acceleration, and thus, the RMS-based acceleration noise is greater unless the mean acceleration is zero. In fact, the SD-based acceleration noise (σ_{SD}) can be mathematically represented using the RMS-based acceleration noise (σ_{RMS}), as follows:

$$\sigma_{SD}{}^2 = \sigma_{RMS}{}^2 - \bar{a}^2 .$$

Thus, the SD-based acceleration noise cannot be larger than the RMS-based acceleration noise.

The cumulative distribution function in Figure 33 indicates that approximately 90% of segmented trips have differences less than 0.25 mph/s (0.37 ft/s/s) and that approximately 30% of the total segmented trips under study have little difference between the two approaches. In other words, the assumption of zero mean acceleration for a trip cannot be applied to about 70% of total segmented trips.

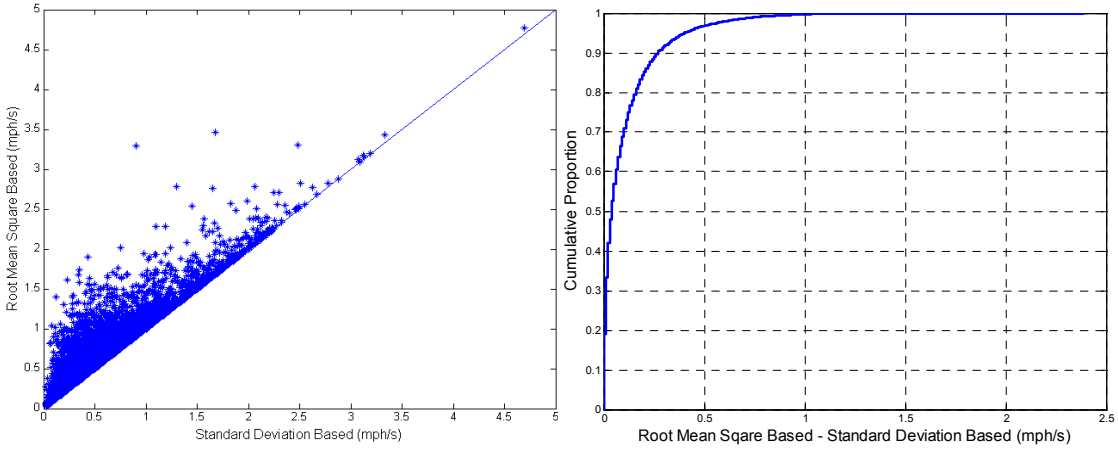

Figure 33: Comparison of Root-Mean-Square-Based and Standard Deviation-Based Acceleration Noise (N=10,465)

The scatter plot in Figure 33 also indicates that some trips have considerably different acceleration noise, depending on the approaches adopted. As a purpose of examining in what situations such big differences occur, the speed profiles of top five trips with the greatest differences were captured and illustrated in Figure 34. These five trips were obtained from five different vehicles and segments, and the differences of acceleration noise are 2.39, 1.78, 1.48, 1.47, and 1.39 mph/s, respectively. As expected, the speeds of the five trips generally continue increasing or decreasing, and the differences between the initial and final speeds are subject to be significant, resulting in a non-negligible average acceleration. Indeed, the average acceleration rates of the five trips are -3.16, -3.02, -2.45, +1.85, and -1.71 mph/s, respectively.

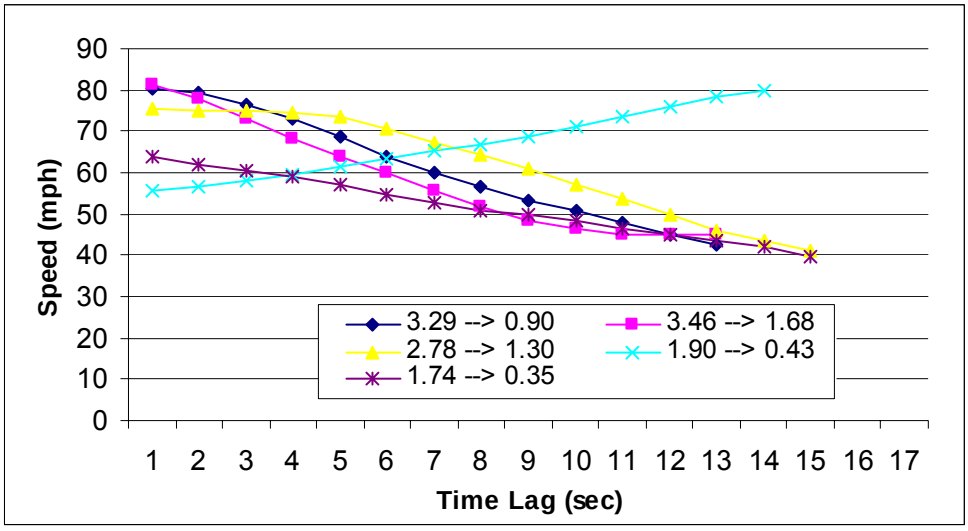

Note: In the legend, "3.29 → 0.90" means the RMS-based value is 3.29 while the SD-based value is 0.90.

Figure 34: Speed Profiles of Trips with High Difference (Top 5 Cases out of 10,465 Cases)

Distribution Comparison Results

The distributions of acceleration noise were compared and tested for the entire data set whether they are statistically different or not. In addition, 95% confidence intervals

around the mean were computed. Figure 35 illustrates the distributions and descriptive statistics, including confidence intervals. The pdf of RMS-based acceleration noise shifts relatively toward right and has a lower peak, implying a higher average value and a higher degree of dispersion than those of SD-based acceleration noise. In fact, the average RMS-based acceleration noise is larger by 0.1 mph/s (0.15 ft/s/s), as is the standard deviation. In addition, the KS test result (p-value = 0.000) and confidence intervals indicated that the two distributions are significantly different.

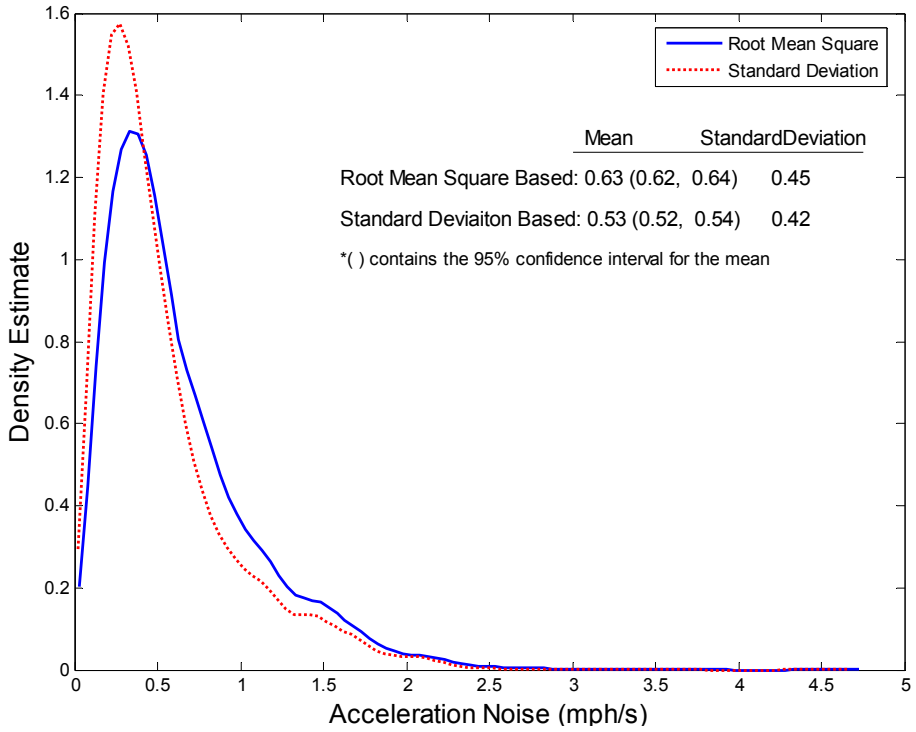

Figure 35: Comparison of Estimated pdfs for Root-Mean-Square-Based and Standard Deviaiton-Based Acceleration Noise

Distribution Comparisons by Level of Service (LOS)

The comparison of distributions, considering traffic conditions, was conducted by segmenting the data set into six groups (A to F) based on the density-based freeway LOS suggested in the Highway Capacity Manual (HCM) 2000. The estimated pdfs are

illustrated in Figure 36, which indicates that the distributions of the RMS-based acceleration noise shift relatively toward right (i.e., higher average values) and have lower peaks (i.e., a smaller degree of dispersion) for all LOS ranges except LOS F. Under LOS F range, the distribution of the SD-based acceleration noise has a higher peak than that of the RMS-based acceleration noise. In addition, the figure indicates that the difference between the two distributions is relatively prominent under LOS E, which is supported by the largest difference in average acceleration noise values under this range. The differences of average values are 0.08, 0.09, 0.09, 0.10, 0.15, and 0.10 mph/s for LOS A-to-F, respectively. On average, the difference becomes more significant as traffic increases, but the difference downturns when traffic conditions reach LOS F. Note that the difference of 0.1 mph/s (0.15 ft/s/s) can be significant when acceleration noise is used as a measure of traffic conditions. For example, the acceleration noise of 0.35 mph/s can be interpreted as the traffic condition of LOS A when the criteria adopted are established based on the RMS-based approach. However, the same level of acceleration noise (0.35 mph/s) is more likely to reflect LOS B condition when SD-based criteria are used since the average SD-based acceleration noise under LOS A is 0.28 (Figure 36). This fact implies that the use of acceleration noise without considering the computation approach may lead to misinterpretation of the results.

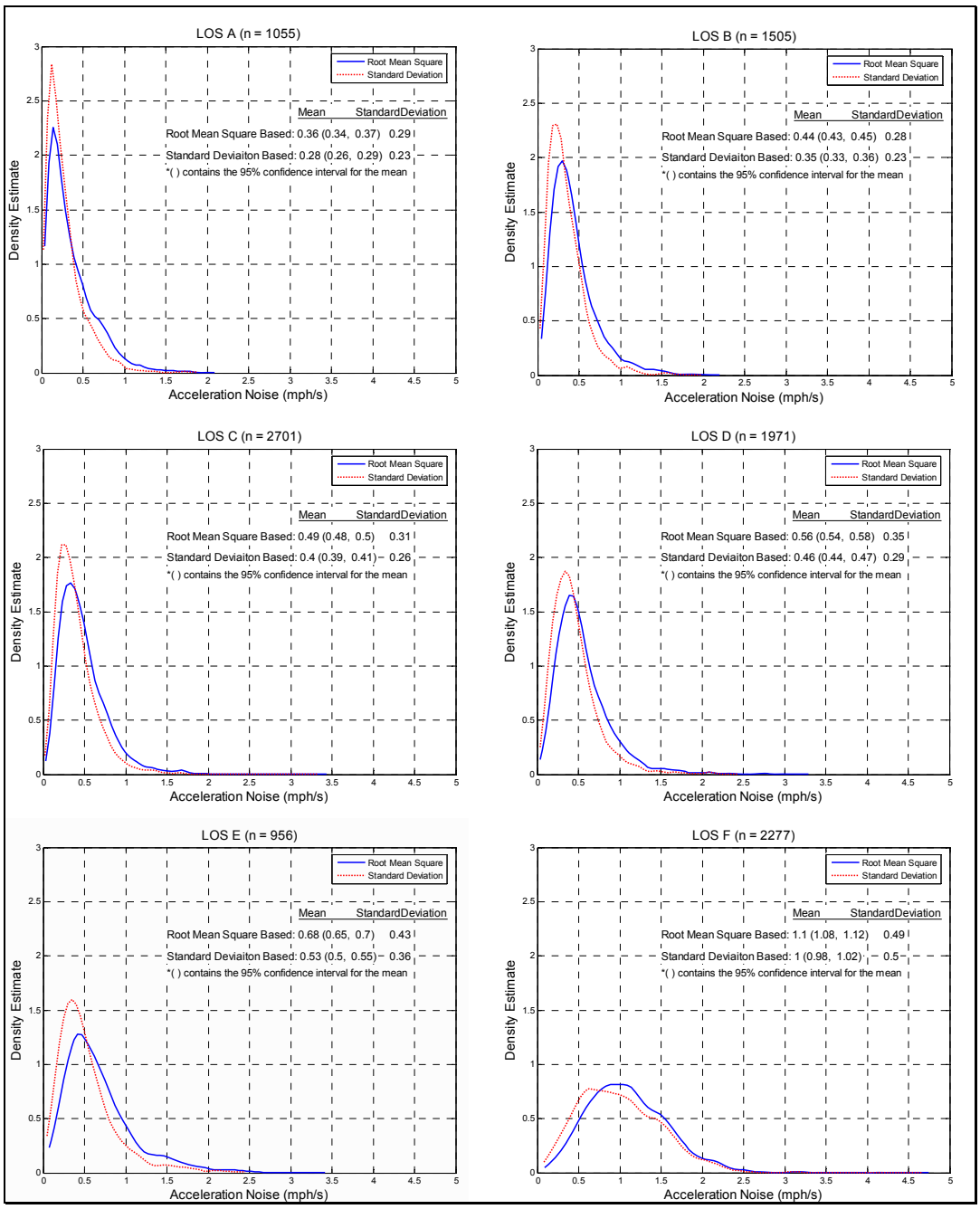

Figure 36: Comparisons of Estimated pdfs for Root-Mean-Square-Based and Standard Deviaiton-Based Acceleration Noise

The KS test results by LOS ranges are summarized in Table 2, which indicates that the distributions from the two approaches are significantly different for all LOS ranges as suggested by small *p*-values. The KS statistics (*T*) in Table 2 also indicate

that LOS E has the largest difference while LOS A and F have relatively smaller differences, which is consistent with the findings from the visual inspection of estimated pdfs. Thus, the difference between results from the two approaches is seemingly more significant under LOS E conditions, suggesting that a more careful interpretation of acceleration noise should be taken under the range.

Table 2: KS Test Results for the Acceleration Noise Distributions from RMS- and SD-Based Approaches

LOS	N	KS Statistic (*T*)	*p*-value
A	1,055	0.120	0.0000
B	1,505	0.165	0.0000
C	2,701	0.146	0.0000
D	1,971	0.151	0.0000
E	956	0.181	0.0000
F	2,277	0.104	0.0000

Comparisons of Difference Distributions by LOS

The distributions of difference (subtraction of the SD-based acceleration noise from the RMS-based acceleration noise) for LOS A-to-F were estimated and compared to examine in what LOS ranges the difference is more significant. The results are shown in Figure 37, which indicates that LOS A has the smallest difference while LOS E has the largest difference compared to other distributions. In particular, the distribution under LOS E has a heavier tail and a lower peak compared to other distributions, implying higher degrees of variance and difference. This fact implies that the average acceleration of a vehicle under LOS E is less likely to be zero since the higher difference means the higher absolute value of average acceleration, as suggested by the relationship between the RMS-based and SD-based acceleration noise. The higher

absolute average acceleration reflects the situation in which vehicles tend to slow down or speed up: a phenomenon that can be observed under unstable traffic conditions like before- or after-breakdowns of traffic flow.

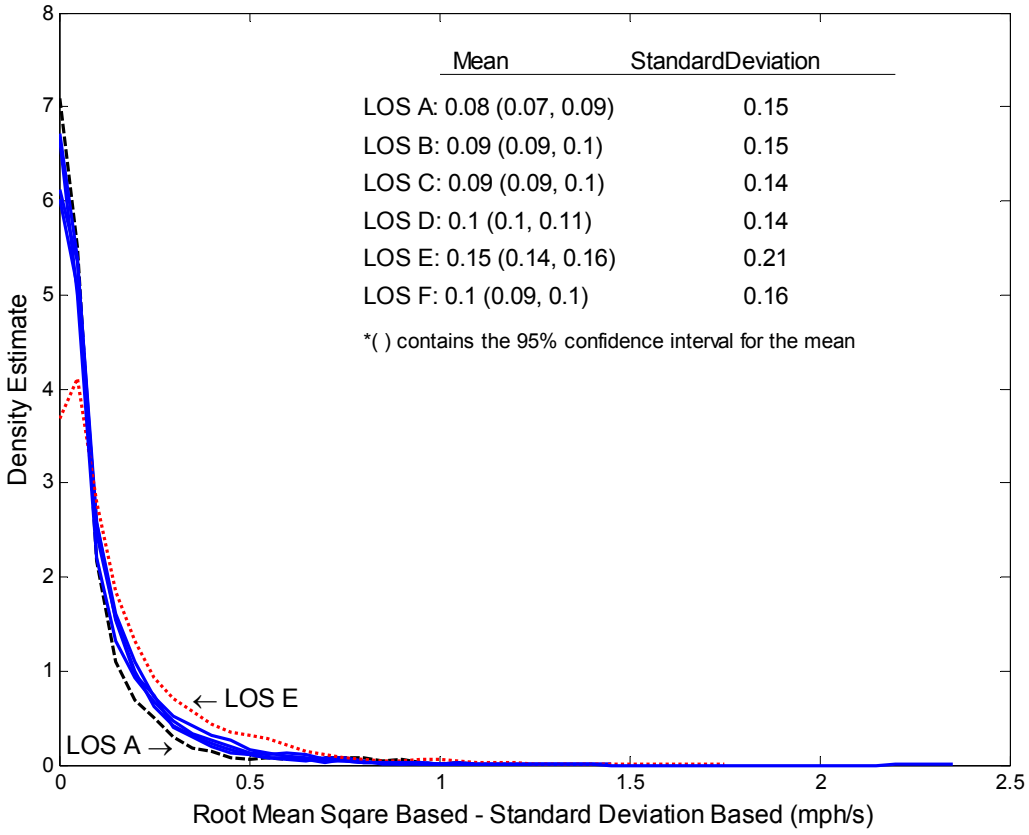

Figure 37: Estimated Difference Distributions by LOS

Similar patterns previously observed are found in the results of the pair-wise KS test, as shown in Table 3. The KS statistics in the table indicate that the difference distributions of LOS A and E are more significantly different from other distributions, as supported by the large KS statistics in the pairs involving LOS A or E. The test results also show that the difference distributions under LOS B and C are not significantly different and that those under LOS B and D are not significantly different

at the significance level of 0.01. Except for these pairs, all the pairs were found to have significantly different distributions, as suggested by low *p*-values.

Table 3: KS Statistics (*T*) and *p*-Values for the Pairwise Comparisons of Difference Distributions

LOS	A	B	C	D	E	F
A	-	0.129 (.000)	0.142 (.000)	0.178 (.000)	0.270 (.000)	0.110 (.000)
B		-	0.016 (.967)	0.050 (.028)	0.146 (.000)	0.064 (.000)
C			-	0.049 (.008)	0.139 (.000)	0.073 (.000)
D				-	0.104 (.000)	0.089 (.000)
E					-	0.173 (.000)
F						-

Note: *p*-values are inside parenthesis.

Summary

The sensitivity of acceleration noise computation approaches— RMS-based and SD-based acceleration noise—was analyzed in this section by examining the distribution characteristics of computed acceleration noise values. Findings from the analysis can be summarized as follows.

- The RMS-based acceleration noise is always equal to or larger than the SD-based acceleration noise, which is supported by the mathematical relationship between the two approaches. The average difference is 0.1 mph/s, which means that the RMS-based acceleration noise is 19% larger than the SD-based acceleration noise.

- Only 30% of the data employed in this study satisfy the assumption that average acceleration should be approximately zero. Thus, the assumption about zero average acceleration for a trip is not true for most cases (at least for the data set employed in this study).
- The greatest differences between the two approaches occur when vehicle speeds have a tendency to continue increasing or decreasing across a segment.
- The two approaches produce statistically different distributions of acceleration noise, and the RMS-based acceleration noise tends to have more variation. These findings are also generally true for the data sets segmented by the density-based LOS.
- The difference between the two approaches becomes significant as traffic congestion increases over the range of LOS A-to-E. In particular, LOS E shows the highest difference.

These findings indicate that the differences between the two approaches may be significant, and thus, some values of acceleration noise in one approach can be interpreted in a different way in the other approach in terms of traffic conditions that the value represents. Thus, when establishing acceleration noise-based criteria, researchers should note the computation approach that they adopt.

The SD-based approach seems to have an advantage in applying acceleration noise as a traffic parameter due to its smaller variance compared with the RMS-based approach. The smaller variance can make the measure more preferable in a statistical meaning. Furthermore, in a sense, the RMS-based approach can be regarded as a

special case of the SD-based approach with zero average acceleration. Based on this notion, hereafter, all the acceleration noise values were computed based on the population standard deviation approach.

On the other hand, the RMS-based approach has a desirable additive property (Drew et al. 1967). If the values of acceleration noise are known together with travel time over consecutive segments, the RMS-based acceleration noise can easily be combined over multiple segments. Thus, acceleration noise obtained over shorter segments can easily be extended to a longer section. In contrast, the SD-based acceleration noise requires additional information on average acceleration for the combining process, rendering the process less practical. Consequently, considering these properties, researchers should select an appropriate approach for their purposes. However, note that the findings reported in this study are limited to the case of 112 vehicles participated in the Commute Atlanta project and a 12-mile freeway corridor segmented into shorter sections within a range of 0.28 to 0.39 miles. Further research efforts would be desirable to confirm the findings in other areas and other driver groups considering more variables including roadway lengths and geometrics.

Sensitivity to Speed Data Sampling Rates

Background

Although this study uses second-by-second GPS data, the data type can be varied depending on data collection devices and study purposes. One such case is the data sampling rate, or number of samples per second denoted by hertz (Hz). The sampling rate can affect the magnitude of acceleration noise values because speed profiles with a

lower sampling rate, equivalently a longer sampling period, are more likely to be smoothed. This study attempted to measure the sensitivity of acceleration noise to the sampling rate, in particular to the sampling rates of 1Hz, 1/3Hz, and 1/5Hz as test cases.

Data

Instrumented Vehicle Trip Data: The data employed in this sensitivity analysis are the same as the previous analysis. However, among the selected 10,465 segmented trips over specific freeway segments, 386 segmented trips were additionally excluded since the number of second-by-second speed observations for the trips was less than ten. For these short time trips, 5-second sampling periods provide only a single data point, and thus, the computation of acceleration noise becomes meaningless. As a result, in total, 10,079 instrumented vehicle trips (segmented trips obtained over northbound GA400 study corridor) were employed in this analysis.

Generation of Lower Sampling Rate Data: Based on the original 1Hz data, acceleration profiles with a lower sampling rate were generated. In this effort, each data point in the new acceleration profiles was set to represent the average acceleration rate over the given sampling period. For example, given a sampling rate of 1/3Hz (i.e., a sampling period of 3 seconds), each data point in a new acceleration profile represents the average acceleration rate over the sampling time period of 3 seconds. This process can be formulated using the following equation:

$$b_i^s = \frac{1}{s}\sum_{m=1}^{s} a_{s(i-1)+m}\ ,\ \ i \le k,$$

b_i^s = ith acceleration rate for the acceleration profile with *1/s* sampling rate

a_i = ith acceleration rate for the second-by-second acceleration profile

s = sampling period (e.g., 3 or 5 seconds)

k = rounded value of n/s to the nearest integer less than or equal to n/s (n is initial data size).

This equation indicates that the initial acceleration rate a_i and the generated acceleration rate b_i is the same when $s = 1$. However, as s increases, the number of data points decreases since i is always less than or equal to k, which is inversely proportional to s. In other words, the longer sampling period means the smaller number of data points in the generated acceleration profile. Table 4 illustrates an example of the process for generating lower sampling rate data from an 1Hz acceleration profile with 10 observations. In the process, the number of data points decreases from 10 to 3, and then 2, as the sampling rate decreases from 1Hz to 1/3Hz, and then 1/5Hz.

Table 4: Data Generation Example (From 1Hz Data to 1/3 and 1/5 Hz data)

Time	1Hz	1/3Hz	1/5Hz
1	0.09		
2	0.55		
3	0.81	0.48	
4	0.84		
5	0.83		0.62
6	0.15	0.61	
7	1.21		
8	0.70		
9	0.39	0.77	
10	0.48		0.59
Acceleration Noise	0.33	0.12	0.02

Results

Using the three different data sets (i.e., the original 1Hz data, generated 1/3Hz and 1/5Hz data), the values of acceleration noise (using SD-based approach) were compared as shown in Figure 38, which indicates that the acceleration noise values from the 1Hz data are greater than those from the other data sets, as expected. In addition, compared to the 1/5Hz data, the acceleration noise values from the 1/3Hz data are closer to thoes from 1Hz data, supported by the R^2 values of 0.95 and 0.88 for 1/3Hz and 1/5Hz data, respectively. These findings clearly indicate that the data with lower sampling frequencies tend to produce lower acceleration noise values. However, the differences seem to be smaller as acceleration noise values increases, implying that the differences may depend on traffic conditions.

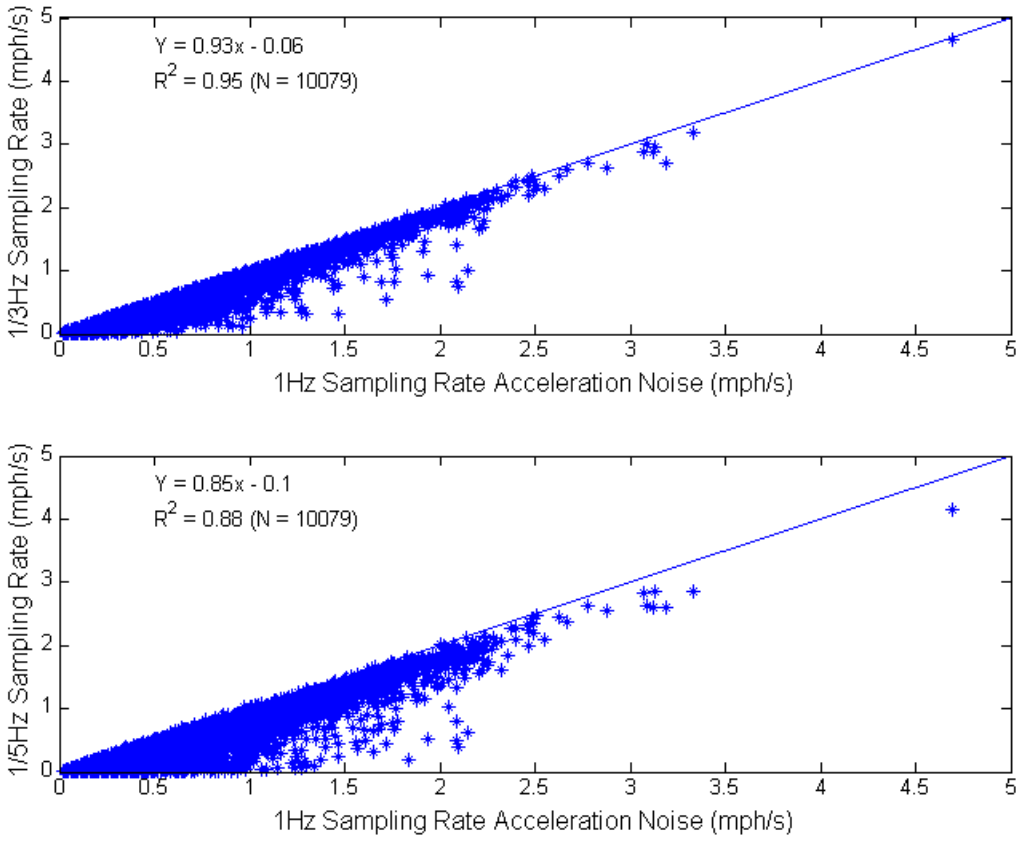

Figure 38: Comparison of Acceleration Noise from the Data with Different Sampling Rates

The acceleration noise values were compared by average speed levels using 10 mph bins. For each bin, acceleration noise values were combined, and 95% confidence intervals were obtained, as illustrated in Figure 39. Consistent with the previous finding, the figure indicates that the data with the lower sampling frequencies produce lower acceleration noise across all speed ranges. In addition, the non-overlapping confidence intervals except for the less than 10mph bin suggest that the acceleration noise values from the three data sets are significantly different. Table 5, summarizing the average acceleration noise values for each speed range, also reveals the trend: the larger differences for higher speed ranges. For example, in case of the comparison between 1Hz and 1/3Hz data sets, the percent decreases of average acceleration noise values for

the speed ranges of 10-20 mph and 70-80 mph are 8.0% and 25.9%, respectively. With respect to the 1Hz data, the overall acceleration noise values were reduced by 17.3% and 32.7% for the 1/3Hz data and the 1/5Hz data, respectively.

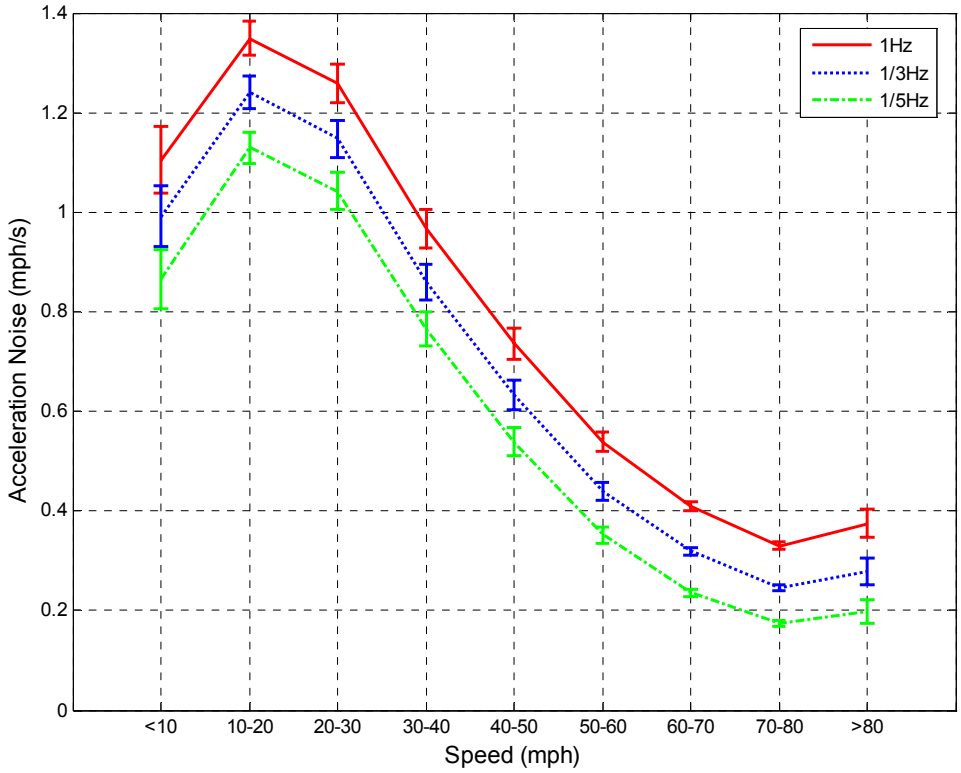

Figure 39: Comparison of Acceleration Noise by Speed Level and Data Sampling Rate

Table 5: Average Acceleration Noise Values for Each Speed Range

Speed (mph)	N	1Hz	1/3Hz		1/5Hz	
		Acceleration Noise	Acceleration Noise	% decrease	Acceleration Noise	% decrease
<10	64	1.10	0.99	(10.3)	0.87	(21.6)
10 - 20	425	1.35	1.24	(8.0)	1.13	(16.3)
20 - 30	586	1.26	1.15	(8.9)	1.04	(17.3)
30 - 40	598	0.97	0.86	(11.1)	0.77	(20.8)
40 - 50	567	0.74	0.63	(14.0)	0.54	(26.8)
50 - 60	1,031	0.54	0.44	(18.6)	0.35	(34.6)
60 - 70	3,237	0.41	0.32	(22.0)	0.24	(42.2)
70 - 80	3,266	0.33	0.25	(25.8)	0.17	(47.1)
>80	305	0.38	0.28	(25.9)	0.20	(47.4)
Overall	10,079	0.54	0.45	(17.3)	0.36	(32.7)

* % decrease was computed with respect to the acceleration noise of 1Hz data.

In addition to the average speed level of the instrumented vehicles, LOS was considered as a covariate affecting the differences, and distributions for each LOS were estimated, as illustrated in Figure 40. Similar to the previous findings, the acceleration noise distributions from the lower frequency data tend to shift toward left with higher peaks across all LOS ranges, yielding the lower acceleration noise and the lower variance. For the test whether the distributions of acceleration noise from the three data sets with the different sampling frequencies have been drawn from the same population, the KS test was implemented, as summarized in Table 6. The results indicate that the three distributions are significantly different (all *p*-values are 0.000) and that the differences become smaller under LOS F range, as indicated by the relatively small K statistics.

Table 6: KS Test Results by LOS

LOS	N	1Hz vs. 1/3Hz		1/3Hz vs. 1/5Hz		1Hz vs. 1/5Hz	
		K	p-value	K	p-value	K	p-value
A	977	0.204	0.000	0.180	0.000	0.357	0.000
B	1,389	0.204	0.000	0.217	0.000	0.390	0.000
C	2,559	0.212	0.000	0.202	0.000	0.383	0.000
D	1,935	0.201	0.000	0.196	0.000	0.365	0.000
E	944	0.185	0.000	0.177	0.000	0.337	0.000
F	2,275	0.093	0.000	0.087	0.000	0.173	0.000
Overall	10,079	0.153	0.000	0.282	0.000	0.423	0.000

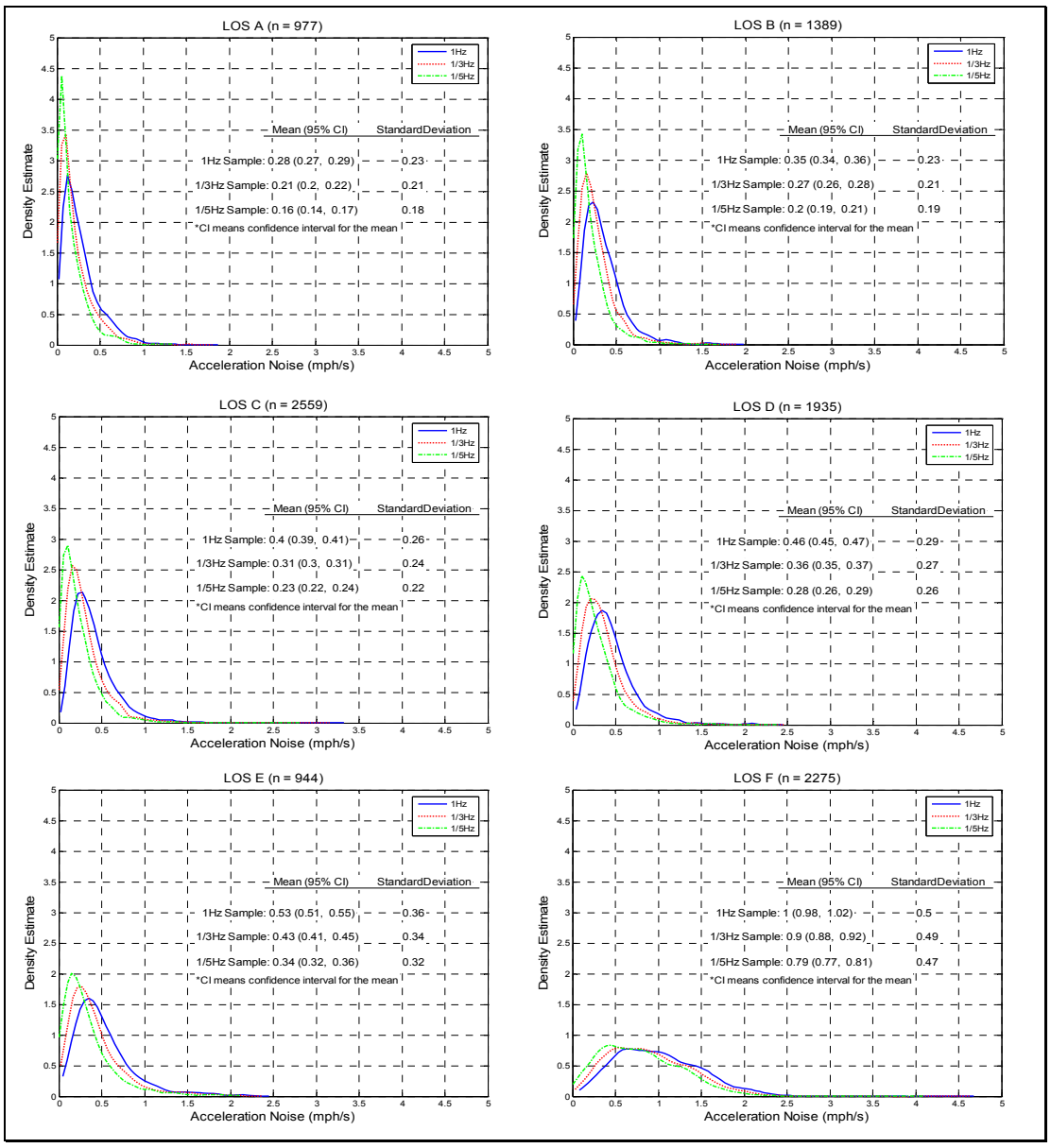

Figure 40: LOS-Based Comparisons of Acceleration Noise Distributions from the Data with Different Sampling Frequencies

Summary

The sensitivity of acceleration noise to the data sampling frequency was analyzed in this section using the three different data sets, among which 1/3Hz and 1/5Hz data were generated based on the 1Hz initial speed profiles. The analysis results clearly indicated that the lower frequency data tend to exhibit lower acceleration noise values, probably

due to the smoothing effect inherent in the lower frequency data. With respect to the 1Hz data, the overall acceleration noise values were reduced by 17.3% and 32.7% for the 1/3Hz data and the 1/5Hz data, respectively. In addition, the differences in the acceleration noise values were more pronounced under the higher speed or better LOS ranges. This phenomenon may be due to the smaller number of GPS data points for the given segment under the better traffic conditions. Note that acceleration noise is defined over a specific roadway segment, and thus, the higher speed means the fewer data points for the segment. Therefore, when the sampling frequency becomes lower, the effect of the data size reduction becomes more critical for the trips with higher speeds. The reduced data size, in turn, results in a smaller acceleration noise because the variation of acceleration is less likely to be captured for the speed profile with smaller data size.

These findings suggest that the understanding of data characteristics such as the sampling frequency would be important to properly apply and interpret the resulting acceleration noise values. In addition, acceleration noise from different research efforts should be carefully compared since they might collect data using different data sources, thus different sampling frequencies.

Chapter 6

Acceleration Noise and Traffic Congestion

Study Objectives and Data

Background

A major issue associated with acceleration noise is whether the parameter can accurately reflect traffic congestion. To answer this question, several research efforts have employed floating car methods to measure acceleration noise under various traffic conditions (Babu and Pattnaik 1997; Croft and Clark 1985). Based on the efforts, the researchers concluded that acceleration noise is associated with traffic congestion. More specifically, they found that acceleration noise increases as traffic congestion worsens. In this chapter, their conclusion is to be affirmed using the instrumented vehicle data which render this research effort unique; unlike previous research efforts in which real-world drivers' behavior could not be observed. In addition, this study compares acceleration noise with vehicle speeds from the viewpoint of the effectiveness in measuring traffic congestion.

Data

This chapter employs the instrumented vehicle trips obtained from 12 segments on northbound GA400 between January 2004 and June 2004 (six months). All the selected segments are basic segments with a speed limit of 65mph and four lanes, minimizing the variation induced by roadway characteristics. In addition, trips were excluded from the data set if the trips were obtained from vehicles which entered or exited the roadway within 0.5 miles on the study segment so that any potential weaving effects were

minimized. The exclusion of entering and exiting trips also prevents the data set from containing accelerating or decelerating vehicle activities not associated with surrounding traffic or roadway characteristics. For such an effort, extended segments, adding 0.5 miles from the both ends of the segment of interest, were established, and only the trips which completely traveled over the extended segments were selected. In addition, weather conditions were also considered since they may affect driver acceleration behavior. To this end, archived hourly precipitation data (obtained from National Climatic Data Center of National Oceanic and Atmospheric Administration) of the nearest station from the study site were utilized, and trips made during any time period with a record of precipitation were excluded from the data set. Finally, daylight conditions were considered. In the consideration, trips made between 7:00am and 7:00pm during a daylight savings time period or between 8:00am and 6:00pm during a non-daylight savings time period were designated as trips under daylight conditions. This study employed only the trips under daylight conditions. As a summary, the data set used in this analysis includes only:

- Trips without entering/exiting activities,
- Trips under potentially non-raining conditions, and
- Trips under daylight conditions.

As a result, 11,500 trips from 177 instrumented vehicles were selected for this analysis, and their statistics by LOS were summarized in Table 7, which indicates that acceleration noise increases with traffic congestion. The estimation of LOS was performed using the one-minute level density data obtained from the synchronized TMC data.

Table 7: Summary Statistics by LOS

LOS	N	Number of Vehicles	Average Speed (mph)	Average Acceleration Noise (mph/s)
A	225	51	73.3	0.25
B	1,827	146	72.5	0.29
C	4,329	159	71.5	0.33
D	2,467	123	68.1	0.41
E	1,083	76	60.3	0.51
F	1,569	75	38.1	0.94
Overall	11,500	177	65.4	0.44

Result

Acceleration Noise, Instrumented Vehicle Speed, and Traffic Density

Acceleration noise was related with instrumented vehicle speeds and traffic density using the whole data set (n = 11,500), as shown in Figure 41. The figure indicates that acceleration noise is negatively correlated with vehicle speeds and positively correlated with density, as suggested by the results of simple linear regression models. Compared to the previous research efforts, the R^2 values for these regression lines appear to be low. For example, a study reported a R^2 value of 0.70 for a linear regression line representing the relationship between acceleration noise and speed from freeway trips (Eisele et al. 1996). In another study, the R^2 value for the linear relationship between acceleration noise and traffic density on freeways was 0.47 (Croft and Clark 1985). In contrast, the R^2 values shown in Figure 41 are limited to only 0.44 and 0.36 for vehicle speeds and density, respectively. These low correlations may be partly due to the data characteristics: the involvement of various vehicles (177 vehicles) and roadway segments (12 basic segments with 65mph speed limit and four lanes). The effects of

roadway characteristics and driver/vehicle will be investigated in detail later in this dissertation.

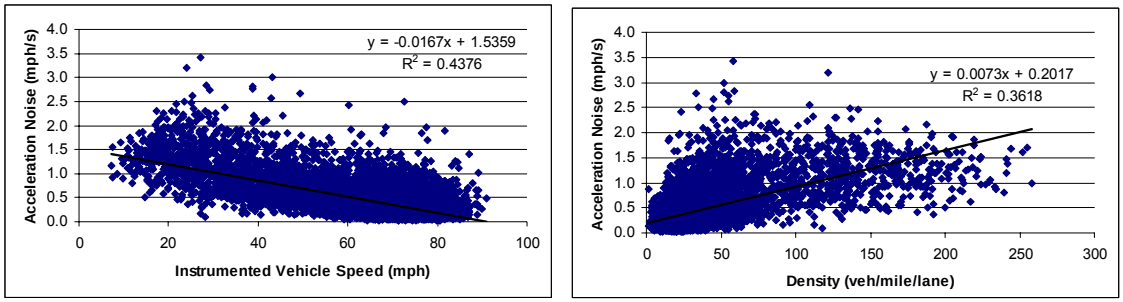

Figure 41: The Relationship among Acceleration Noise, Instrumented Vehicle Speed, and Density (n=11,500)

The relationship was examined on a segment-by-segment basis. In this examination, cubic polynomial regression models, theoretical relationships proposed by Drew (1968), were computed in addition to linear models, and their results (R^2) are summarized in Table 8. The R^2 values for the relationship with vehicle speeds lie between 0.35 and 0.60 for the linear models while the cubic polynomial models exhibited R^2 values between 0.38 and 0.63. The increases of the R^2 values for the cubic polynomial models can be expected since the more explanatory variables provide more explanatory powers for the model. However, the test using the adjusted R^2 values, for which the number of parameters is incorporated, and the models with more variables are penalized, indicated that the effect of the increased number of explanatory variables is negligible, implying that the cubic polynomial fitting may be more appropriate for the relationships, as proposed by Drew (1968). This phenomenon was also found for the relationships between density and acceleration noise, but their relationships exhibited lower R^2 values than those for the relationships between vehicle speed and acceleration noise.

Table 8: Coefficients of Determination for Linear and Cubic Regression Models

Segment	N	Vehicle Speed vs. Acceleration Noise		Density vs. Acceleration Noise	
		Linear	Cubic	Linear	Cubic
NB10	924	0.44	0.50	0.41	0.44
NB11	982	0.35	0.38	**0.28**	**0.30**
NB12	1,018	0.40	0.48	0.38	0.39
NB13	929	0.44	0.49	0.36	0.38
NB14	892	0.39	0.42	0.38	0.40
NB15	921	0.39	0.41	0.33	0.35
NB17	923	0.39	0.43	0.40	0.44
NB19	891	0.43	0.46	0.36	0.38
NB20	1,034	0.36	0.41	0.30	0.33
NB21	1,047	0.48	0.54	0.40	0.44
NB22	1,044	0.54	0.58	0.42	0.50
NB24	895	0.60	0.63	**0.46**	**0.52**
Overall	11,500	0.44	0.48	0.36	0.40

Comparison with the Energy Model

The energy model proposed by Drew (1968) established the theoretical relationships among acceleration noise, speed, and density. The results of the energy model were examined by comparing them with the relationships obtained from the instrumented vehicle data. For the comparison, scatter plots which show the relationships among acceleration noise, vehicle speed, and density were obtained for a single segment (NB 24, n = 895) so that a clearer relationship should be observed by eliminating the segment-by-segment variation. The relationship is illustrated in Figure 42, in which the estimated cubic polynomial regression models are also reported. In contrast to the energy model, acceleration noise seems to stay or decrease, rather than continue increasing, when vehicle speeds are significantly low (i.e., less than 20mph). Similarly, the regression line representing the relationship between acceleration noise and density more clearly indicates that the values of acceleration noise may downturn after some

point (e.g., about 130 veh/mile/lane in Figure 42). This observation of downturn may be plausible since vehicle movements can be extremely restricted under severe traffic conditions, and thus, the speed changes of the vehicle can be minimal under the conditions. These findings imply that the relationships dictated by the energy model may not be maintained under the boundary conditions imposed by the extremely heavy traffic conditions, as argued by Winzer (1981).

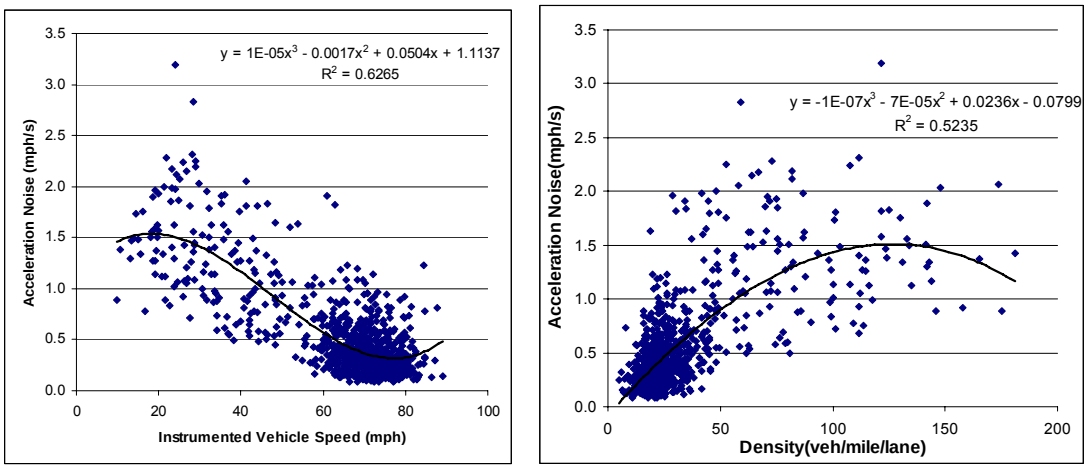

Figure 42: Relationships among Acceleration Noise, Vehicle Speed, and Density for the Trips on NB24 (N = 895)

For a further examination, trips from only three vehicles, top 3 vehicles showing the highest number of trips among 149 vehicles observed on segment NB24, were selected so that vehicle-by-vehicle variation can be examined. Using these trips, the relationships among acceleration noise, speed, and density were obtained, as shown in Figure 43, in which totally 158 trips (Vehicle 1: 48; Vehicle 2: 50; and Vehicle 3: 59) were utilized. Similar trends observed in the previous analysis were found in the plots, and the phenomenon of the downturn seemed more pronounced for the trips of Vehicle

1, as suggested by the fitted cubic polynomial regression lines. However, Vehicles 2 and 3 show a trend that acceleration noise continues increasing as speed decreases or density increases. However, this phenomenon may be attributed to the data range, and thus, the use of more congested data (i.e., vehicle speed less than 20 mph) would provide clearer ideas about the trends. In addition to the shapes of the curves, the varied magnitudes of acceleration noise for the same level of traffic conditions indicate that drivers may differently respond to the surrounding traffic conditions. These findings suggest that the factors induced by driver/vehicle affect the values of acceleration noise.

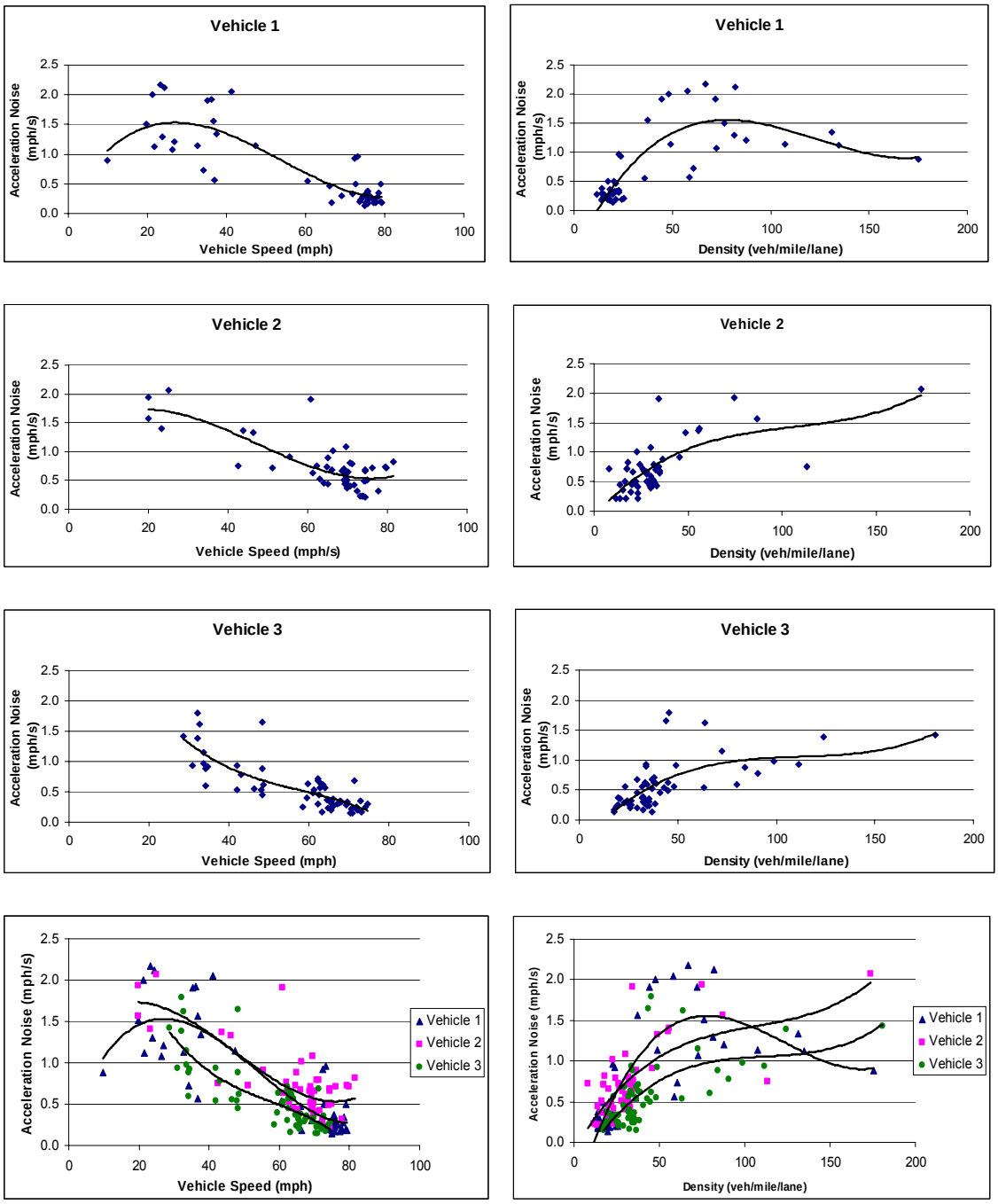

Figure 43: Relationships among Acceleration Noise, Vehicle Speed, and Density for the Trips on NB24 from Three Vehicles (48, 51, and 59 Trips for Vehicles 1, 2, and 3)

Acceleration Noise Distributions by LOS range

The distributions of acceleration noise by LOS ranges were examined. In this examination, speed distributions were also examined for comparison. At first, 95%

confidence intervals for the mean for each LOS range were obtained, as shown in Figure 44. The figure clearly indicates that acceleration noise increases and speed decreases as traffic congestion worsens. None of the confidence intervals overlap except for the speed confidence intervals of LOS A and B ranges, indicating no significant difference of mean speeds for the ranges at a significance level of 0.05. This situation can be expected since speed is not sensitive to traffic conditions under the free-flow conditions. Indeed, HCM 2000 suggests that the minimum speeds for LOS A and B are exactly the same if the free-flow speed for the basic segment is less than 70mph. Even in the case of the segment with a free-flow speed of 75mph, the minimum speeds for LOS A and B are 75.0 and 74.8mph, respectively, and thus, they show little difference. However, the acceleration noise confidence intervals reveal significant differences between LOS ranges, implying its capability to discern traffic conditions even for LOS A and B ranges.

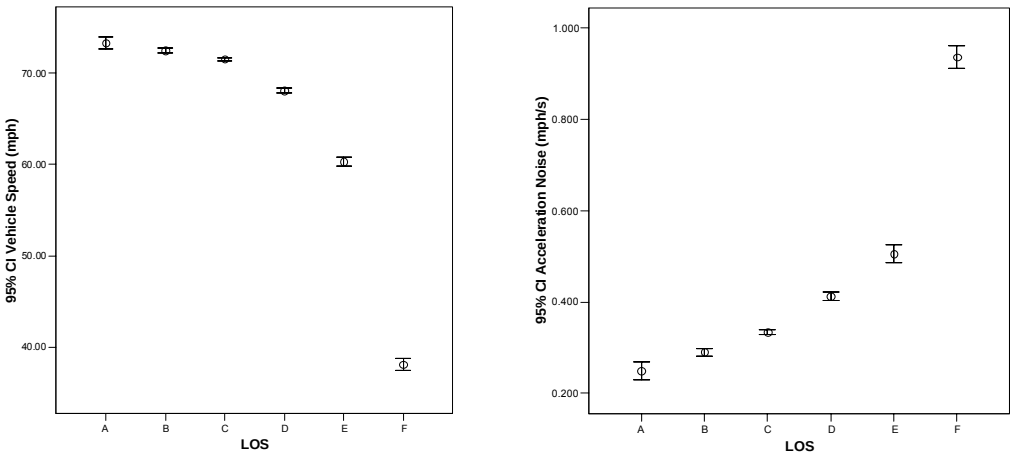

Figure 44: Confidence Intervals for Means of Acceleration Noise and Vehicle Speeds by LOS Ranges

In addition to the confidence interval analysis, a KS test was performed in an attempt to quantify the magnitude of differences among distributions. The resulting KS statistics and *p*-values for each LOS pair are summarized in Table 9. The table indicates that all the distributions are significantly different for both acceleration noise and speed distributions at a significance level of 0.05, as suggested by the low *p*-values in parentheses. However, the *p*-value of 0.036 for the pair of LOS A and B of speed distributions suggests the two distributions may not be significantly different at a higher

significance level (i.e., 1%). In fact, the lowest KS statistics 0.099 for the pair implies that the two distributions are closer than any other pairs. An examination of KS statistics reveals that acceleration noise may be more indicative of traffic conditions under LOS A-to-C, which is supported by the larger KS statistics for the pairs of acceleration noise distributions under LOS A-to-C ranges. In contrast, speed seems to be more indicative of traffic conditions under LOS D-to-F ranges for the same reason. This finding is interesting since a combination of acceleration noise with speed may enhance the capability of the probe vehicle-based traffic congestion monitoring systems, which have relied on solely speed data.

Table 9: KS Statistics and p-Values for the Pairwise Comparisons of Acceleration Noise and Speed Distributions by LOS Ranges

	LOS	A	B	C	D	E	F
Acceleration Noise	A	-	**0.122**	**0.220**	0.336	0.455	0.726
			(0.005)	(0.000)	(0.000)	(0.000)	(0.000)
	B		-	**0.115**	0.239	0.365	0.683
				(0.000)	(0.000)	(0.000)	(0.000)
	C			-	0.151	0.279	0.628
					(0.000)	(0.000)	(0.000)
	D				-	0.134	0.530
						(0.000)	(0.000)
	E					-	0.436
							(0.000)

	LOS	A	B	C	D	E	F
Vehicle Speed	A	-	**0.099**	**0.172**	0.371	0.705	0.952
			(0.036)	(0.000)	(0.000)	(0.000)	(0.000)
	B		-	**0.081**	0.302	0.649	0.920
				(0.000)	(0.000)	(0.000)	(0.000)
	C			-	0.238	0.602	0.902
					(0.000)	(0.000)	(0.000)
	D				-	0.442	0.863
						(0.000)	(0.000)
	E					-	0.713
							(0.000)

Note: *p*-values are inside parenthesis.

Confidence Regions for Acceleration Noise and Vehicle Speed by LOS

As mentioned before, a combination of acceleration noise and vehicle speed may provide more helpful information about traffic conditions. Thus, an examination of unified acceleration noise and speed was performed as an attempt to better understand their relationships with traffic conditions. In this study, their relationships were identified based on the confidence region analysis, a multivariate statistical analysis technique. In the technique, the confidence region for the mean μ of a *p*-dimensional normal population can be derived from:

$$P\left[n(\bar{x}-\mu)' S^{-1}(\bar{x}-\mu) \le \frac{p(n-1)}{(n-p)} F_{p,n-p}(\alpha) \right] = 1-\alpha ,$$

where *n*, $\bar{x}$, and *S* represent sample size, a vector of sample mean, and covariance matrix, respectively (Johnson and Wichern 1992). Thus, a *100(1-α)%* confidence region for the mean μ of a *p*-dimensional normal population is the set determined by all μ such that:

$$n(\bar{x}-\mu)' S^{-1}(\bar{x}-\mu) \le \frac{p(n-1)}{(n-p)} F_{p,n-p}(\alpha) .$$

As suggested in the assumptions for constructing confidence regions, each variable (in this case, acceleration noise and speed) should be normally distributed. However, an examination of acceleration noise distributions revealed that they may not be normally distributed. Fortunately, the violation of the normal distribution assumption could be mitigated by taking log, for which detailed explanations will be provided in the next chapter.

The constructed confidence regions based on the 895 instrumented vehicle trips from NB24 were illustrated in Figure 45, in which six confidence ellipses represent the

confidence regions for six LOS ranges, and the centroid for each region was marked by the corresponding letter, A-to-F. The confidence regions clearly indicate that the lower acceleration noise and the higher speed are more likely to be experienced for better traffic conditions. However, the distinctions between LOS ranges do not appear to be clear because of the significant overlaps, implying a large amount of variation for acceleration noise and vehicle speed within or between HCM LOS ranges. In particular, the confidence region for LOS D range overlaps with all the other confidence regions. These findings suggest that the current HCM LOS system may not effectively reflect drivers' experience, represented by acceleration noise and speed.

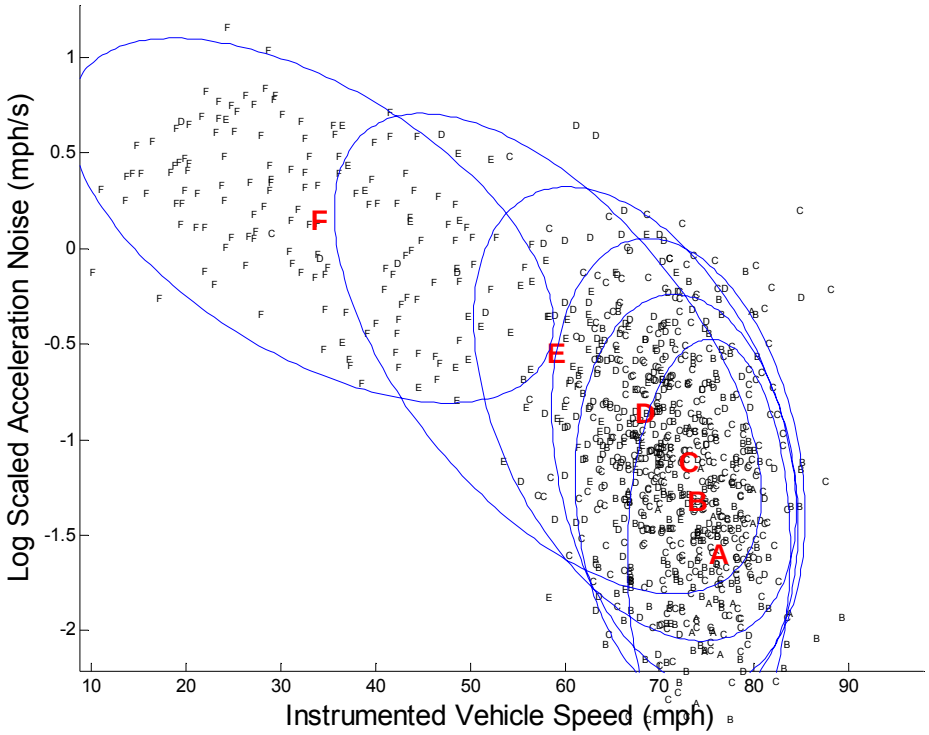

Figure 45: 90% Confidence Regions for Acceleration Noise and Vehicle Speed (NB24)

Summary

In this chapter, the relationships between acceleration noise and traffic congestion measured by traffic density and vehicle speed were investigated. The investigation suggested that acceleration noise can be an indicator of traffic conditions, in particular for LOS A-to-C ranges. Under the free-flow conditions, vehicle speed is only a weak indicator of traffic conditions since speed changes marginally under the ranges. However, acceleration noise appears to be non-linearly correlated with traffic conditions, and thus, a sole use of acceleration noise for measuring traffic conditions may mislead researchers, in particular for highly congested conditions. Consequently, this study suggests that a combined use of acceleration noise with speed may be more effective for measuring traffic conditions. In addition, the confidence region analysis indicated that the current HCM LOS system may not effectively reflect the drivers' experience represented by speed and acceleration noise. Thus, the use of speed and acceleration noise may be able to provide another perspective for the traffic flow quality experienced by drivers.

Chapter 7

Acceleration Noise and Roadway Characteristics

Study Objectives and Data

Background

Roadway characteristics, including the number of lanes, speed limit, grade, curvature, and operational type (e.g., basic, on/off ramp segments), affect acceleration noise. Although some research efforts have attempted to identify the relationship between acceleration noise and roadway characteristics, their efforts were limited to the experimental level, and thus, their findings may not truly reflect real-world situations experienced by real-world drivers. In the real world, the effects may be interactive. In other words, their effects may vary by traffic condition, requiring a more systematic approach to identify the relationships. In addition, the previous research efforts have a weakness in that the data employed in the studies were obtained from a single or just a few test vehicles, not from real-world vehicles. Although the test vehicles might represent the general driver/vehicles and control variability introduced by drivers, it is still suspected whether they could truly represent the general public. This study attempts to establish the relationship between acceleration noise and roadway characteristics using statistical models based on the instrumented vehicle data driven by real-world drivers. In particular, such models were developed by LOS range, and thus, the interaction of roadway characteristics and traffic conditions is expected to be revealed.

Data

The initial instrumented vehicle data for this study were collected over all segments (89 segments) of GA400 during the time period between March and May 2004 (three months period). However, TMC data for two segments (SB5 and NB23) were not available during the time period, and thus, the data from the two segments could not be used in this study. In addition, a visual examination of data quality revealed that the TMC data from the camera station covering the segment of SB40 might not be reliable because of the suspect data clustered at the right-bottom corner in Figure 46, which illustrates TMC speed versus instrumented vehicle speed. The erroneous data are likely to be associated with equipment errors or malfunctions for the camera station. The data from the suspect camera station were also utilized to obtain the macroscopic traffic data for the segment SB39, and thus, the TMC data for SB39 was also expected to be unreliable. Consequently, the two segments were also excluded from the analysis. Finally, preliminary analyses were implemented as an attempt to capture segments inducing abnormal vehicle activities, resulting an exclusion of ten additional three-lane segments (northbound only) located between four-lane and two-lane roadways. Vehicle activities on the three-lane segments were significantly influenced by lane-reduction in addition to the general roadway characteristics. Consequently, 14 segments were excluded from the analysis, and thus, instrumented vehicle trips from 75 segments were utilized for this analysis.

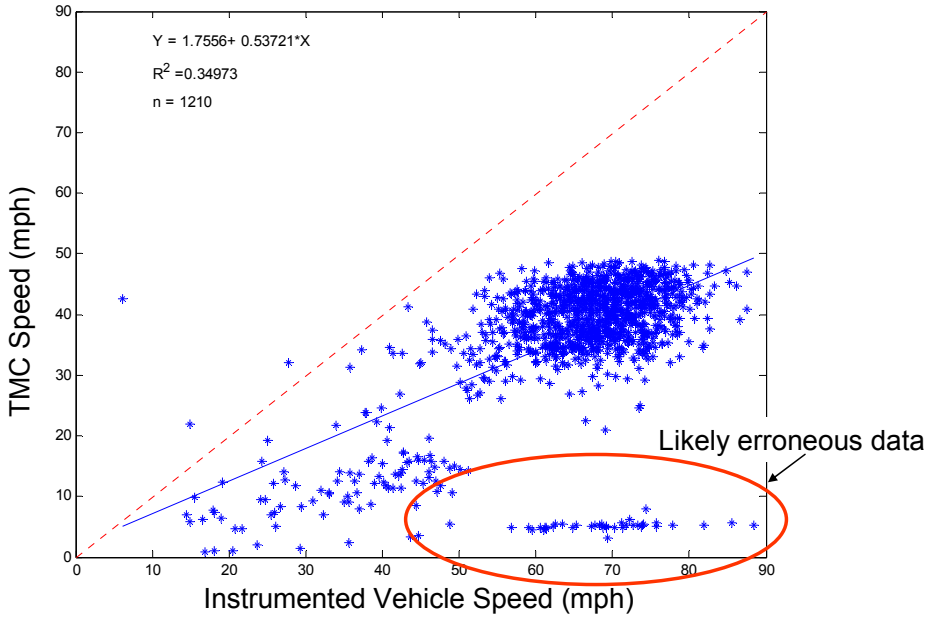

Figure 46: Visual Examination of Data Quality

In addition to the segment-wise data screening, night-time trips, entering and exiting trips, and trips under potentially raining conditions were also excluded (see Chapter 6). Consequently, 31,916 trips from 174 vehicles over 75 segments were employed in this analysis. Table 10 summarizes the selected trip data by LOS range, and Figure 47 illustrates the changing pattern of the average instrumented vehicle speed and acceleration noise by LOS range, indicating that vehicle speed decreases and acceleration noise increases as traffic congestion worsens.

Table 10: Data Summary by LOS Range

LOS	N	Number of vehicles	Number of segments	Speed (mph)	Acceleration Noise (mph/s)
A	502	55	74	73.2	0.27
B	4,369	142	75	72.2	0.30
C	12,403	165	75	70.4	0.34
D	7,390	164	75	66.7	0.42
E	2,779	127	75	60.0	0.52
F	4,473	109	75	36.1	0.97

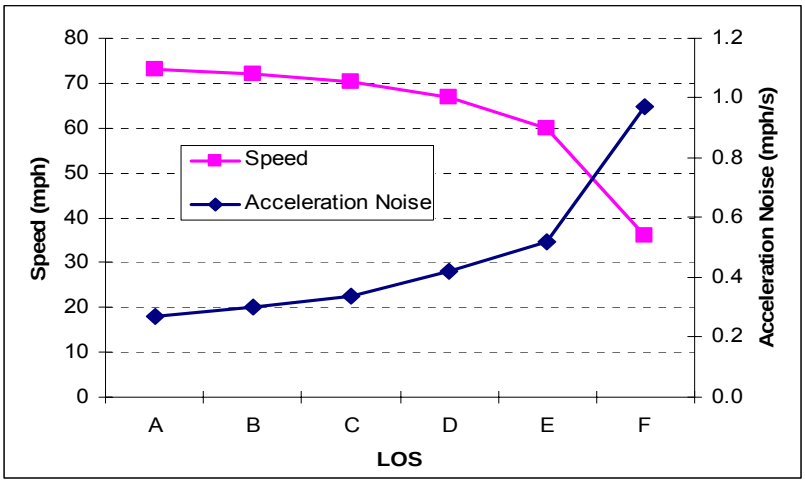

Figure 47: Average Instrumented Vehicle Speed and Acceleration Noise by LOS Ranges

Model Development

Methodology - Random Intercept Model

An important feature of the data set used in this study is that the sampled trips are repeated measurements from the sampled drivers/vehicles, indicating potential correlations among observations from the identical driver/vehicle. Thus, statistical models with a capability of handling the correlation or cluster effects by subject (in this case, driver/vehicle) should be applied. Considering this circumstance, this study uses random coefficient models, which are similar to ordinary regression models except that the random coefficient model contains an additional term to help explain the within-cluster correlation (random effects). Thus, the random coefficient model is composed of two parts: fixed and random effects. When the functional form of the model is assumed to be linear, and the random effects can be represented by random intercepts, the model (random intercept model) can be represented by

$$y_{ij} = \alpha + x_{ij}\beta + \delta_j + \varepsilon_{ij},$$

where y_{ij} is the ith response variable for subject j, and x_{ij} represents explanatory variables for the ith observation from subject j. In addition, β represents the vector of fixed-effect parameters to be estimated, and δ_j and ε_{ij} are mutually independent samples from $N(0, \tau^2)$ and $N(0, \sigma^2)$, respectively (Longford 1993). The variances σ^2 and τ^2 are referred to as elementary- and cluster-level variance components, and this random intercept model becomes identical to an ordinary regression model when $\tau^2 = 0$. The random intercepts for subject j are represented by the term δ_j. If two observations in the same cluster are correlated:

$$\text{var}(y_{ij}) = \sigma^2 + \tau^2 \ ,$$

$$\text{cov}(y_{ij,} y_{i'j}) = \tau^2 \quad (i \neq i') \ .$$

The correlation of two outcomes from the same subject is represented by

$$\rho = \frac{\tau^2}{\sigma^2 + \tau^2} \ ,$$

which is referred to as the variance component ratio and indicates the fraction of the residual variance attributed to between-cluster variation.

The parameters can be obtained from the maximum likelihood (ML) estimation or alternatively the restricted maximum likelihood (REML). The REML estimation was proposed to mitigate the problem of the biased estimator of the residual variance in the ML estimation. However, in most cases, the results of ML and REML estimation almost coincide unless the number of parameters with respect to the sample size is comparatively large (Longford 1993). The model parameter estimation was implemented using REML in this study.

Acceleration Noise Data Transformation

Like the ordinary regression model, the random intercept model also requires the normally distributed dependent variables. Thus, acceleration noise distributions were examined to determine whether they are normally distributed. The examination revealed that the distributions are closer to the log-normal distributions, rather than the normal distributions, requiring an appropriate data transformation. Thus, the original acceleration noise data were transformed by taking log, and the resulting distributions were re-examined, as shown in Figure 48. The distributions obtained from the transformation appear to be closer to normal distributions. The transformation effects were measured through one-sample normal KS tests as shown in Table 11, which suggests that the degree of normality was significantly enhanced after the transformation, in particular for LOS A and B ranges. The enhancement of normality is supported by the smaller test statistics (K) after the transformation, although the test results suggest that even the log-transformed distributions for LOS C, D, and F ranges are still significantly different from normal distributions. Note that the KS test applies the stricter threshold with the sample size. (The data sizes for LOS C and D ranges are relatively large.)

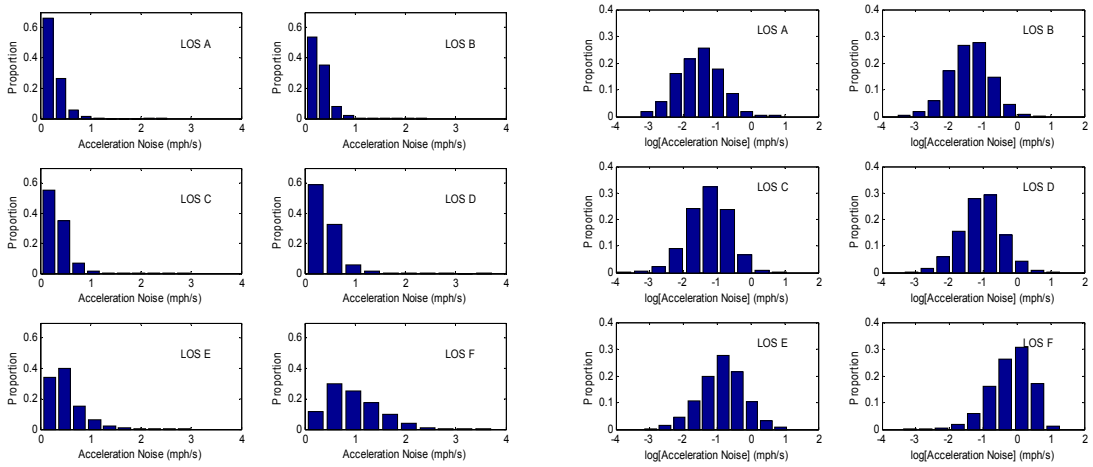

Before **After**

Figure 48: Log Transformation of Acceleration Noise Data

Table 11. Results of One-Sample Normal KS Tests for Before and After Log-Transformation

LOS	Before		After	
	K	p-value	K	p-value
A	0.153	0.000	0.033	0.662
B	0.112	0.000	0.018	0.102
C	0.104	0.000	0.016	0.004
D	0.118	0.000	0.023	0.001
E	0.123	0.000	0.028	0.026
F	0.066	0.000	0.051	0.000

Model Specification

The models to be developed in this chapter use log-transformed acceleration noise as the dependent variable. For their explanatory variables, the models use five roadway characteristics: facility type (basic segment, on-ramp, and off-ramp), grade, curvature, speed limit (55 and 65 mph), and number of lanes (2, 3, and 4 lanes). Naturally, such variables as facility type, speed limit, and number of lanes were treated as discrete variables. In addition, grade and curvature were also treated as discrete variables by binning them. For binning grade, two break points (i.e., -2 and +2%) were used, resulting in three grade groups: less than -2%, -2 – +2%, and greater than +2%. The use

of the break points (±2%) is based on the fact that HCM defines level terrain as the segments which include short grades of no more than 2 percent (TRB 2000). In addition, the grade range for the study data set (-3.7 - 3.4%) implies that the breakpoints may be appropriate in terms of the potential data size for each grade bin. In case of curvature, a single breakpoint (1.5 in a unit of 10000/radius of curvature) was used, resulting in two curvature groups. The determination of the breakpoint was based on the results of the regression tree analysis, a statistical tool splitting data into partitions with minimizing the sum of the squared deviations from the means in the partitioned groups (Breiman et al. 1984). In particular, the result from the data set under LOS A condition was referred because the LOS A data provided better fitting results than the other data sets. The breakpoint of 1.5 appears to be reasonable in terms of the curvature range for the data set (0.04 and 3.00).

Model Estimation Results

Six random intercept models for each LOS range were estimated, as shown in Tables 12-14. The validity of the estimated model can be examined through the residual distributions, which is supposed to be normally distributed by the model assumption, and the reasonableness of the estimated parameters. First, the normality of residuals was examined through the Q-Q plots of residuals as shown in Figure 49, which indicates the residuals do not significantly deviate from the normal distribution except for the residuals of LOS F model. Second, the sign of the estimated parameters were examined. For all six models, the sign of the estimated parameter seems to be intuitively correct. For example, the negative signs for the variable of the basic segment

indicate that basic segments tend to induce less acceleration noise, compared to off-ramp segments. As an another example, the positive signs for the variable of the segments with two lanes mean that such segments tend to induce larger acceleration noise, compared to the segments with four lanes. Finally, the significant variances for the random intercepts, suggested by the low *p*-values for the variables, justify the use of the random intercept models, implying the importance of driver/vehicle effects. If the variance of the random intercept is not significant, the ordinary regression model would be enough for the data set. Consequently, the estimated model was concluded to be valid from these perspectives.

Meanwhile, the estimated models resulted in considerably low coefficients of determination (R^2) which ranges from 0.09 (LOS F) to 0.20 (LOS A), implying the low explanatory power of the employed independent variables. This situation can be expected as the developed models are unlikely to remove all the variances induced by various drivers/vehicles and localized traffic conditions (e.g., interaction with other vehicles, location within a platoon, etc.). In addition, within the same LOS range, different levels of traffic conditions may induce variances, in particular for LOS F range defined by a wider traffic density range, simply larger than 45veh/mile/lane. However, the estimated models seem to be sufficient to identify the effects of roadway characteristics on acceleration noise.

Table 12: Model Estimation Results for LOS A and B Ranges

LOS A (N = 502)

Variables		Estimate	t	Sig.
Intercept		**-1.518***	**-4.369**	**0.000**
Facility Type	Basic Segment	-0.073	-0.960	0.337
	On-ramp area	-0.011	-0.116	0.907
	Off-ramp area			
Grade	Less than -2%	0.053	0.731	0.465
	Greater than +2%	-0.039	-0.540	0.589
	Between -2 and +2%			
Curvature (10000/radius of curvature in feet)	Greater than 1.5	**0.189***	**2.328**	**0.020**
	Less than or equal to 1.5			
Number of lanes	2 lanes	**0.294***	**2.408**	**0.016**
	3 lanes	-0.053	-0.624	0.533
	4 lanes			
Speed limit	55 mph	**0.185***	**2.368**	**0.018**
	65 mph			
Variance of residual		0.322		0.000
Variance of random intercept		0.112		0.003
Coefficient of determination			0.20	

LOS B (N = 4,369)

Variables		Estimate	t	Sig.
Intercept		**-1.392***	**-5.062**	**0.000**
Facility Type	Basic Segment	**-0.107***	**-4.067**	**0.000**
	On-ramp area	-0.031	-0.976	0.329
	Off-ramp area			
Grade	Less than -2%	**0.058***	**2.391**	**0.017**
	Greater than +2%	-0.038	-1.562	0.118
	Between -2 and +2%			
Curvature (10000/radius of curvature in feet)	Greater than 1.5	0.018	0.640	0.522
	Less than or equal to 1.5			
Number of lanes	2 lanes	**0.307***	**7.029**	**0.000**
	3 lanes	0.010	0.371	0.711
	4 lanes			
Speed limit	55 mph	**0.150***	**5.965**	**0.000**
	65 mph			
Variance of residual		0.302		0.000
Variance of random intercept		0.074		0.000
Coefficient of determination			0.17	

* indicates the estimated parameter is significant at a 0.05 level.

Table 13: Model Estimation Results for LOS C and D Ranges

Variables		Estimate	t	Sig.
Intercept		**-1.321***	**-5.266**	**0.000**
Facility Type	Basic Segment	**-0.040***	**-2.602**	**0.009**
	On-ramp area	0.012	0.591	0.554
	Off-ramp area			
Grade	Less than -2%	**0.037***	**2.582**	**0.010**
	Greater than +2%	-0.018	-1.302	0.193
	Between -2 and +2%			
Curvature (10000/radius of curvature in feet)	Greater than 1.5	-0.012	-0.765	0.444
	Less than or equal to 1.5			
Number of lanes	2 lanes	**0.261***	**10.859**	**0.000**
	3 lanes	0.008	0.531	0.595
	4 lanes			
Speed limit	55 mph	**0.136***	**9.633**	**0.000**
	65 mph			
Variance of residual		0.303		0.000
Variance of random intercept		0.062		0.000
Coefficient of determination			0.17	

LOS D (N = 7,390)

Variables		Estimate	t	Sig.
Intercept		**-1.176***	**-5.148**	**0.000**
Facility Type	Basic Segment	-0.011	-0.579	0.562
	On-ramp area	**0.143***	**5.294**	**0.000**
	Off-ramp area			
Grade	Less than -2%	**-0.040***	**-2.255**	**0.024**
	Greater than +2%	0.002	0.105	0.917
	Between -2 and +2%			
Curvature (10000/radius of curvature in feet)	Greater than 1.5	-0.012	-0.579	0.563
	Less than or equal to 1.5			
Number of lanes	2 lanes	**0.182***	**7.072**	**0.000**
	3 lanes	0.004	0.180	0.857
	4 lanes			
Speed limit	55 mph	**0.035***	**2.047**	**0.041**
	65 mph			
Variance of residual		0.318		0.000
Variance of random intercept		0.051		0.000
Coefficient of determination			0.14	

* indicates the estimated parameter is significant at a 0.05 level.

Table 14: Model Estimation Results for LOS E and F Ranges

Variables		Estimate	t	Sig.
Intercept		**-0.796***	**-3.192**	**0.003**
Facility Type	Basic Segment	**-0.114***	**-4.073**	**0.000**
	On-ramp area	**0.321***	**6.148**	**0.000**
	Off-ramp area			
Grade	Less than -2%	**-0.190***	**-6.500**	**0.000**
	Greater than +2%	0.040	1.271	0.204
	Between -2 and +2%			
Curvature (10000/radius of curvature in feet)	Greater than 1.5	0.058	1.590	0.112
	Less than or equal to 1.5			
Number of lanes	2 lanes	0.033	0.856	0.392
	3 lanes	-0.016	-0.341	0.733
	4 lanes			
Speed limit	55 mph	**-0.132***	**-4.286**	**0.000**
	65 mph			
Variance of residual		0.342		0.000
Variance of random intercept		0.060		0.000
Coefficient of determination			0.17	

LOS F (N = 4,473)

Variables		Estimate	t	Sig.
Intercept		-0.228	-1.210	0.235
Facility Type	Basic Segment	-0.017	-0.700	0.484
	On-ramp area	**0.153***	**4.850**	**0.000**
	Off-ramp area			
Grade	Less than -2%	**-0.080***	**-3.647**	**0.000**
	Greater than +2%	**0.070***	**3.002**	**0.003**
	Between -2 and +2%			
Curvature (10000/radius of curvature in feet)	Greater than 1.5	0.033	1.183	0.237
	Less than or equal to 1.5			
Number of lanes	2 lanes	0.024	0.726	0.468
	3 lanes	0.000	0.009	0.993
	4 lanes			
Speed limit	55 mph	**-0.083***	**-3.812**	**0.000**
	65 mph			
Variance of residual		0.324		0.000
Variance of random intercept		0.034		0.000
Coefficient of determination			0.09	

* indicates the estimated parameter is significant at a 0.05 level.

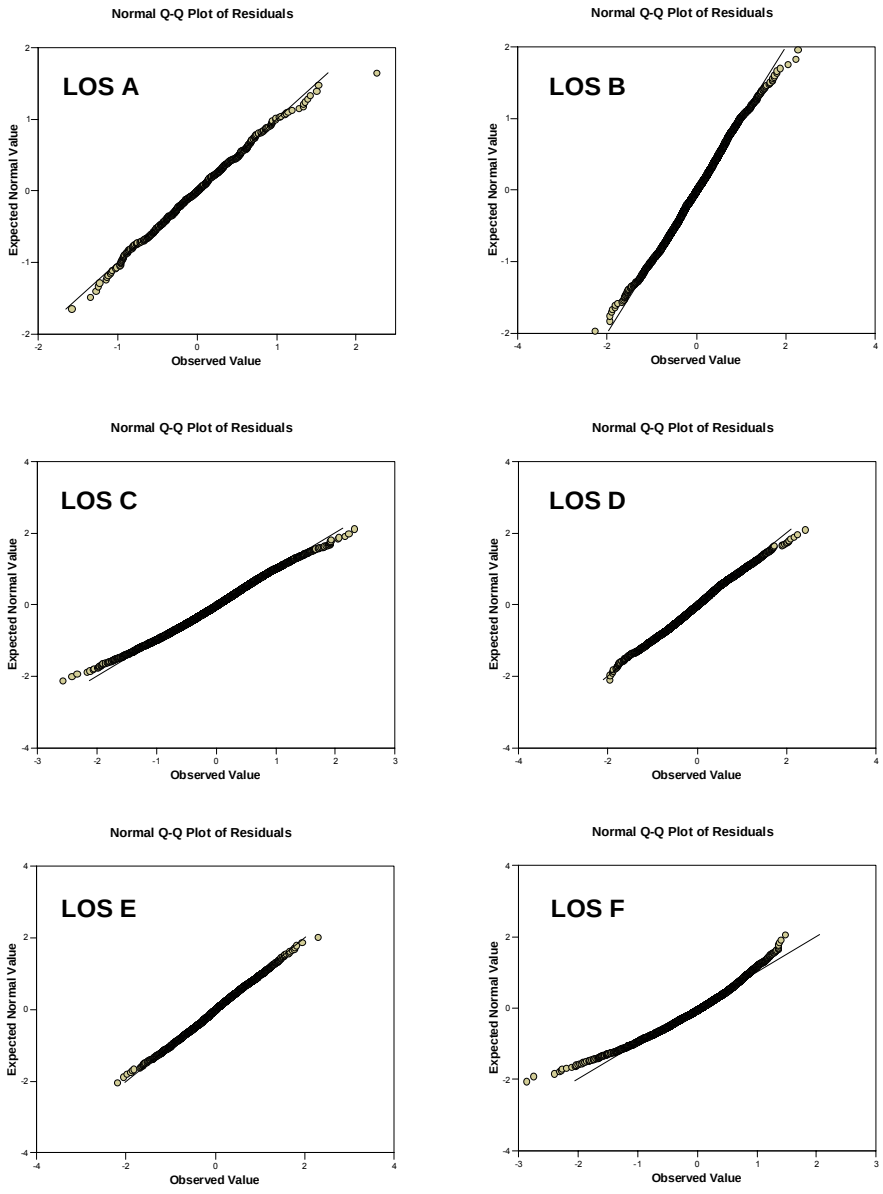

Figure 49: Normal Q-Q Plots of Residuals for Acceleration Noise Models

Interpretation of the Estimated Parameters

The interpretation of the estimated parameters in the model is not straightforward since the dependent variable, acceleration noise, was taken with logs, and thus, the effect of a unit change in independent variables varies depending on the location of the starting point of the independent variables, as in the case of logistic regression models (Neter et al. 1996). This aspect can be mathematically demonstrated using a fitted simple

regression function, $\ln(y) = a + bx$. Based on this function, an initial value, when x=x_1, can be expressed in the following way:

$$\ln(Y_1) = a + bx_1 .$$

In addition, the value reflecting a unit change in the independent variable can be expressed as:

$$\ln(Y_2) = a + b(x_1 + 1) .$$

Thus, $Y_1 = \exp(a + bx_1)$, and $Y_2 = \exp(a + bx_1 + b)$. Using these equations, the difference between Y_2 and Y_1 becomes:

$$Y_2 - Y_1 = e^{a+bx+b} - e^{a+bx} = e^{a+bx}(e^b - 1).$$

Consequently, the effect of the unit increase is a function of x, which implies that the effect depends on the magnitude of x, and thus, the interpretation of the estimated parameter becomes difficult. However, the ratio of Y_2 to Y_1 can cancel out the term that includes x and produces a meaningful value indicating the percent change in acceleration noise for each additional unit of independent variables. The percent change can be expressed as follows:

$$\left(\frac{Y_2}{Y_1} - 1\right) \times 100 = \left(\frac{e^{a+bx+b}}{e^{a+bx}} - 1\right) \times 100 = (e^b - 1) \times 100 \ .$$

For example, when the estimated parameter for a variable is 0.5, the percent change of acceleration noise contributed by the variable is $(e^{0.5} - 1) \times 100$, that is 65%. When the estimated parameter is zero, the percent change reasonably becomes zero. The corresponding metric to the percent change is odds ratio in logistic regression models (Neter et al. 1996).

Effects of Roadway Characteristics on Acceleration Noise

Based on the percent change approach, the effects of facility type were examined by LOS range, as shown in Figure 50, in which the reference variable is off-ramp segment, and thus, it does not appear in the graph. The graph suggests that the effects of facility type vary, depending on traffic conditions. For example, on-ramp segments seldom affect acceleration noise under LOS A-to-C ranges, but they significantly increase acceleration noise after LOS D conditions. This situation may justify the introduction of ramp-metering after LOS D conditions as an attempt to prevent the traffic flow quality of the mainline from degrading because of entering vehicles. The graph also suggests that basic segments tend to exhibit lower acceleration noise than on/off ramp segments.

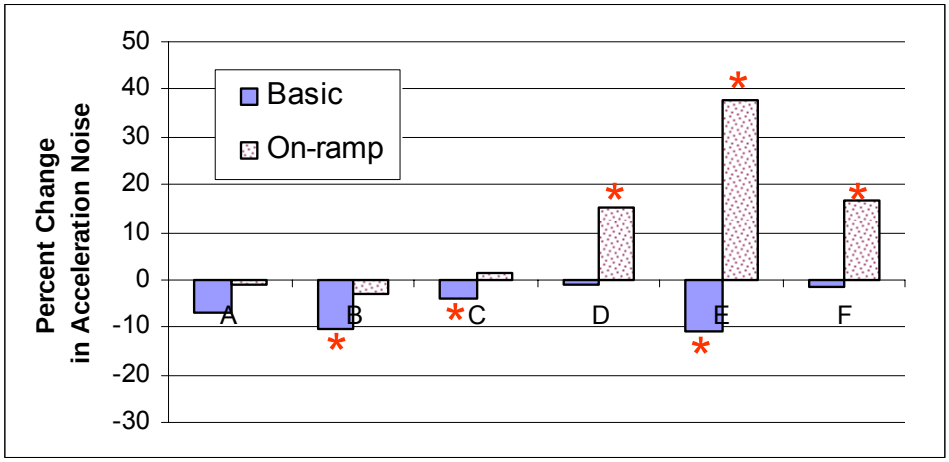

* indicates the variable is significant at a level of 0.05.

Figure 50: Effects of Facility Type on Acceleration Noise (Reference Variable = Off-ramp)

The percent change approach was also applied for capturing the impacts of grade, as shown in Figure 51. The figure indicates that roadway grades can affect acceleration noise in an opposite manner, depending on traffic conditions. Downhill grades (in this study, less than -2%) increase acceleration noise under LOS A-to-C

conditions while they decrease acceleration noise under LOS D-to-F conditions. A possible explanation for this phenomenon is that under free-flow conditions on downgrades, drivers are likely to adjust their speeds to avoid gaining too much speed and running out of control, resulting in an increase of speed fluctuations. Jones and Potts (1962) also reported the trend of increasing acceleration noise for the downhill runs using the data collected during off-peak period, thus free-flow conditions. In contrast, under forced-traffic conditions restricting high-speeding operations, the downgrades may help the traffic flow smoothly move. In case of upgrades (> +2%), the estimated parameter was significant under only LOS F condition, indicating greater acceleration noise for uphill driving with respect to the level terrain (-2 - +2%). This phenomenon appears to reasonably reflect traffic flow quality experienced by drivers because uphill grades generally induce more speed fluctuations under congested conditions, thus low-speed driving. Note that the study corridor contains grades only between -3.7 – 3.4%, meaning that the use of different data set with steeper grades may exhibit different results.

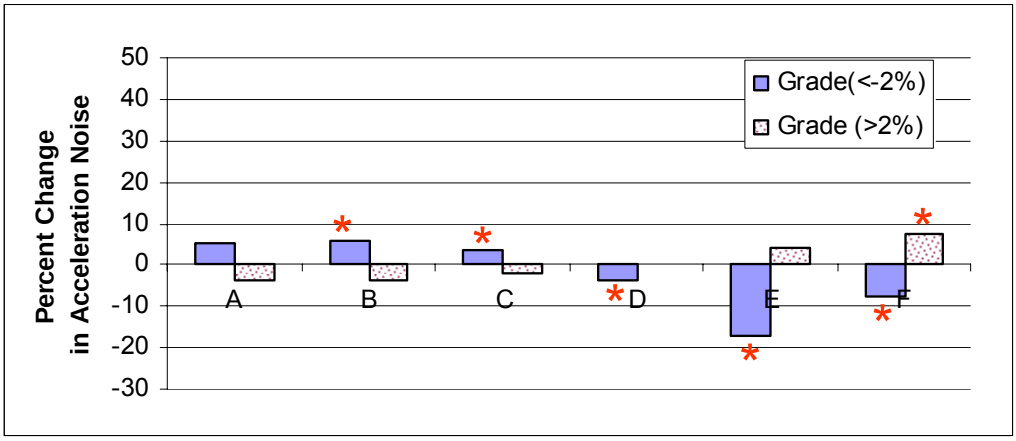

* indicates the variable is significant at a level of 0.05.

Figure 51: Effects of Grade on Acceleration Noise (Reference Variable = Grade between -2 - +2%)

The effects of curvature were also analyzed, as shown in Figure 52, indicating that the degree of curvature plays a significant role under only LOS A conditions. This phenomenon seems reasonable because speeding, requiring a negotiation with roadway curvature, is more likely to occur under LOS A.

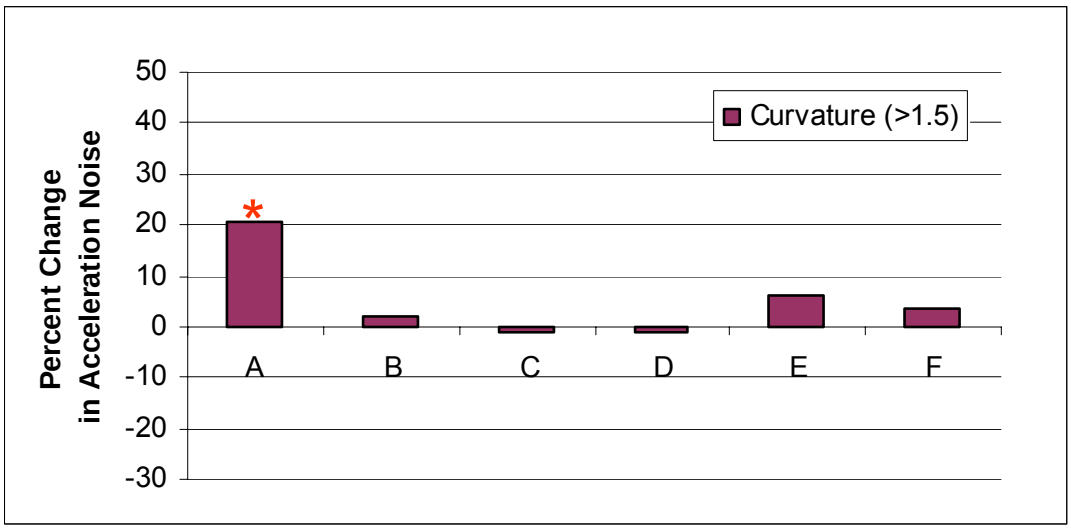

* indicates the variable is significant at a level of 0.05.

Figure 52: Effects of Curvature on Acceleration Noise (Reference Variable = Curvature ≤ 1.5)

In addition, the effects of the number of lanes were analyzed, as shown in Figure 53. The figure indicates that three-lane and four-lane segments have little difference while two-lane segments tend to considerably increase acceleration noise under LOS A-to-D conditions. However, the effects of the number of lanes seemingly disappear under LOS E and F conditions.

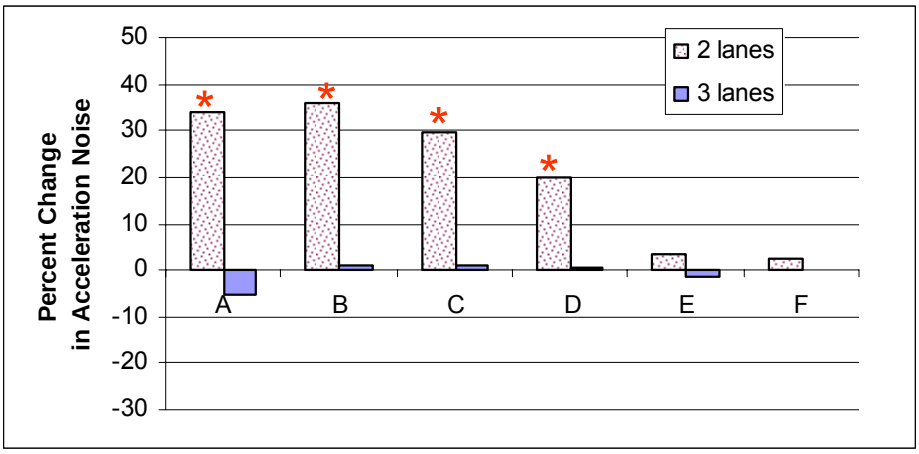

* indicates the variable is significant at a level of 0.05.

Figure 53: Effects of the Number of Lanes on Acceleration Noise (Reference Variable = 4 lanes)

Finally, the effect of speed limit was examined, as illustrated in Figure 54. The figure indicates that the segments with a speed limit of 55 mph tend to increase acceleration noise under LOS A-to-D ranges, as can be expected. However, this phenomenon reverses under LOS E and F ranges, in which speed limit may have little effects on vehicle operations because of the constrained traffic conditions. One possible reason for this phenomenon is the relative traffic flow quality with respect to speed limit. In other words, for the same travel speed below speed limit, the relative traffic flow quality would be better for the trips made under the segments with a lower speed limit. An important implication associated with this fact (the better traffic flow quality for the lower speed limits under LOS E and F ranges) is that the postponement of the onset of system breakdown may be possible by lowering speed limit. However, the verification of this conjecture requires more detailed investigation.

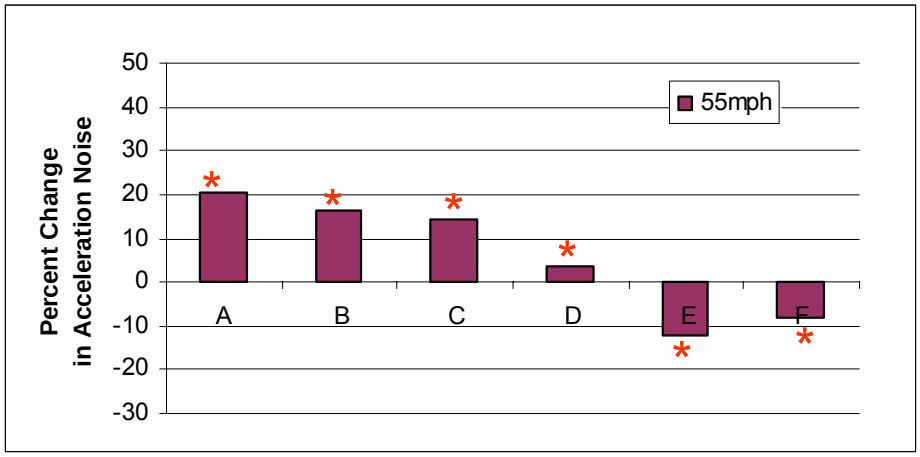

* indicates the variable is significant at a level of 0.05.

Figure 54: Effects of Speed Limit on Acceleration Noise (Reference Variable = 65mph)

LOS-by-LOS Effects

In the previous section, the effects of roadway characteristics were examined on a variable-by-variable basis, revealing the dynamics of the effects depending on traffic conditions. Such dynamics was examined as shown in Figure 55, which displays the changing pattern of percent changes depending on LOS ranges for all the variables considered in the models. The figure indicates that the number of lanes is the most significant factor under LOS A-to-C conditions, implying that acceleration noise tends to considerably increase on two-lane roadway segments. In addition, the graph reveals that number of lanes (i.e., two-lane segments) and facility types (i.e., on-ramp segments) are almost equally the most significant factors under LOS D range. However, under LOS E and F ranges, facility types (i.e., on-ramp segments) appear to be the most significant factor while the significance of the number of lanes becomes noticeably weak. In addition to the number of lanes and facility type, speed limit seems significant under LOS A-to-C ranges, implying that operational characteristics of the roadway are more influential than roadway geometrics such as grade and curvature, at least for the

study corridor. This phenomenon may be reasonable in that the study area is a freeway corridor of which geometric conditions cannot be severely poor due to its higher roadway design standards.

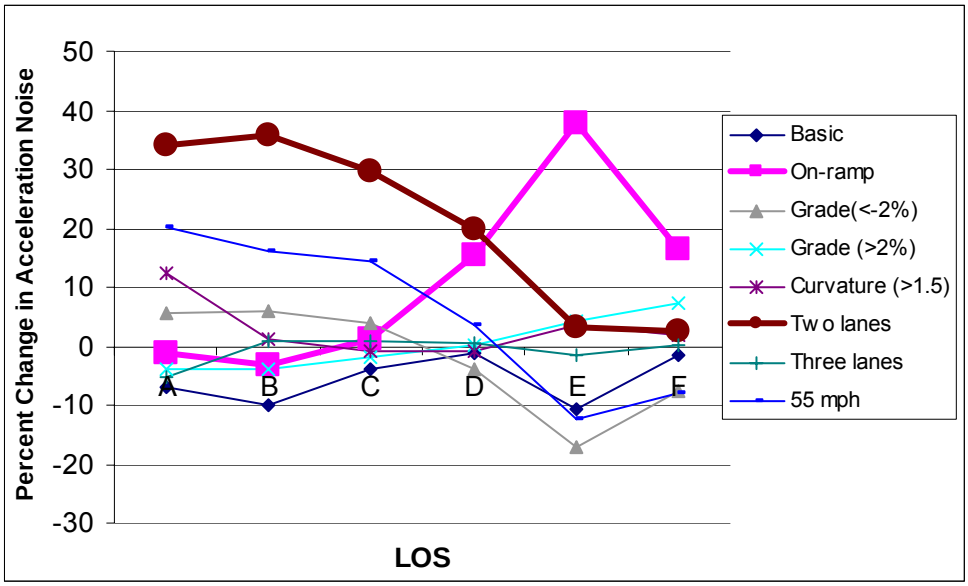

Figure 55: LOS-by-LOS Effects of Roadway Characteristics

Summary

In this chapter, the effects of roadway characteristics were analyzed using the random intercept models developed for six LOS ranges, with the aim of investigating their varied effects depending on traffic conditions. Models were successfully developed although their explanatory power appeared to be low, as suggested by the low R^2 values (e.g., at most 0.20 for the LOS A model). The estimated parameters appeared to be intuitively correct, and they reflected the effects of considered variables depending on traffic conditions. The findings obtained from the analysis can be summarized as follows:

- In general, basic segments provide better traffic flow compared to on/off-ramp areas. However, the differences among the facility types do not appear under LOS A conditions.
- As traffic conditions become unstable, traffic flows on on-ramp areas are detrimentally degraded. In fact, the effects of on-ramp areas under LOS E conditions showed the greatest effects in terms of the metric, percent change.
- For the study data set, no difference was found between four-lane and three-lane segments. However, two-lane roadways appeared to significantly increase acceleration noise under LOS A-to-D ranges.
- The effects of curvature are only pronounced under LOS A condition, implying that only high-speeding vehicles may be affected by the degree of curvature. As the degree of curvature increases, acceleration noise tends to increase.
- Grade effects appeared to be complex, as suggested by the change of the direction of effects. This aspect may require a more detailed analysis for the grade effects. However, the grade effects were found to be minimal compared to other variables for the study site.
- The operational characteristics (number of lanes, speed limit, and facility type) of freeway were found to be more influential than roadway geometry (i.e., grade and curvature).

The analysis results suggest that the effects of roadway characteristics can interact with traffic conditions, implying that the consideration of the interaction effects may enhance the understanding of traffic flow characteristics.

Chapter 8

Acceleration Noise and Driver/Vehicle Characteristics

Study Objectives

Researchers have argued that acceleration noise is affected by vehicle/driver as well as by traffic conditions and roadways. However, the evidence of this aspect has not yet been satisfactorily provided, mainly due to the difficulty in recruiting various drivers/vehicles for such study. In fact, previous research efforts employed only a small number of vehicles/drivers, and thus, could not effectively and objectively identify driver/vehicle effects on acceleration noise. The instrumented vehicle data employed in this study provide a unique research opportunity to effectively examine the effects of vehicle/driver characteristics using the larger driver/vehicle group. Thus, based on the instrumented vehicle data, this study attempts to develop statistical models showing the relationships between acceleration noise and such variables as driver age, gender, household income, vehicle body type, and vehicle age. In addition to the acceleration models, speed models were also developed so that the question—how differently the driver/vehicle characteristics affect speed and acceleration noise—can be examined by comparing the two models. In the model development, the data set was segmented by LOS ranges, and separate models for each LOS range were developed, in an attempt to capture the various behavioral responses of drivers to the different level of traffic conditions. In the attempt, only LOS A-to-D ranges were considered since driver and

vehicle behavioral differences are less likely to appear under the forced traffic conditions, LOS E and F.

Data

Data Collection Time Period and Roadway Segments

The initial data set for this analysis of driver/vehicle effects was obtained from four segments of GA400 during the time period between October 2003 and August 2004 (excluding trips under potentially raining conditions, see Chapter 7). Only four segments were selected for the following reasons. First, the data size for the entire segments was far too large to handle. In fact, approximately 265,000 segmented trips were collected over the 89 segments during the eleven months, and thus, computational burden was expected for the use of the entire data set. Second, the use of trip data from various roadway segments complicates the analysis. As suggested by the analysis results reported in the previous chapter, acceleration noise can be affected by roadway characteristics, requiring an isolation of geometric effects for a proper assessment of driver/vehicle effects. The four segments were selected based on the following criteria: 1) two sites per direction, 2) a mixture of different roadway characteristics, 3) basic segments only, 4) minimal grade and curvature, and 5) maximizing sample size. Items 1 and 2 pursue the even distribution of segments in terms of location and characteristics, and items 3 and 4 pursue the minimization of geometric disturbances that might affect acceleration noise. Unlike other studies in which test vehicles travel along designated routes during specific time periods, the data collection approach of this study is less controlled but yields a large data set.

Exclusion of Shared Vehicles

As dictated by the study objective of this chapter, the appropriate identification of the driver for any specific instrumented vehicle is critical. However, the identification becomes difficult if the vehicle is significantly shared by multiple persons in the household. To avoid this problem, this research referred to the vehicle sharing percentages obtained from the survey in which the project participants were asked to list each household vehicle, provide the primary driver of the vehicle, any secondary drivers, and the estimated amount of driving by each driver (Ogle 2005). Based on this reported vehicle sharing information, this research excluded the trips made by the vehicles with the primary drivers' driving time percentages lower than 90%. This data screening criteria resulted in reducing the number of vehicles by 7% (6% for the number of trips).

Data Summary

Table 15 summarizes the characteristics of the selected four segments. As mentioned earlier, the table indicates that two basic segments for each direction and two 3-lane and two 4-lane segments were selected. Table 16 summarizes data size, average speed and acceleration noise for each LOS range, indicating the data set is composed of 6,271 trips from 224 instrumented vehicles.

Table 15: Characteristics of Selected Segments

Segment	Length (mile)	Speed Limit (mph)	Grade (%)	Curvature	Number of Lanes	Facility Type
SB13	0.25	65	+1.35	0.2	3	Basic
SB35	0.32	65	+1.78	0.5	4	Basic
NB17	0.20	65	-0.20	0.4	4	Basic
NB34	0.23	65	+1.00	1.5	3	Basic

* Curvature was computed as 10,000/radius of curvature in feet.

Table 16: Average Values of Speed and Acceleration Noise and Sample Size by LOS

LOS	Average Speed (mph)	Average Acceleration Noise (mph/s)	Sample Size	Number of Vehicles/Drivers
A	71.5	0.23	965	136
B	71.4	0.26	1,983	194
C	70.9	0.30	2,297	183
D	65.9	0.37	1,026	125
Overall			6,271	224

Driver/Vehicle Distributions

The sampled driver/vehicle distributions are illustrated in Figure 56 and they are briefly compared with the national average. The comparison with the national percentages of licensed drivers by age group indicates that the sample size for the age group under 25 is smaller (7% vs. national average 13%) while the sample size for the age group of 35-45 seems larger (28% vs. national average 21%). However, the general pattern does not significantly deviate from the national average. In case of gender, the distribution is close to the national trend which indicates that the number of male drivers is slightly higher than that of female drivers (50.1% versus 49.9%). (The values of the national average are based on (FHWA 2003) In case of household income, the sampled data illustrate that the proportion of high income households is large while the proportion of low income households is small. Thus, the income distribution for the selected data set is biased toward high income households (Ogle et al. 2005).

In case of vehicle body type, passenger cars occupy the largest portion (i.e., about 59%). This proportion is similar to the national average 56.8% (based on the vehicle file of the 2001 National Household Travel Survey published by the U.S. Department of Transportation), and the proportion of vans (9% vs. national average 9.1%) is also similar. However, the percentages of SUVs (18%) and pick-ups (14%) show somewhat different values from the national average (SUVs- 11.9%; pick-ups – 18.3%). The distribution of vehicle age was compared with the national distribution used in the MOBILE6 model, an emissions analysis tool developed by the Environmental Protection Agency (EPA). The comparison indicates that the sampled data contain fewer older vehicles. For example, the percentages of vehicles older than 10 years are 17% and 33% for the sampled data and the national average, respectively. The major reason for the smaller portion of old vehicles is because only vehicles traveled more than 3,000 miles/year were instrumented in the Commute Atlanta project (Ogle et al. 2006), and thus, older vehicles in the participants' households are likely to be removed from the target of the instrumentation. However, the general patterns of the vehicle age distributions are not significantly different from the national average. Figure 56 also indicates that LOS-by-LOS distributions do not significantly differ.

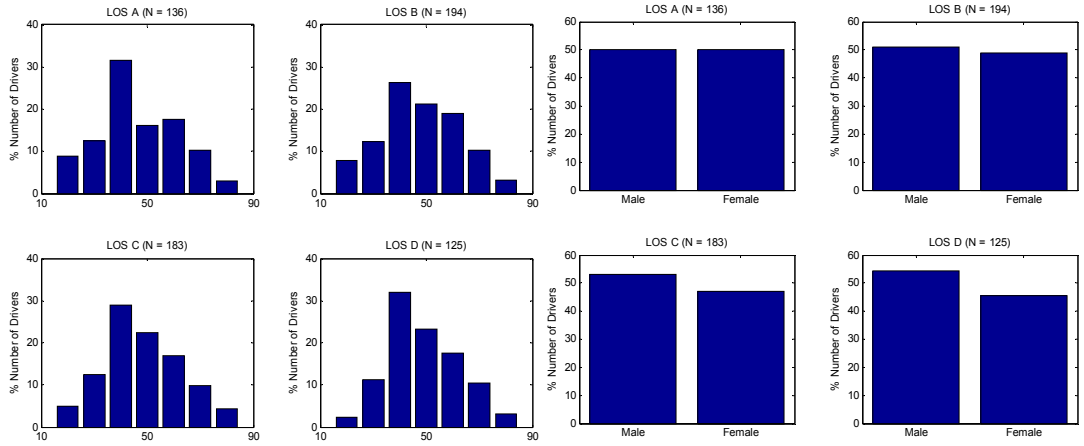

(a) Age (b) Gender

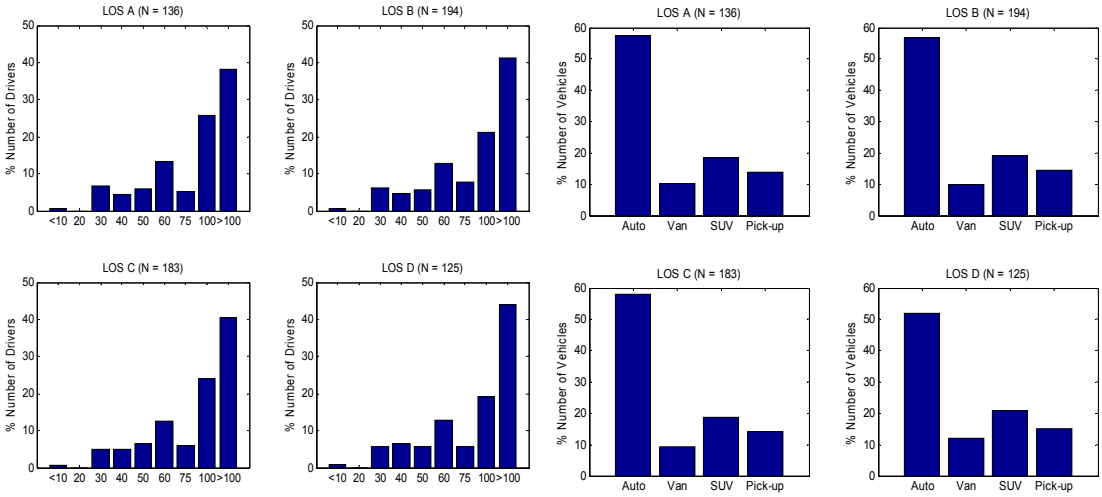

(c) Household Income (unit: $1000) (d) Vehicle Body Type

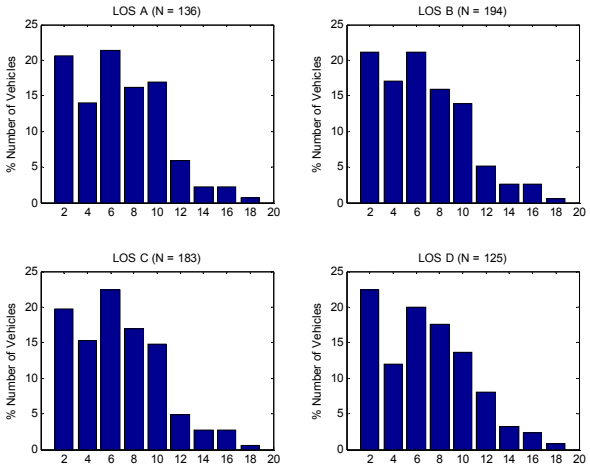

(e) Vehicle Age

Figure 56: Distributions of Driver and Vehicle (N = 224)

Relationships Among Driver/Vehicle Characteristics

The relationships among driver and vehicle characteristics were examined for the selected 224 drivers/vehicles by obtaining distributions or scatter plots. First, the relationship between driver gender and vehicle type was examined, as shown in Figure 57. The figure, illustrating the distributions of the number of male and female drivers by vehicle type, indicates that vans are more likely to be driven by female drivers and that a majority of pick-up trucks in the data set were driven by male drivers. In fact, the data set contains only two female drivers out of 32 pick-up truck drivers. This situation seems to coincide with the general expectations associated with the pattern of vehicle usage, indicating the appropriateness of the selected data set.

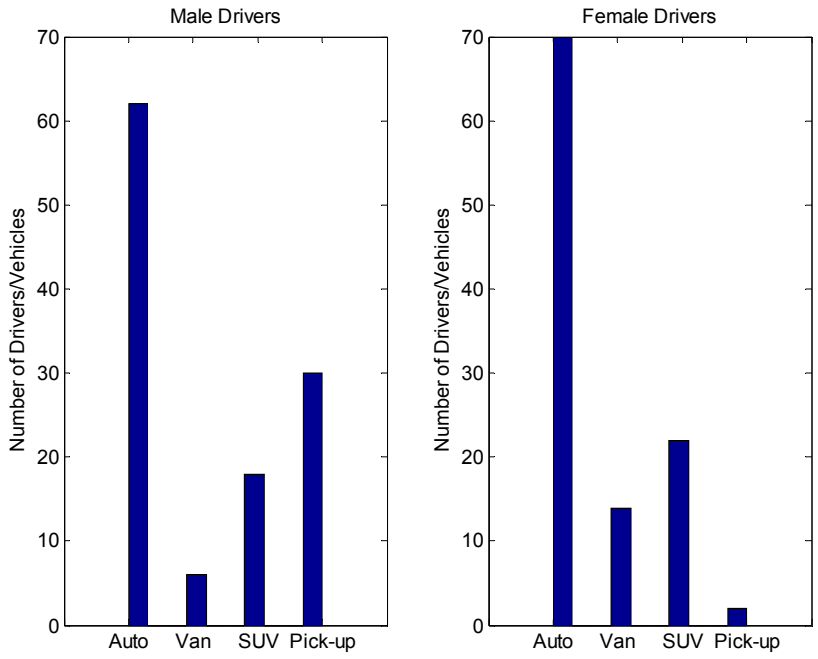

Figure 57: Distributions of Number of Male and Female Drivers by Vehicle Body Type (N=224)

Second, the relationships between vehicle type, driver age, and vehicle age were examined by obtaining scatter plots, as shown in Figure 58. The figure indicates that

vans or pick-up trucks are less likely to be driven by younger drivers (i.e., younger than 35 years old). However, significant correlations are not found between vehicle type and driver age. The scatter plot showing the relationship between vehicle type and vehicle age also indicates that they have no significant correlations. Third, the relationship between driver age and gender was examined (Figure 59), suggesting no significant correlations between the two driver characteristics. The mean ages are 50 and 45 years old for male and female drivers, respectively. In addition, any significant correlations between the other driver/vehicle characteristics were not found although their scatter plots are not reported in this dissertation.

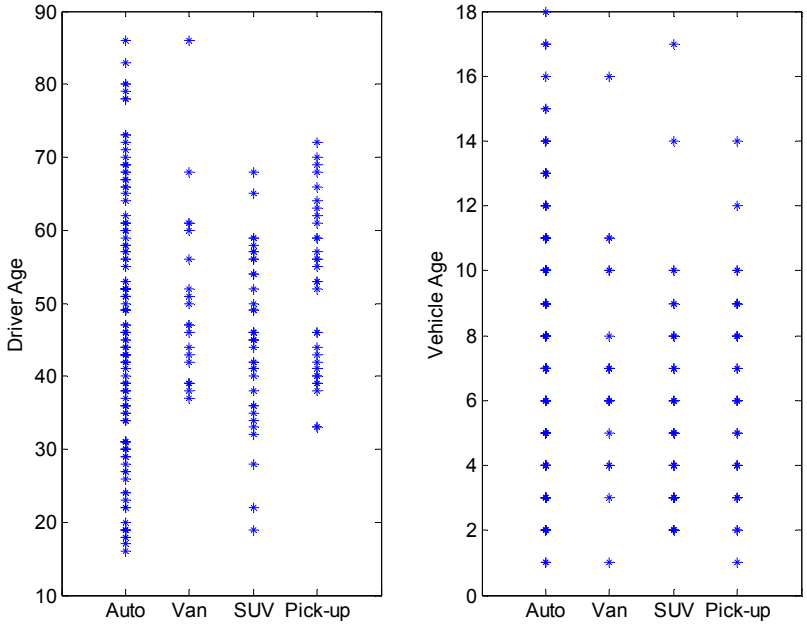

Figure 58: Relationships between Vehicle Type, Driver Age, and Vehicle Age (N=224)

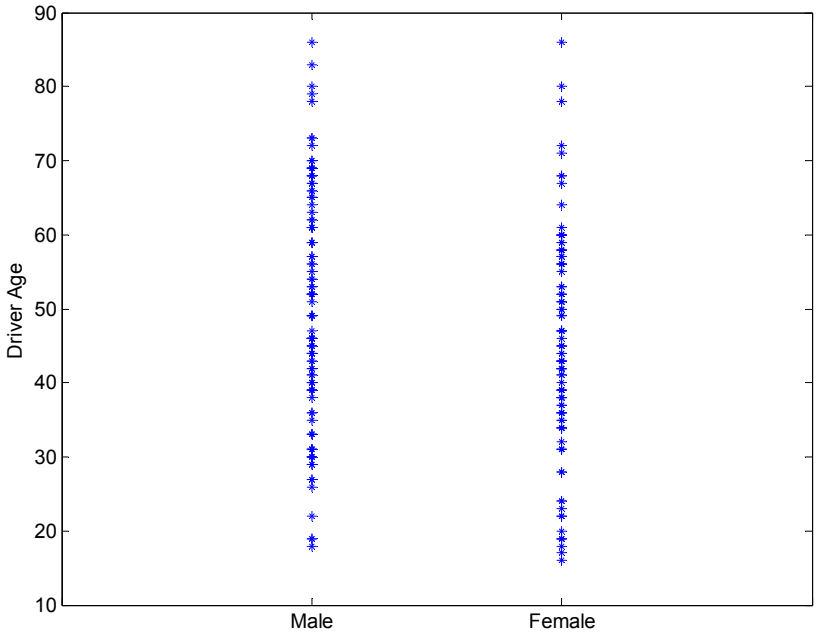

Figure 59: Relationship between Driver Age and Gender (N=224)

Model Development

Explanatory and Response Variables

The explanatory variables of the statistical model developed in this analysis are driver age, gender, annual household income, vehicle body type, and vehicle age. Among them, annual household income was aggregated into three categories: less than $50,000; $50,000 - $100,000; and greater than $100,000. This aggregation was performed since the initial nine classes, requiring eight parameters to be estimated, were considered excessive, and the sample size of the low-income group was too small. In addition, driver age and vehicle age were also aggregated into four (younger than 20, 20 – 39, 40 – 59, and older than or equal to 60 years old) and three categories (younger than 5, 5 – 9, and older than or equal to 10 years old), respectively, and thus, these variables were used as discrete variables, rather than continuous variables. This data binning is based on the notion that the variables (driver age and vehicle age) may not be linearly related

to dependent variables (vehicle speed or acceleration noise). For example, an increase in driver age by one may have different effects on driver speeding behavior, depending on the reference ages (e.g., from 19 to 20 years old vs. from 59 to 60 years old).

For the model development, only main effects were considered, and thus, interaction effects between explanatory variables were not included in the model. The consideration of interaction effects is not practical because of the following two reasons: 1) complexity of model development and interpretation and 2) occurrence of missing factor combinations. For example, a consideration of interaction effects between driver age and vehicle type introduces additional 15 variables (four driver age groups × four vehicle types – one reference variable), resulting in a complex model output and correspondingly complicated interpretations. In addition, the limited number of drivers/vehicles may produce zero degrees of freedom (no data) for some factor combinations. In fact, the selected data set does not include even a single trip made by female pick-up drivers under LOS A condition. As another example, the data set does not include van or pick-up drivers younger than 20 years old (Figure 58), resulting in zero degrees of freedom for the combinations of such driver age group and van (or pick-up). Although the exclusion of interaction effects may not fully describe the causal relationships between the independent and dependent variables, general ideas may be obtained by considering the main effects only.

In addition to the variables associated with driver/vehicle characteristics, daylight conditions, which may affect vehicle speed profiles, were also considered as an explanatory variable. In a simple manner as explained in the previous chapter, if a trip was made between 7:00am and 7:00pm during a daylight savings time period or

between 8:00am and 6:00pm during a non-daylight savings time period, the trip was designated as a trip under daylight conditions. Otherwise, the trip was designated as a non-daylight trip. The location of a trip was also considered since different geometrics can affect vehicle speed profiles. Thus, in an attempt to isolate the geometric effects from the model, each segment was employed as a dummy variable.

As a response variable, acceleration noise was taken with a natural log so that its distribution would be closer to normal, as shown in Figure 60. In fact, the transformation enhanced the normality of the data set, as suggested in Table 17. The table exhibits the results of one-sample KS normal tests, indicating that the log-transformed data are not significantly different from normal distributions at a level of 0.05.

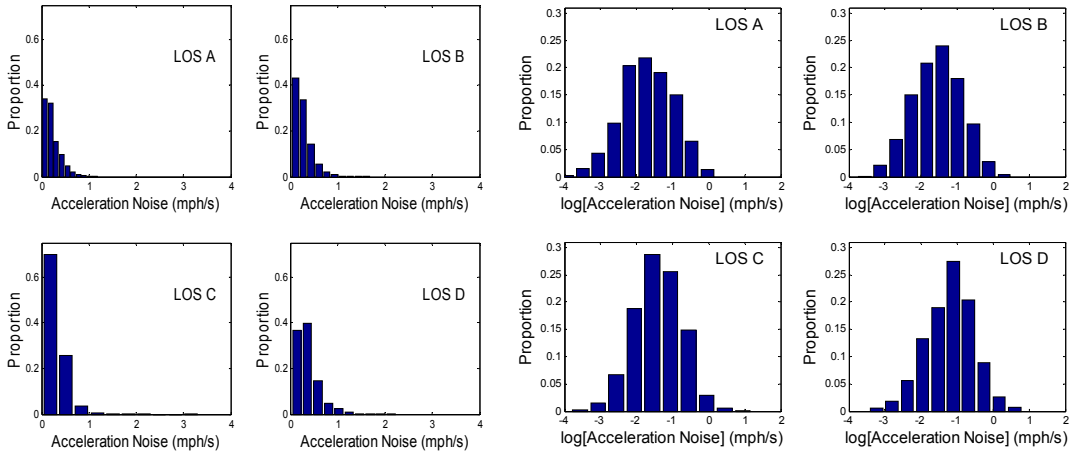

Figure 60: Log Transformation of Acceleration Noise

Table 17: Results of One-Sample Normal KS Tests for Before and After Log-Transformation

LOS	Before		After	
	K	p-value	K	p-value
A	0.134	0.000	0.027	0.506
B	0.119	0.000	0.022	0.302
C	0.121	0.000	0.021	0.271
D	0.124	0.000	0.036	0.146

Model Results

In total, eight random intercept models (acceleration noise and speed models for each LOS A-to-D ranges) were developed. For these models, the normality of residuals was examined by plotting normal Q-Q plots for residuals, as shown in Figure 61. Although the figure indicates that the residuals for the speed model under LOS D appear to have a large number of outliers, which may be attributed to the instability of traffic conditions under the range, it generally supports the normality assumption. In addition to the residual plots, the variances for random intercepts were examined. As a result, they were found to be highly significant, as suggested by the low *p*-values, supporting the validity of random intercept models. If the variances are not significant, the application of random intercept model becomes meaningless, and thus, the ordinary regression model is enough to evaluate the causal relationships between acceleration noise and the independent variables.

The explanatory power of the models was examined by the coefficients of determination (R^2). The R^2 values were within the range of 0.18 – 0.22 and 0.27 – 0.42 for the acceleration noise and speed models, respectively. These low R^2 values, in particular for the acceleration noise models, may suggest that vehicle speed profiles were affected by numerous factors in addition to the variables considered in the models.

Table 18: Model Estimation Results for LOS A Range

LOS A (N = 965)

Variables		Log (Acceleration Noise)		Speed	
Intercept		**-1.795***	**(0.000)**	**68.092***	**(0.000)**
Driver Age (years)	< 20	-0.112	(0.600)	**10.004***	**(0.000)**
	20 - 39	-0.071	(0.567)	**6.141***	**(0.000)**
	40 - 59	0.026	(0.814)	**4.247***	**(0.000)**
	≥ 60		.		.
Gender	Male	0.034	(0.713)	1.441	(0.072)
	Female		.		.
Household Income ($1,000's)	< 50	0.030	(0.811)	-0.253	(0.813)
	50 - 100	-0.080	(0.404)	-0.697	(0.393)
	> 100		.		.
Vehicle Type	Van	-0.147	(0.270)	-1.754	(0.129)
	SUV	-0.125	(0.278)	-0.780	(0.431)
	Pick-up	**-0.304***	**(0.023)**	1.315	(0.250)
	Passenger Car		.		.
Vehicle Age (years)	0 - 4	0.127	(0.259)	-0.470	(0.625)
	5 - 9	0.089	(0.368)	-0.711	(0.401)
	≥ 10		.		.
Segment	SB13	-0.004	(0.962)	-0.389	(0.534)
	NB17	0.067	(0.358)	0.173	(0.750)
	NB34	**0.189***	**(0.012)**	**-1.459***	**(0.008)**
	SB35		.		.
Daylight Condition	No	-0.018	(0.731)	**-1.669***	**(0.000)**
	Yes		.		.
Variance of residual		0.393	(0.000)	20.878	(0.000)
Variance of random intercept		0.097	(0.000)	8.814	(0.000)
Coefficient of determination		0.22		0.27	

Note: p-values are inside parentheses, and * indicates that the estimated parameter is significant at a 0.05 level.

Table 19: Model Estimation Results for LOS B Range

LOS B (N = 1,983)

Variables		Log (Acceleration Noise)		Speed	
Intercept		**-1.769***	**(0.000)**	**71.127***	**(0.000)**
Driver Age (years)	< 20	**0.382***	**(0.026)**	**5.720***	**(0.000)**
	20 - 39	0.089	(0.310)	**3.805***	**(0.000)**
	40 - 59	0.122	(0.128)	0.983	(0.182)
	≥ 60		.		.
Gender	Male	0.061	(0.357)	**1.271***	**(0.040)**
	Female		.		.
Household Income ($1,000's)	< 50	-0.031	(0.728)	-1.427	(0.082)
	50 - 100	-0.078	(0.256)	-0.133	(0.833)
	> 100		.		.
Vehicle Type	Van	-0.002	(0.983)	-0.603	(0.505)
	SUV	0.047	(0.573)	-0.765	(0.323)
	Pick-up	-0.114	(0.221)	-0.796	(0.357)
	Passenger Car		.		.
Vehicle Age (years)	0 - 4	-0.021	(0.805)	0.437	(0.569)
	5 - 9	0.129	(0.088)	-0.135	(0.846)
	≥ 10		.		.
Segment	SB13	-0.077	(0.110)	**-2.516***	**(0.000)**
	NB17	-0.019	(0.624)	**-1.074***	**(0.001)**
	NB34	0.087	(0.055)	**-4.482***	**(0.000)**
	SB35		.		.
Daylight Condition	No	-0.011	(0.733)	**-2.014***	**(0.000)**
	Yes		.		.
Variance of residual		0.355	(0.000)	21.746	(0.000)
Variance of random intercept		0.085	(0.000)	8.614	(0.000)
Coefficient of determination		0.18		0.32	

Note: *p*-values are inside parentheses, and * indicates that the estimated parameter is significant at a 0.05 level.

Table 20: Model Estimation Results for LOS C Range

LOS C (N = 2,297)

Variables		Log (Acceleration Noise)		Speed	
Intercept		**-1.593***	**(0.000)**	**69.336***	**(0.000)**
Driver Age (years)	< 20	0.290	(0.169)	**5.523***	**(0.003)**
	20 - 39	0.174	(0.058)	**4.015***	**(0.000)**
	40 - 59	0.080	(0.325)	**1.945***	**(0.007)**
	≥ 60		.		.
Gender	Male	0.071	(0.298)	0.921	(0.126)
	Female		.		.
Household Income ($1,000's)	< 50	-0.057	(0.542)	-0.878	(0.287)
	50 - 100	-0.003	(0.965)	0.403	(0.504)
	> 100		.		.
Vehicle Type	Van	**-0.227***	**(0.025)**	-1.179	(0.188)
	SUV	-0.065	(0.454)	-0.618	(0.421)
	Pick-up	**-0.284***	**(0.003)**	0.100	(0.906)
	Passenger Car		.		.
Vehicle Age (years)	0 - 4	**0.177***	**(0.045)**	-0.003	(0.997)
	5 - 9	0.098	(0.195)	-0.375	(0.575)
	≥ 10		.		.
Segment	SB13	**-0.103***	**(0.005)**	**-2.280***	**(0.000)**
	NB17	-0.034	(0.256)	**-1.550***	**(0.000)**
	NB34	**0.166***	**(0.016)**	**-6.391***	**(0.000)**
	SB35		.		.
Daylight Condition	No	0.042	(0.225)	**-1.344***	**(0.000)**
	Yes		.		.
Variance of residual		0.329	(0.000)	24.534	(0.000)
Variance of random intercept		0.080	(0.000)	6.490	(0.000)
Coefficient of determination		0.19		0.30	

Note: *p*-values are inside parentheses, and * indicates that the estimated parameter is significant at a 0.05 level.

Table 21: Model Estimation Results for LOS D Range

LOS D (N = 1,026)

Variables		Log (Acceleration Noise)		Speed	
Intercept		**-1.217***	**(0.000)**	**66.088***	**(0.000)**
Driver Age (years)	< 20	0.313	(0.385)	3.846	(0.286)
	20 - 39	0.015	(0.905)	**3.244***	**(0.010)**
	40 - 59	-0.015	(0.889)	1.164	(0.263)
	≥ 60		.		.
Gender	Male	0.076	(0.398)	-0.108	(0.903)
	Female		.		.
Household Income ($1,000's)	< 50	-0.071	(0.564)	-1.804	(0.145)
	50 - 100	0.045	(0.620)	1.251	(0.163)
	> 100		.		.
Vehicle Type	Van	-0.104	(0.397)	0.438	(0.715)
	SUV	-0.015	(0.891)	-0.958	(0.377)
	Pick-up	**-0.421***	**(0.001)**	1.293	(0.278)
	Passenger Car		.		.
Vehicle Age (years)	0 - 4	-0.003	(0.980)	1.479	(0.179)
	5 - 9	0.046	(0.646)	0.906	(0.355)
	≥ 10		.		.
Segment	SB13	**-0.145***	**(0.014)**	**-1.435***	**(0.020)**
	NB17	**-0.100***	**(0.029)**	**-4.316***	**(0.000)**
	NB34	**0.727***	**(0.000)**	**-22.430***	**(0.000)**
	SB35		.		.
Daylight Condition	No	-0.032	(0.539)	**-1.897***	**(0.001)**
	Yes		.		.
Variance of residual		0.331	(0.000)	36.657	(0.000)
Variance of random intercept		0.081	(0.001)	7.042	(0.002)
Coefficient of determination		0.21		0.42	

Note: *p*-values are inside parentheses, and * indicates that the estimated parameter is significant at a 0.05 level.

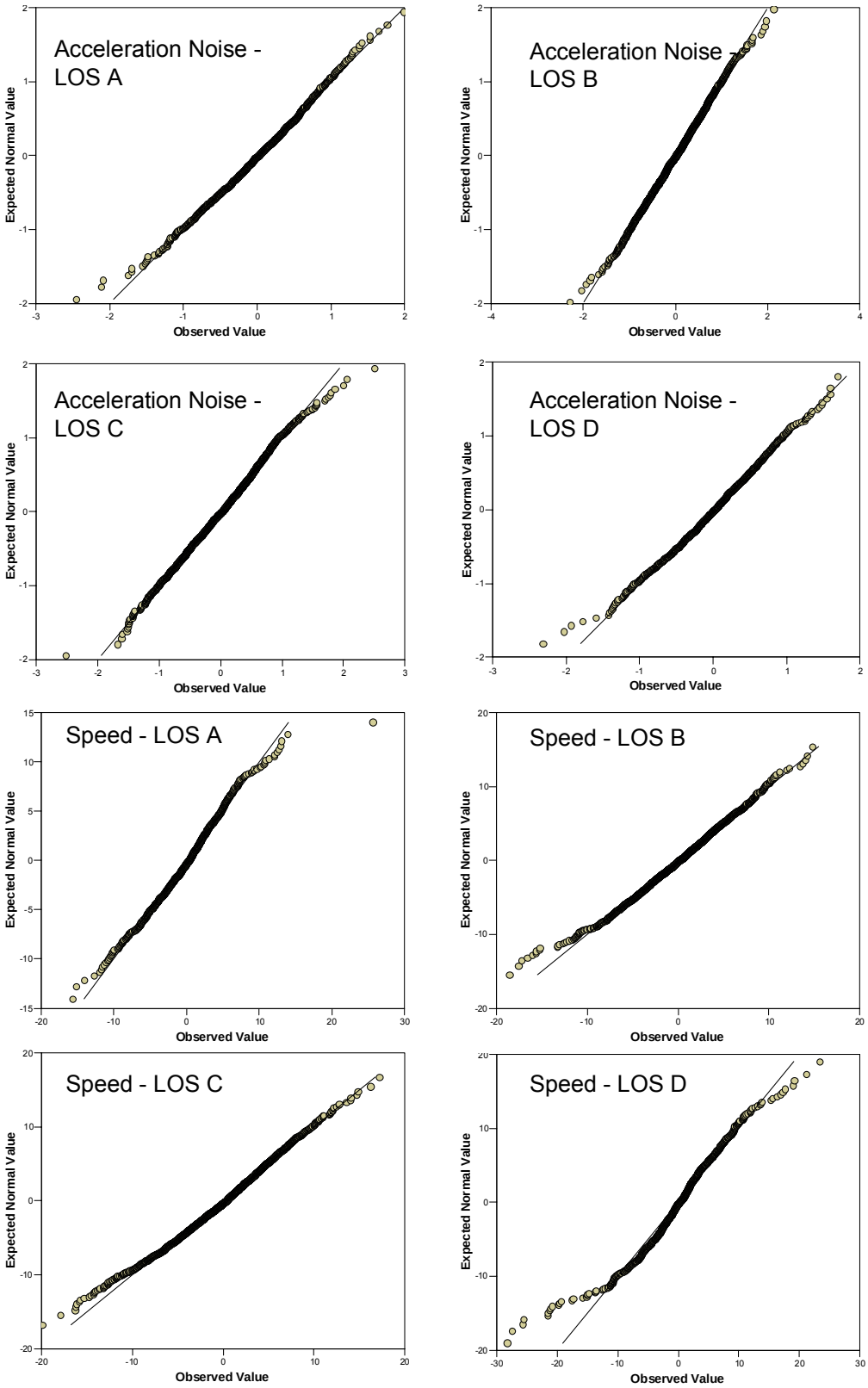

Figure 61: Normal Q-Q Plots of Residuals for Acceleration Noise and Speed Models

Effects of Driver Characteristics

The estimated results indicate that driver age is the most important variable among the driver characteristics. Also, the significance levels indicate that the effect of age is more pronounced for speed for all considered LOS ranges while the effect of age on acceleration noise is significant only for the LOS B model. The acceleration noise model for LOS B range implies that the young drivers (less than 20 years old) exhibit higher acceleration noise than the other age groups. The signs and magnitudes of the driver age parameters imply that the younger drivers tend to drive faster than the other age groups. For example, the speed model for LOS A indicates that drivers younger than 20 years old tend to drive faster than drivers older than 60 years old by 10 mph on average. In addition, the effects of driver age on speed appear to diminish as traffic conditions become worse, as suggested by the magnitude of the parameters (i.e., for the age group less than 20 years old, LOS A: 10.0; LOS B: 5.7; LOS C: 5.5; and D: 3.8). This finding implies that the developed models appropriately reflect the interactions of driver behavior and traffic conditions. Meanwhile, gender is insignificant for all models at a level of 0.05 except for the LOS B speed model. The model indicates that male drivers tend to drive faster than female drivers by 1.3 mph on average. Any significant differences between male and female drivers are not found for acceleration noise. In case of household income, the variable is insignificant in all models, indicating little associations between household income and speed/acceleration behavior. This phenomenon may be partly attributed to the biased sample toward high-income group.

The changing patterns of *p*-values by LOS levels were illustrated in Figures 62 and 63, in which the variable is considered significant at a significance level of 0.05 if

p-value is less than 0.05. Figure 62 clearly suggests that the variable of age is significant for all speed models while the variable is insignificant for all acceleration noise models except for LOS B range. Meanwhile, gender is significant at a level of 0.05 only for the speed model of LOS B, indicating that gender is not a significant variable for acceleration noise, at least for the data set. These findings imply that acceleration noise may be less sensitive to drivers' characteristics than speed.

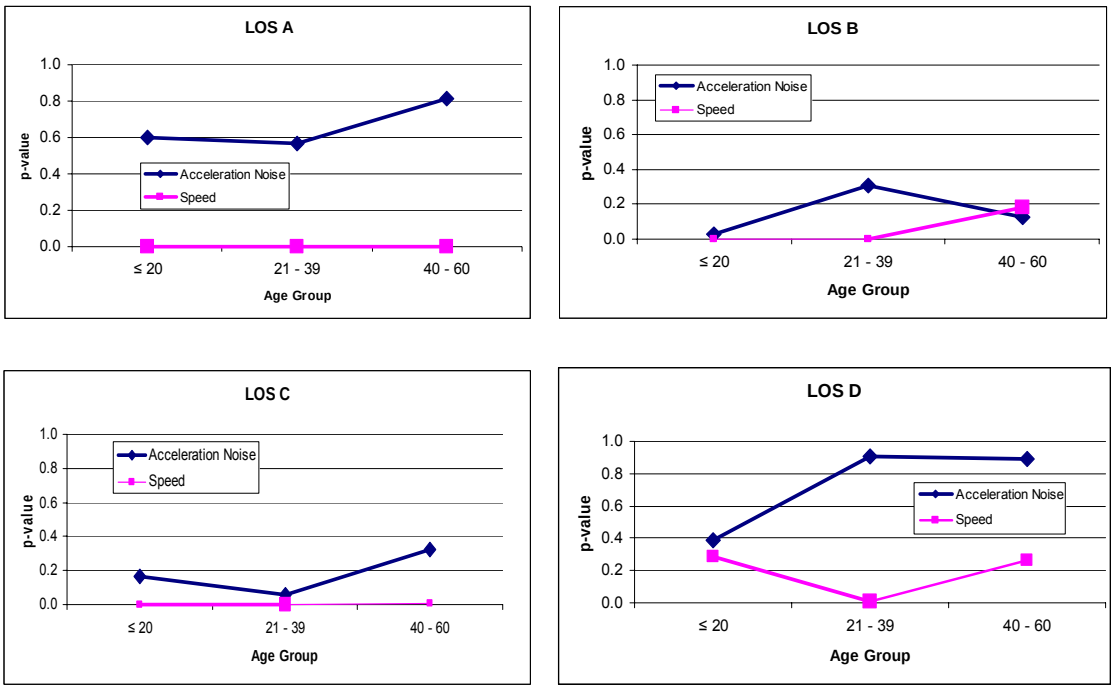

Figure 62: Changing Patterns of *p*-values for Age Groups by LOS Range

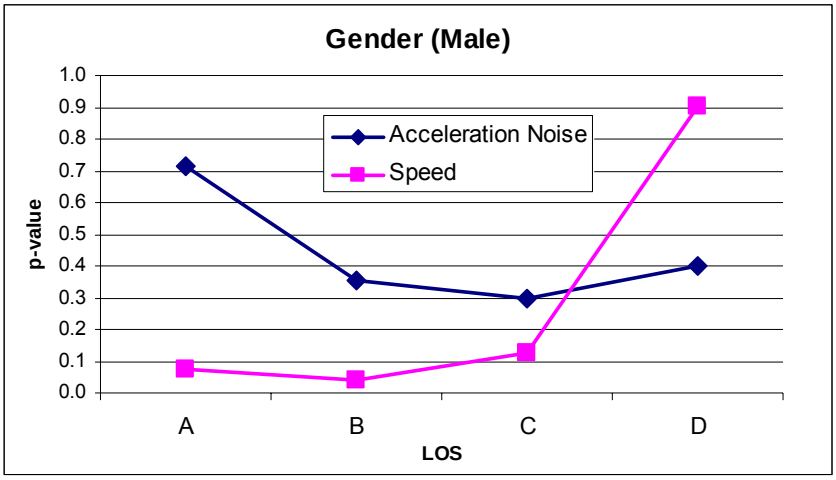

Figure 63: Changing Patterns of *p*-values for Gender by LOS Range

Effects of Vehicle Characteristics

In case of vehicle characteristics, the developed speed models imply that speed is less sensitive to vehicle characteristics. Indeed, variables related to vehicle characteristics are insignificant for all speed models. In contrast, acceleration noise appears to be more affected by vehicle characteristics. For example, acceleration noise of passenger cars tends to be larger than any other types, as shown in Figure 64. In particular, this situation appears to be more pronounced in LOS C and D ranges than LOS A and B ranges, under which acceleration or deceleration vehicle activities are less likely to occur compared to worse traffic conditions. The figure also suggests that no significant differences exist between passenger cars and SUVs for all LOS ranges. Meanwhile, older vehicles exhibited lower acceleration noise under LOS C condition, which is the only traffic condition in which vehicle age appears to be significant. More specifically, the resulting parameter (i.e., 0.177 for vehicle age 0 – 4 years old) in the LOS C acceleration noise model implies that vehicles less than 5 years old tend to exhibit 19% (i.e., $(e^{0.177} - 1)\times 100$) higher acceleration noise values than vehicles older than 9 years.

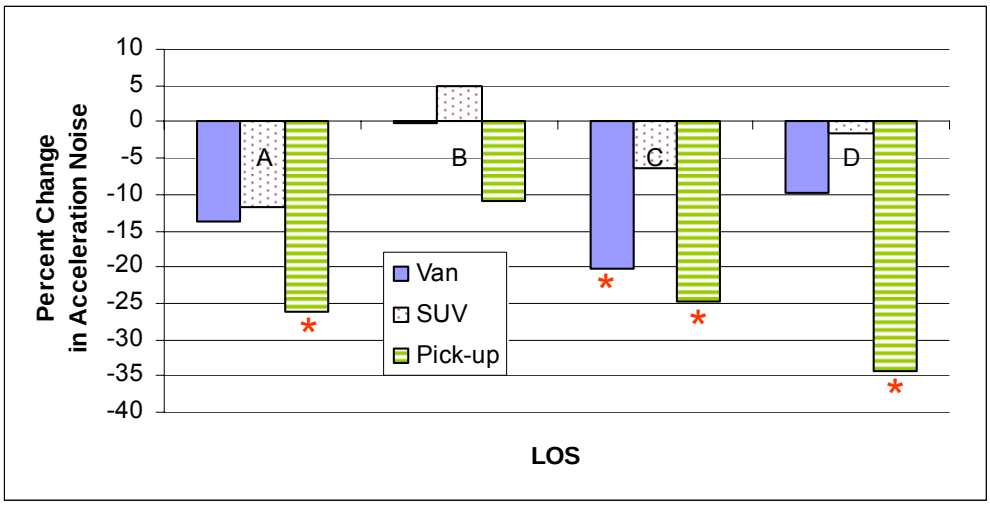

Figure 64: Effects of Vehicle Type on Acceleration Noise

The findings noted in the previous section suggest that vehicle performance associated with acceleration capabilities may be closely related with the magnitude of acceleration noise. As an attempt to verify this aspect, the power-to-weight ratio, which is regarded as a measure of vehicle performance (a vehicle with a higher ratio is expected to accelerate faster than a vehicle with a lower value), was calculated for a portion of the instrumented vehicles (154 vehicles out of 224 vehicles, 69%) for which vehicle specifications are available. In the calculation, curb weight (the total weight of a vehicle with standard equipment, oil, lubricants, coolant, a full tank of fuel and not loaded with either passengers or cargo) was used for the vehicle weight. As a result, the average power-to-weight ratios, measured in horsepower per ton (hp/t), were 131, 107, 101, and 100 for passenger cars, SUVs, pick-ups, and vans, respectively. This finding suggests that acceleration noise may be closely correlated with vehicle performance, although the modeling results indicate that vans tend to have greater acceleration noise values than pick-ups unlike their similar power-to-weight ratios. Note that the actual

vehicle weight depends on loaded passengers and cargo, and thus, the power-to-weight ratio can be changed depending on situations.

Variance Component Ratio

Variance component ratio (ρ), the fraction of the residual variance attributed to between-driver/vehicle variation, was compared by models, as shown in Figure 65. This graph indicates that the ratio for speed models decreases with congestion, suggesting smaller between-driver variances under worse traffic conditions. In other words, as traffic congestion increases, drivers are less likely to have the chance to select their desired speed, and thus, speed differences between drivers becomes smaller. However, the variance component ratio for acceleration noise models is relatively stable regardless of traffic congestion levels, and the ratio is always smaller than that of speed except for LOS D, suggesting that acceleration noise is less likely determined by the characteristics of driver/vehicle than speed at least under LOS A-to-C ranges. In addition, the less dependency on drivers/vehicles may be attributed to the fact that acceleration noise is more affected by numerous localized traffic conditions such as traveling lanes and positions in a platoon.

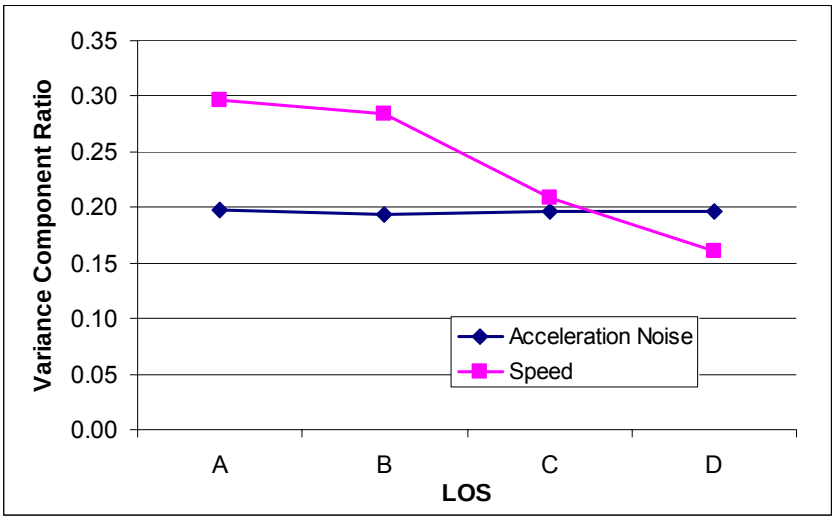

Figure 65: Variance Component Ratio by LOS

Stability in Acceleration and Speed Behavior

An investigation of the degree of stability in acceleration/deceleration can provide insights into driver behavior. To this end, the correlation between two acceleration noise values and speeds obtained from any two randomly selected trips from the same vehicles was examined, as shown in Figure 66. In the sample selection, trips under only free-flow conditions (LOS A) were considered so that the effects of traffic should be minimized for the selection of speed or acceleration noise. The resulting coefficients of correlation were 0.2 and 0.38 for acceleration noise and speed, respectively. Compared to an existing study in which speed correlation coefficients lie within a range between 0.49 and 0.81 (Haglund and Aberg 2002), the correlation coefficient 0.38 for speed is rather low. Figure 66 indicates that acceleration noise is less consistent for a driver than speed. This phenomenon implies that acceleration noise is more likely to be determined by factors other than driver/vehicle, even under free-flow conditions, supporting the findings from the variance component ratio analysis.

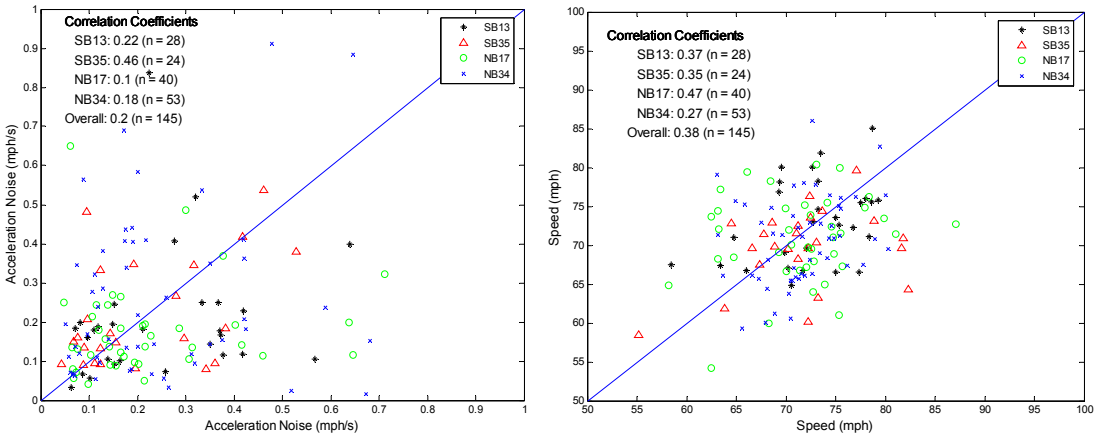

Figure 66: Correlation of Speed and Acceleration Noise Obtained from Randomly Selected Two Free-Flow Trips

Summary

In this chapter, the effects of driver/vehicle characteristics on acceleration noise were analyzed using the instrumented vehicle data obtained from the four segments of GA400 over eleven months. The data were employed for developing LOS-by-LOS (A-to-D) random intercept models, for which driver age, gender, household income, vehicle type, and vehicle age were used for explanatory variables, and log-transformed acceleration noise was used as the response variable. In addition to the acceleration noise models, speed models, based on the same data set and the same explanatory variables as acceleration noise models, were also developed for comparison.

The developed models indicated that driver age is the most significant variable among the driver characteristics for both acceleration noise and speed models. The modeling results indicated that the younger drivers generally tend to drive faster with greater acceleration noise. However, driver age appeared to more strongly influence speed than acceleration noise, as suggested by the significance levels (*p*-values). Drivers' gender seemed not important for acceleration noise model for all LOS ranges,

while speed is influenced by gender under LOS A and B ranges at a significance level of 0.1. The modeling results indicated that male drivers tend to drive faster than female drivers.

In contrast to the driver characteristics, acceleration noise appeared to be more influenced by vehicle characteristics than speed, in particular under LOS C and D ranges. Generally, passenger cars and SUVs tend to exhibit greater acceleration noise, indicating the correlation between acceleration noise and vehicle performance, as verified by the examination of power-to-weight ratio. In addition, the analysis of variance component ratio was performed, suggesting that acceleration noise is less affected by driver/vehicle characteristics than speed under LOS A-to-C ranges. This aspect was also confirmed by the correlation analysis using the two-sampled trips from the same vehicles under LOS A conditions. The analysis indicated that drivers' speed choice is more consistent than acceleration noise.

However, the weak explanatory power of the developed models, as suggested by the low R^2 values, implies that vehicle speed profiles may be affected by numerous factors other than the explanatory variables employed in this study. Potentially, localized traffic conditions, including vehicle positions in a platoon and interactions with heavy vehicles, might play a role for the unexplained variability. In addition, the purpose of driving (e.g., commuting, sales, leisure, etc) might influence the speed profiles because drivers' attitude can be affected by such factors. The consideration of such variables is expected to produce interesting results, enhancing the explanatory power for the relationship between acceleration noise and driver/vehicle characteristics.

Chapter 9

Measurement of Traffic Flow Quality Using GPS-Equipped Vehicles

Composite Index

Previous analysis results suggested that the degree of speed variation, measured by acceleration noise, appears to have a potential for evaluating the traffic flow quality experienced by drivers. For example, acceleration noise was more sensitive to traffic conditions and less sensitive to drivers/vehicles than speed under LOS A-to-C ranges. However, the analysis showed that acceleration noise may have weaknesses in that it is non-linearly correlated with traffic conditions, as suggested by the potential downturn under the highly congested conditions. These observations suggest that the combination of acceleration noise and speed may generate a better measure than either one by complementing each other. Thus, this study proposes a composite index, representing the traffic flow quality experienced by drivers, using acceleration noise and speed together, as suggested in Figure 67.

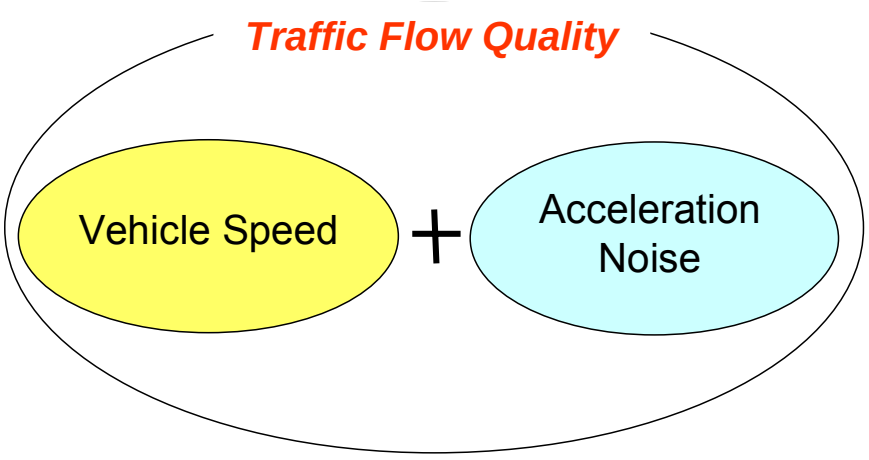

Figure 67: Concept of Proposed Traffic Flow Quality

The proposed approach seems to be consistent with the concept of LOS defined by HCM, which states that

> "*Level of service (LOS) is a quality measure describing operational conditions within a traffic stream, generally in terms of such service measures as speed and travel time, freedom to maneuver, traffic interruptions, and comfort and convenience*" (TRB 2000).

Since acceleration noise is closely associated with the degree of freedom to maneuver, traffic interruptions, and comfort and convenience, the proposed approach combining acceleration noise and speed matches well with the concept of LOS in the HCM.

Fuzzy Inference System

As an approach to combining two measures (speed and acceleration noise), the fuzzy inference system was proposed in the previous section. The fuzzy logic was initially proposed by Zadeh 1965 and has been applied to solve various real-world problems including transportation (Klir and Yuan 1995; Teodorovic and Vukadinovic 1998). The main reason why fuzzy logic is popular for solving the real-world problems is its feature for handling uncertainties often observed in the real world. The uncertainty may lie in the evaluation of traffic conditions, which is more or less subjective and depends on the perception of individuals. Thus, finite ranges, dividing acceptable and unacceptable traffic conditions, may not exist. Furthermore, an aggregation of different measures induces greater uncertainty. Based on this notion, researchers have attempted to apply the fuzzy inference system when combining multiple congestion indices and proved that

the approach could be an effective methodology (Hamad and Kikuchi 2002; Vaziri 2002).

In this study, the purpose of the fuzzy inference system is to map two crisp inputs (acceleration noise and speed) into a crisp output (composite traffic flow quality index). The mapping can be achieved through four steps: the fuzzification of inputs, the application of fuzzy rules, the aggregation of outputs, and deffuzificaiton. The first step, the fuzzification of inputs, is to take the values of acceleration noise and speed and determine the degree for each pre-specified fuzzy sets through membership functions. The second step, the application of fuzzy rules, is to evaluate the degree of traffic flow quality based on fuzzy rules. The fuzzy rules, called if-then rules, take the following form:

If (acceleration noise is x) and (speed is y), then (the degree of traffic flow quality) is z,

where x, y and z represent linguistic values such as "Good" or "Bad". The fuzzy inference system is usually composed of multiple rules, and each pair of input elements is evaluated for every rule. Then, the outputs generated by the rules are aggregated via specified operators such as maximum, probabilistic *or*, and sum. These operators provide the approach how the outputs are combined, resulting in a single combined fuzzy set. In the last step, the aggregated output, encompassing a range of values, is converted into a crisp number, which is called defuzzification. The defuzzification can be performed by several methods such as centroid method, mean of maximum, largest of maximum, smallest of maximum, and so on. Among them, the centroid method is

the most popular and used in this study. The structure of the fuzzy inference system is summarized in Figure 68.

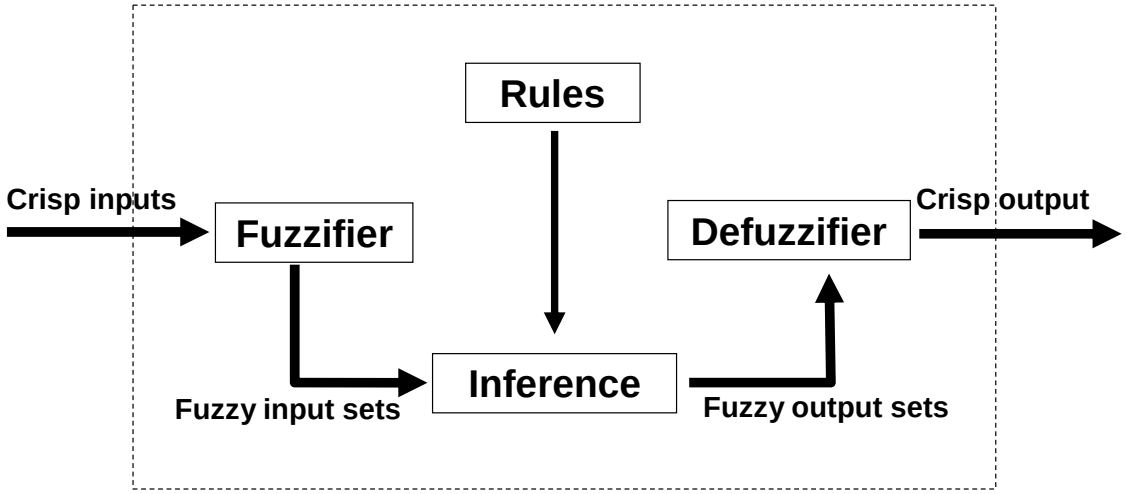

Source: (Mendel 2001)

Figure 68: Structure of Fuzzy Inference System

Application

Membership Functions for Acceleration Noise and Speed

The application of the fuzzy inference system requires the establishment of membership functions for the two inputs: acceleration noise and speed. In general, the membership functions can be established using opinion surveys asking the drivers' perceived traffic flow quality under various traffic conditions. However, in this study, no such survey could be implemented due to the constraints of cost and time. Thus, as an alternative, the acceleration noise and speed distributions obtained from the instrumented vehicle trips, collected over the segments with four lanes and a speed limit of 65mph on northbound GA400 (see chapter 6), were utilized. In particular, the distributions were obtained for each LOS range using the Gaussian kernel density estimation technique, as

shown in Figure 69. The distributions suggest the ranges of acceleration noise and speed values for each LOS range and relative occurrence probabilities for specific values. For example, the acceleration noise value of 1.5 mph/s is much less likely to be observed under LOS A-to-E ranges while the value is more likely to be observed under LOS F range, as suggested by the pdfs. As an attempt to quantify this probability over the whole range, normalized probability curves were obtained by assuming the normal and log-normal distributions for vehicle speed and acceleration noise, respectively, as shown in Figure 70. These assumptions, reflecting the shapes of the pdfs in Figure 69, facilitated the calculations of the probabilities across all ranges. The curves obtained indicate that the acceleration noise value of 2.0, for example, is most likely to be observed under LOS F condition with a probability of 0.85. However, the probability becomes 0.1 under LOS E, and then, it becomes only marginal for the other LOS ranges, A-to-D. Note that the summation of the probabilities from the six LOS ranges for any specific values of acceleration noise is equal to one, indicating that they are the relative occurrence probabilities. In the same manner, the curves for vehicle speed indicate that the speed of 30mph is only observed under LOS F with a probability of one. Thus, such feature of the normalized probability curves could be utilized for establishing the membership functions for acceleration noise and vehicle speed.

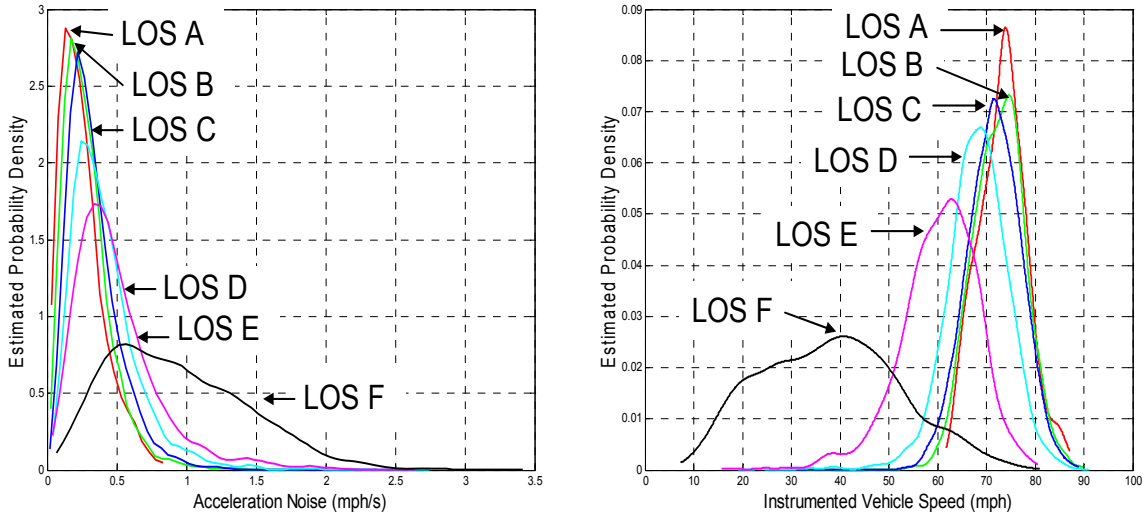

Figure 69: LOS-by-LOS Estimated pdfs for Acceleration Noise and Vehicle Speed

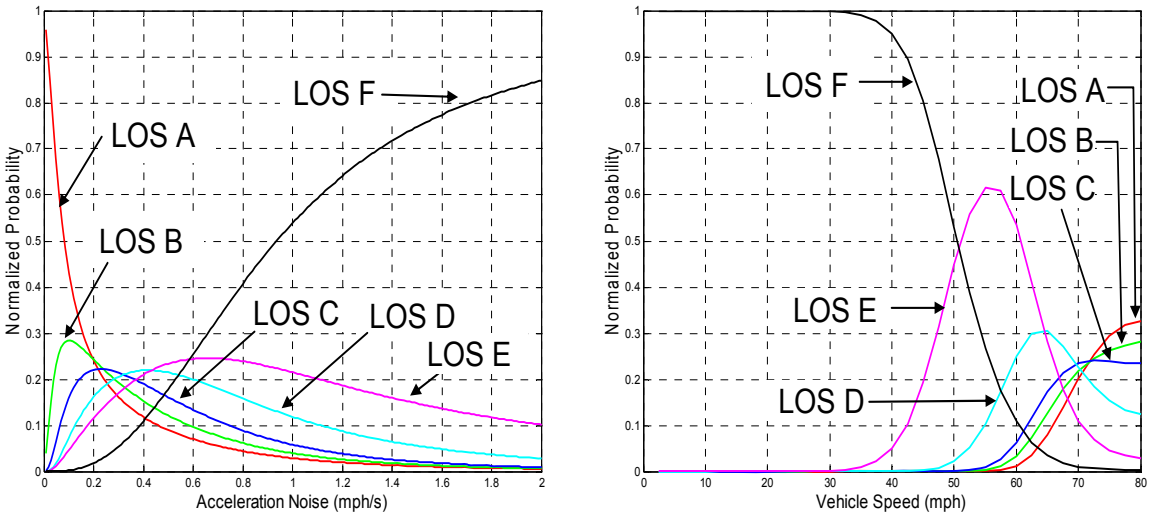

Figure 70: Normalized Probability Curves for Acceleration Noise and Vehicle Speed

Based on the normalized curves, membership functions for acceleration noise and speed were established as shown in Figure 71, in which four linguistic values—"Best", "Good", "Bad", and "Worst"—were adopted. The membership function of acceleration noise for the linguistic value "Best" approximates the normalized probability curve for LOS A condition while the speed membership function for "Best" approximates the curves of LOS A-to-C conditions. For speed, the membership

functions for “Good”, “Bad”, and “Worst” reflects the pattern of the normalized probability curves for LOS D, E, and F, respectively. Meanwhile, the membership function of “Good” for acceleration noise approximates the curves of LOS B and C, and the “Bad” membership function approximates the curves for LOS D and E. Similarly, the membership function of “Worst” for acceleration noise approximates the shape of the LOS F curve. All the established membership functions were formed using straight lines, simplifying the shape of the functions. The established membership functions indicate that traffic flow quality should be the worst when acceleration noise is larger than 2.5 or vehicle speed is less than 40mph, approximating the normalized probability curves in Figure 70.

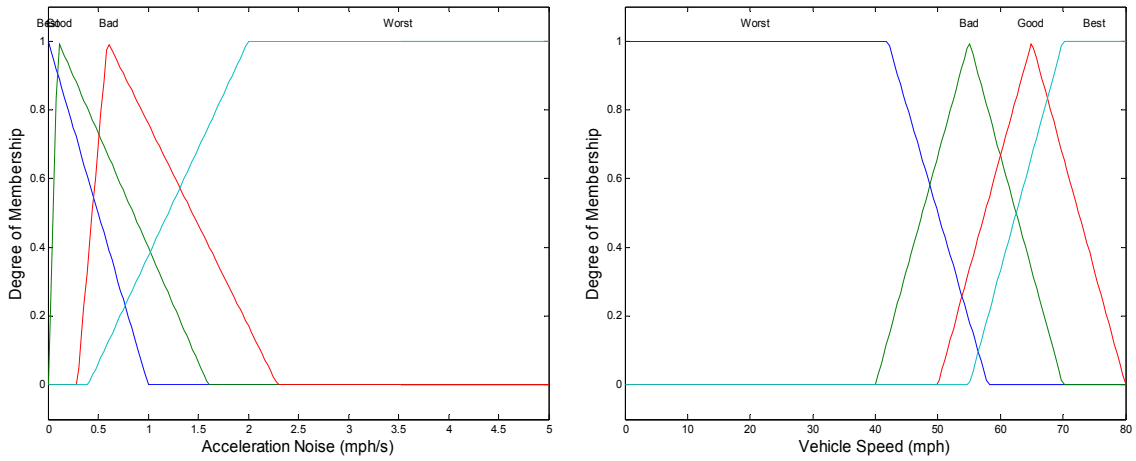

Figure 71: Membership Functions for Acceleration Noise and Vehicle Speed

Membership Functions for Traffic Flow Quality

The membership functions for the traffic flow quality, represented by four linguistic values (“Best”, “Good”, “Bad”, and “Worst”), were established in a simple manner by applying four triangular membership functions with the same size, as shown in Figure 72.

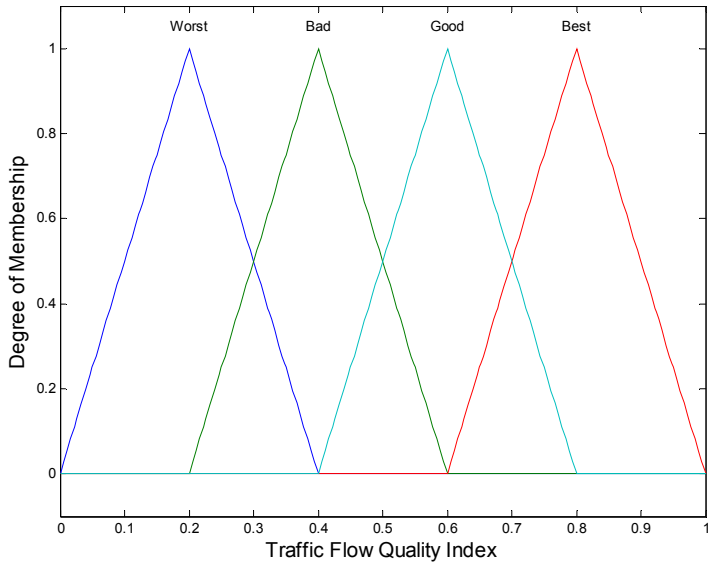

Figure 72: Membership Functions for Traffic Flow Quality

Fuzzy Rules

In the fuzzy inference system, 13 if-then rules, formulating the conditional statements, were established as shown in Table 22. The table indicates that if both acceleration noise and speed are "Best", then the traffic flow quality is also regarded as "Best". However, it also indicates that even when speed is "Best", traffic flow quality can be "Bad" if acceleration noise is "Bad" or "Worst", reflecting the more weights to acceleration noise under this traffic condition. This rule is consistent with the finding that speed is less sensitive to traffic under LOS A-to-C conditions. Meanwhile, if speed is too low ("Worst" condition), the traffic flow quality is regarded as "Worst" regardless of acceleration noise values. This rule reflects the finding that acceleration noise may downturn as traffic conditions extremely worsen.

Table 22: Established Fuzzy Rules

		Acceleration Noise			
		Best	Good	Bad	Worst
Speed	Best	**Best**	**Good**	**Bad**	**Bad**
	Good	**Good**	**Good**	**Bad**	**Bad**
	Bad	**Bad**	**Bad**	**Bad**	**Worst**
	Worst	**Worst**	**Worst**	**Worst**	**Worst**

Summary of the Fuzzy Inference System

The adopted fuzzy inference system for the measurement of traffic flow quality is represented in Figure 73, which indicates that the system is composed of two inputs and one output. In addition, the system contains 13 if-then rules supporting Mamdani-type fuzzy inference system. The Mamdani-type fuzzy inference system is distinguished by the linguistic if-then rules (Mendel 2001).

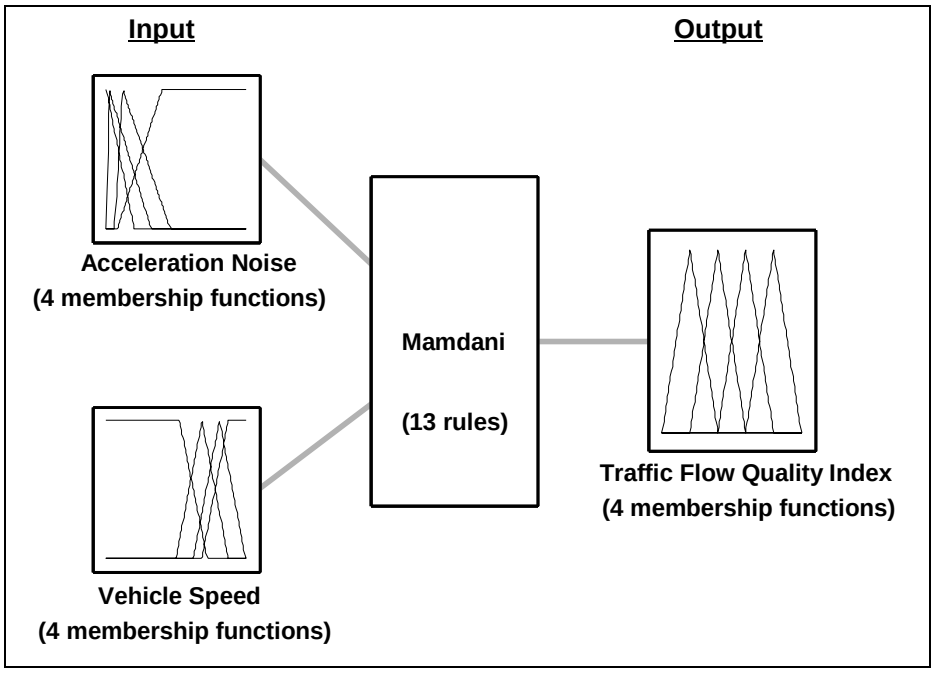

Figure 73: Fuzzy Inference System Applied for Evaluating Traffic Flow Quality

Based on the membership functions and the fuzzy rules specified in the previous sections, the traffic flow quality index, ranging from 0.2 to 0.8, is determined, as shown in Figure 74. The figure illustrates how the traffic flow quality index is affected by the two inputs: acceleration noise and speed. As can be expected, the higher speed combined with the lower acceleration noise results in a higher traffic flow quality index. In contrast, the lower speed and the higher acceleration noise result in the lower value of the traffic flow quality index.

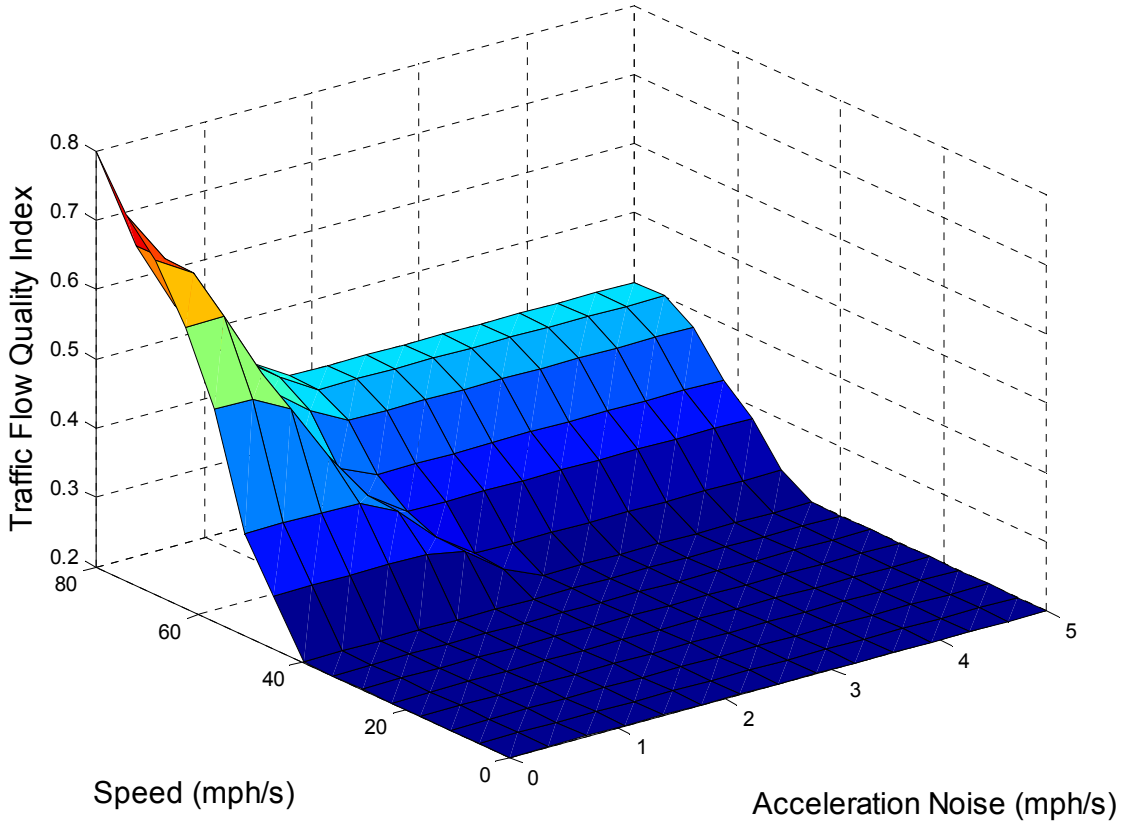

Figure 74: Relationship among Acceleration Noise, Speed, and Traffic Flow Quality Index

Application to a Single Segment

The proposed fuzzy inference system was applied to the instrumented vehicle data collected over one segment (NB24), as an illustration purpose. The resulting traffic

flow quality index was compared with acceleration noise and speed, as shown in Figure 75. The figure indicates that the traffic flow quality index is generally proportional to speed and inversely proportional to acceleration noise. However, a large amount of variation is found in the plot, implying that the index is not determined by either speed or acceleration noise alone. In particular, the variation is notable for high-speed trips. For example, the range of traffic flow quality index for the trips with speed higher than 65 mph is between 0.3 and 0.7. In addition, the relationship between the traffic flow quality index and the HCM LOS was illustrated in Figure 76, in which the distributions of the index values and the confidence intervals for the means of the index values were plotted. The plots suggest that the index generally agrees with the LOS system and that a significant amount of variation exists at the same time, consistent with the findings provided by the confidence region analysis in chapter 6.

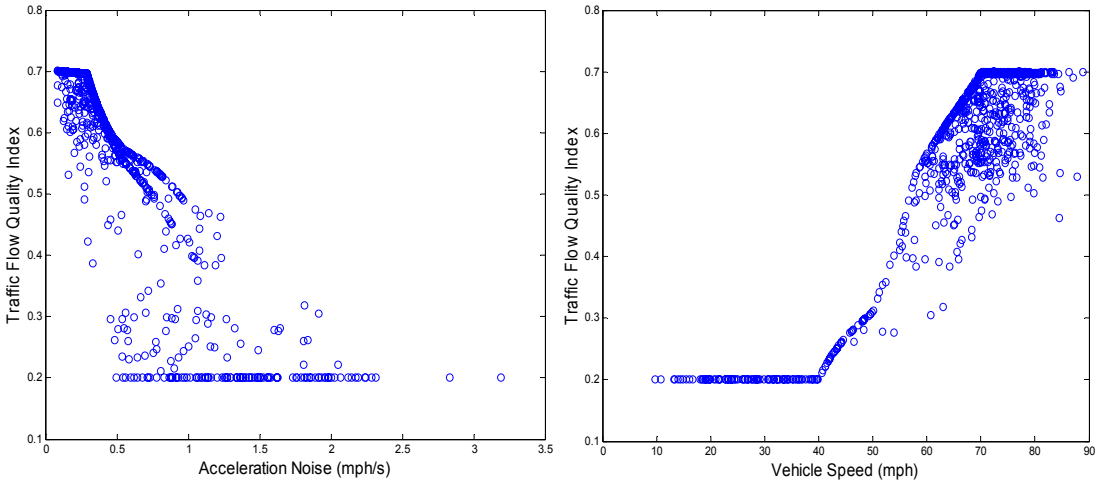

Figure 75: Relationships between Acceleration Noise, Vehicle Speed, and Traffic Flow Quality Index

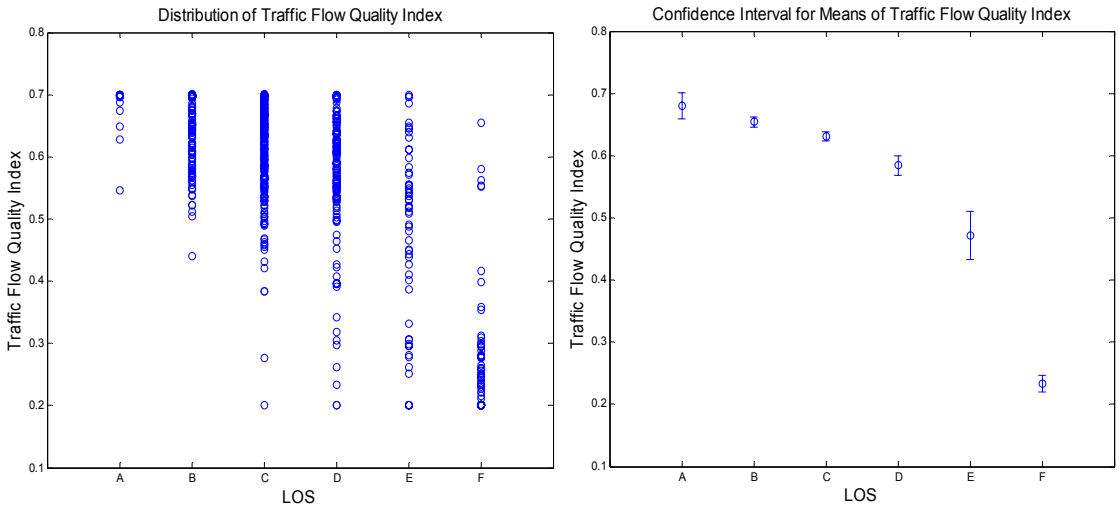

Figure 76: Relationships between Level of Service and Traffic Flow Quality Index

Application to Freeway Network

The developed methodology was applied to the wider freeway network in the metro Atlanta area using the instrumented vehicle data obtained during the weekdays over three months (January to March 2006). For the application, a freeway polygon system, composed of 1,451 polygons created around 209 centerline-miles of freeway networks, was developed. Based on the polygons (each polygon covers both directions), the locations of instrumented vehicles were identified, and speed and acceleration noise were computed over the polygons, of which average length is 0.14 miles. Then, the fuzzy inference system was applied to each polygon. Although the instrumented vehicle data were not available for all the segments, the traffic flow quality for the most major corridors could be identified, as shown in Figure 77. The figure graphically illustrates the estimated levels of traffic flow quality (multiplied by 100 for a display purpose) for morning (7 to 8am) and afternoon (5 to 6pm) peak times. The patterns shown in the figure generally coincide with the expectation.

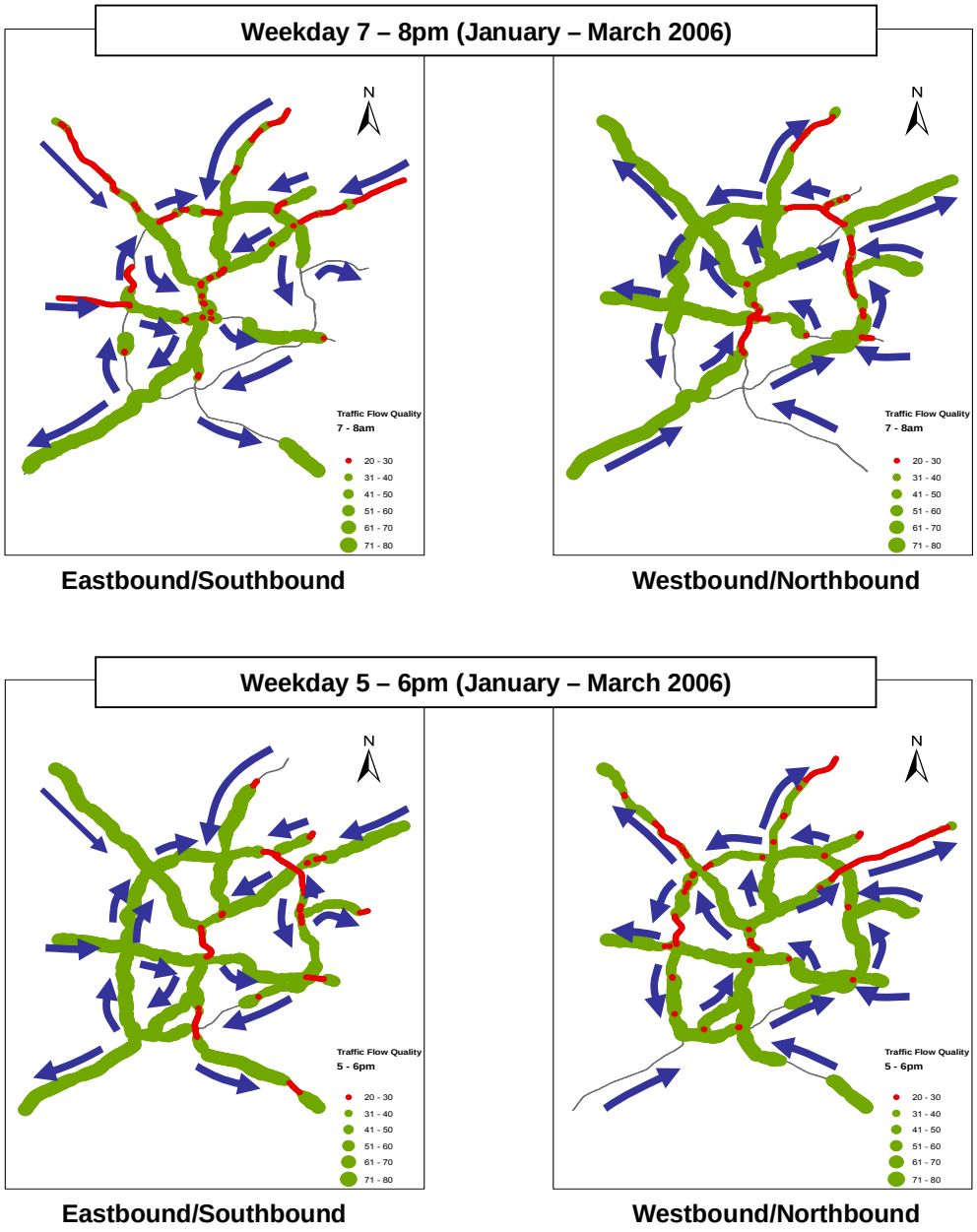

Figure 77: Traffic Flow Quality Measured from the Fuzzy Inference System

In addition to the traffic flow quality maps, the average traffic flow quality index was computed by averaging the resulting indices across all the segments, as shown in Figure 78. The figure clearly shows that traffic flow quality experienced by the instrumented vehicle drivers were worse during peak hours. The map suggests that the

peak hours are 7 to 9 am and 5 to 7 pm. In contrast, traffic flow quality appears to be better during 11 am to 2 pm.

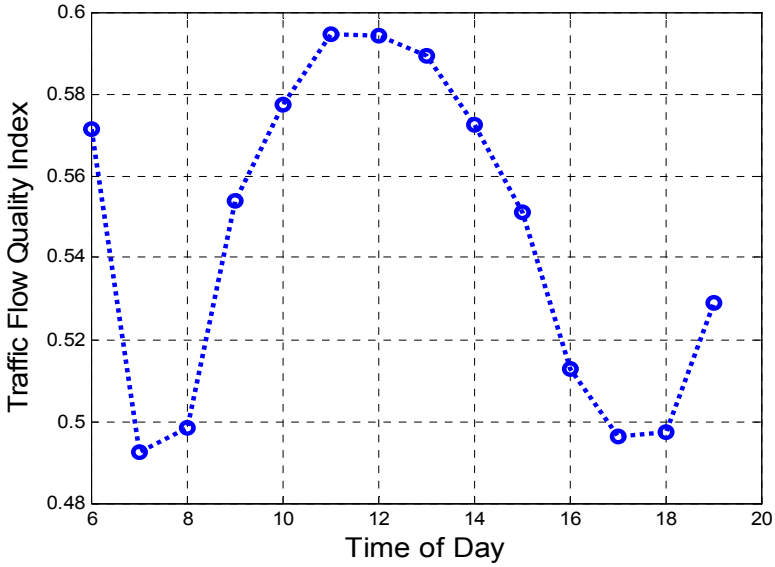

Figure 78: Average Traffic Flow Quality Index by Time of Day

Summary

A fuzzy inference system-based approach, combining vehicle speed and acceleration noise obtained from GPS-equipped instrumented vehicles, was proposed for evaluating traffic flow quality on freeways. The composite index appears to be advantageous in that the two measures can complement each other. For example, under free-flow conditions (i.e., LOS A-to-C), acceleration noise may complement vehicle speed which is insensitive to traffic conditions. Meanwhile, speed can complement the weakness of acceleration noise (i.e., potential downturn) under congested conditions. In fact, this aspect was incorporated into the fuzzy rules in the application step. The application results indicated that the proposed approach may be practical and promising for evaluating traffic flow quality. In particular, the application to a larger freeway network

produced reasonable outcomes, providing general insights into the network-wide traffic flow conditions experienced by the instrumented drivers. However, more detailed analyses are required so that the characteristics of the resulting index should be fully understood.

Further research work is required to understand the drivers' perception about traffic flow quality. Although this research effort assumes that the speed variation of a vehicle and speed can measure the degree of traffic flow quality experienced by drivers, the assumption needs to be closely investigated whether the measures truly reflect the traffic flow quality. The investigation should be designed to identify critical factors determining the level of perceived traffic flow quality and breakpoints (in the factors) partitioning acceptable and unacceptable traffic flow quality.

Chapter 10
Conclusions

Summary and Contributions

Summary

This study analyzed the characteristics of speed variation, in particular measured by acceleration noise which has been considered as a traffic parameter representing traffic flow quality from the perspective of individual drivers. In addition, this study proposed a fuzzy inference system-based approach that generates the index of traffic flow quality, combining vehicle speed and acceleration noise. This work utilized a rich set of the GPS-equipped instrumented vehicle data which provide second-by-second speed and location over a 12-mile freeway corridor, GA400 in Atlanta, Georgia. The employment of the real-world instrumented vehicle data rendered this work unique, compared to previous research efforts which have been limited to the experimental level. As a result of this unique research effort, various aspects of acceleration noise were revealed in a quantitative manner. Such findings can be summarized as follows.

- Acceleration noise depends on traffic, roadway, and driver/vehicle. Seemingly, traffic is the most influential factor among the three factors. Although their relative explanatory powers for acceleration noise were not closely examined, the resulting R^2 values imply this aspect.
- Other than the three major factors, acceleration noise may be also affected by various factors associated with localized traffic conditions such as vehicle

positions in a queue. This aspect may be suggested by the large variance or the low R^2 values of the models developed in this study.

- Traffic conditions and acceleration noise may not be linearly correlated, as suggested by the downturn under heavily congested conditions. This aspect indicates the weakness of acceleration noise as a measure of traffic conditions.
- Acceleration noise may be a better measure for measuring traffic conditions under LOS A-to-C ranges than speed, which was supported by the greater sensitivity of acceleration noise under the ranges. This finding is important since it implies that the capability of probe vehicle-based traffic congestion monitoring system can be enhanced by incorporating acceleration noise as a complementing measure.
- Roadway characteristics, including geometrics, capacity and facility type, can affect the magnitude of acceleration noise. Interestingly, the roadway conditions can interact with traffic conditions. For example, acceleration noise on on-ramp areas becomes notably larger under LOS E conditions, compared to the other LOS ranges.
- Acceleration noise is less sensitive to driver/vehicle characteristics than speed under LOS A-to-C ranges, as clearly suggested by the results of variance component ratio and correlation analyses. This aspect implies that acceleration noise may be more desirable as a measure of traffic conditions under the ranges.

- Consequently, the combined measure utilizing both speed and acceleration noise may produce a better measure for evaluating the traffic flow quality experienced by individual drivers.
- The fuzzy inference system, as an approach to combining the two measures, may be effectively applied to measuring traffic flow quality.

In addition to these findings, sensitivity analyses indicate that the values of acceleration noise can be affected by computation approaches and data types (e.g., data sampling rate), requiring the careful interpretation of the actual values of acceleration noise. In other words, an attachment of too much significance to the actual values of acceleration noise may not be safe.

Contributions

This research work takes advantage of a rich set of the instrumented vehicle data collected from real-world drivers and vehicles. In particular, the instrumented vehicle data were synchronized with TMC data so that the macro-level traffic conditions which the instrumented vehicles experienced can be captured. The employment of the unique data set enables this research work to contribute in several ways which has not yet been shown in existing studies. The major contributions of this research work can be briefly summarized as follows:

- Demonstrate the application of GPS-equipped instrumented vehicle data for the evaluation of traffic flow conditions

- Provide various analysis results about the characteristics of acceleration noise
- Provide new perspectives for the evaluation of traffic conditions (traffic flow quality)
- Provide the fuzzy inference system-based framework for the evaluation of traffic flow quality.

Recommendation for Future Work

User perceptions about traffic flow quality

In this research work, the traffic flow quality was assumed to be proportional to speed and inversely proportional to acceleration noise. Although this assumption may be generally reasonable, the degree of user satisfaction for a specific range of acceleration noise or speed should be fully understood. In particular, the relationship between acceleration noise and the degree of satisfaction should be carefully investigated since acceleration noise, unlike speed, is a rather unfamiliar concept to the general public. The lack of the understanding of the user perception may mislead the acceleration noise-based evaluation of roadway service quality.

Expansion to Other Sites

This research work focused on only one freeway corridor, GA400 in Atlanta, Georgia. Thus, the observable characteristics of roadway and drivers/vehicles are limited to this corridor, resulting in a loss of generality to some degree in some aspects. This limitation may be overcome by expanding the study site to other areas which contain

different characteristics. The expansion is likely to provide an opportunity to investigate the characteristics of speed variation using a wider range of variables, and thus, meaningful outcomes enhancing the understanding of traffic flow characteristics can be expected.

Expansion to Arterials

Although this research work was conducted focusing only on freeway, the same research framework can be applied to arterials. In the application, more variables should be considered since vehicle activities on arterials are subject to be significantly influenced by various factors, including signals and roadside activities by pedestrian and parked cars. Although the effective consideration of the numerous variables can pose a challenge, it may provide an opportunity to explore the characteristics of speed variation and traffic flow quality under various traffic/roadway conditions.

APPENDIX A

Drew's Energy Momentum Theory

The purpose of this appendix is to provide detailed mathematical background for the Drew's energy momentum theory introduced in Chapter 2. In particular, the relationship between acceleration noise and speed is mathematically established based on Drew (1968)'s work. Although this appendix provides only the acceleration noise-speed relationship, such relationships for other parameters—density and volume—also easily obtained in the similar manner.

Relationship between Density and Kinetic Energy

Let's assume that the kinetic energy in a traffic flow system can be represented by $\alpha k u^2$, which is the correspondence of $\frac{1}{2}\rho v^2$ in the hydrodynamic system. In the equation, α, k, and u represent the kinetic energy correction factor, density, and speed, respectively. In addition, ρ and v are the counterparts of k and u, respectively. Again, the kinetic energy (E) is defined by:

$$E = \alpha k u^2 .$$

Meanwhile, the well-known generalized equations of state obtained from the principle of fluid mechanics dictate that

$$u = u_f \left[1 - \left(\frac{k}{k_j} \right)^{\frac{n+1}{2}} \right], n > -1,$$

and thus,

$$q = ku = ku_f \left[1 - \left(\frac{k}{k_j} \right)^{\frac{n+1}{2}} \right], n > -1.$$

In the equations above, u_f and k_j represent free-flow speed and jam density, respectively. In addition, n determines the shape the curves illustrating the relationships among speed, density, and volume. For example, when $n = 1$, Greenshields' linear model is obtained while parabolic model is obtained when $n = 0$. In addition, exponential model is obtained when $n = -1$. Such model names follow the shape of the u-k curves.

Now, the kinetic energy can be represented as follows:

$$E = \alpha k u^2$$

$$= \alpha k u_f^{\,2} \left[1 - \left(\frac{k}{k_j} \right)^{\frac{n+1}{2}} \right]^2$$

$$= \alpha k u_f^{\,2} \left[1 - 2\left(\frac{k}{k_j} \right)^{\frac{n+1}{2}} + \left(\frac{k}{k_j} \right)^{n+1} \right], n > -1.$$

Using the equation above, the following curve, showing the relationship between density and the kinetic energy, is obtained.

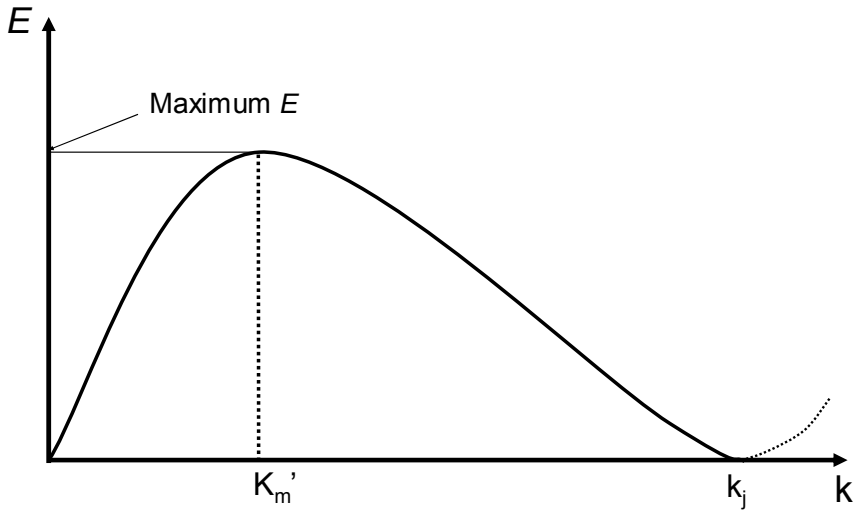

Figure 79: Relationship between Density and Kinetic Energy

Now, the value of k_m' can be computed by differentiating the equation above with respect to density and setting as zero. That is,

$$\frac{dE}{dk} = \alpha u_f^{\,2}\left[(1-\left(\frac{k}{k_j}\right)^{\frac{n+1}{2}})^2 + 2k\left[1-\left(\frac{k}{k_j}\right)^{\frac{n+1}{2}}\right]\frac{(n+1)}{2}\left[-\left(\frac{1}{k_j}\right)^{\frac{n+1}{2}}\right]k^{\frac{n-1}{2}}\right]$$

$$= \alpha u_f^{\,2}\left[1-\left(\frac{k}{k_j}\right)^{\frac{n+1}{2}}\right]\left[1-\left(\frac{k}{k_j}\right)^{\frac{n+1}{2}} - (n+1)\left(\frac{k}{k_j}\right)^{\frac{n+1}{2}}\right] .$$

Thus, the condition, $\frac{dE}{dk} = 0$, can be achieved when $k = k_j$. However, when $k \neq k_j$, k should satisfy the following condition:

$$\left(\frac{k}{k_j}\right)^{\frac{n+1}{2}}(n+2) = 1 .$$

Thus, by solving the equation above, k_m' at which the kinetic energy is maximized is obtained as follows:

$$k_m' = \left(\frac{1}{n+2}\right)^{\frac{2}{n+1}} k_j, \; n > -1.$$

In addition, u_m' at which the kinetic energy is maximized is computed using the following relationship:

$$u = u_f \left[1 - \left(\frac{k}{k_j}\right)^{\frac{n+1}{2}}\right], \; n > -1.$$

In the equation above, the replacement of k with k_m' results in u_m', which depends on free-flow speed as follows:

$$u_m' = u_f \left[1 - \left[\frac{k_j}{k_j}\left(\frac{1}{n+2}\right)^{\frac{2}{n+1}}\right]^{\frac{n+1}{2}}\right]$$

$$= u_f \left(1 - \frac{1}{n+2}\right)$$

$$= u_f \left(\frac{n+1}{n+2}\right), \; n > -1$$

Relationship between Acceleration Noise and Speed

Two assumptions—1) total energy (T) in a traffic stream is a sum of kinetic energy (E) and internal energy (I) and 2) the internal energy is expressed by acceleration noise σ—generates the following equations:

$$T = E + I$$

$$= \alpha k u^2 + \sigma .$$

The equation dictates that $T = E$ when $\sigma = 0$. Note that the zero acceleration noise means the optimum condition of the traffic flow and that it can be achieved when the kinetic energy is maximized. Thus, total energy when acceleration noise is zero can be represented using k_m' and u_m' as follows:

$$T_{\sigma=0} = E$$

$$= \alpha k_m' (u_m')^2$$

$$= \alpha \left(\frac{1}{n+2} \right)^{\frac{2}{n+1}} \left(\frac{n+1}{n+2} \right)^2 k_j u_f{}^2 .$$

Thus, when $n = 1$ (equivalent to the assumption of the linear relationship between speed and density),

$$T_{\sigma=0} = \alpha \left(\frac{4}{27} \right) k_j u_f{}^2 .$$

Meanwhile, when the kinetic energy is zero, acceleration noise is maximized, and thus, $T_{E=0} = \sigma_{\max}$. Under this condition,

$$T_{E=0} = \alpha k u^2 + \sigma$$

$$= \sigma_{\max} .$$

Consequently, acceleration noise can be represented as follows:

$$\sigma = \sigma_{\max} - \alpha k u^2 .$$

The replacement of k with $k_j\left(1-\frac{u}{u_f}\right)^{\frac{2}{n+1}}$ results in the following equation showing the relationship between acceleration noise and speed.

$$\sigma = \sigma_{\max} - \alpha k_j u^2 \left(1-\frac{u}{u_f}\right)^{\frac{2}{n+1}}$$

Again, when n = 1, the equation above becomes:

$$\sigma = \sigma_{\max} - \alpha k_j u^2 + \frac{\alpha k_j}{u_f} u^3 .$$

In this equation, α can be obtained by equating $T_{E=0}$ and $T_{\sigma=0}$, which is based on the energy conservation rule. That is:

$$\alpha\left(\frac{4}{27}\right) k_j {u_f}^2 = \sigma_{\max} .$$

Thus, the kinetic energy correction factor is expressed as follows:

$$\alpha = \left(\frac{27}{4}\right)\frac{\sigma_{\max}}{k_j {u_f}^2} .$$

Finally, by replacing α, the relationship between acceleration noise and speed can be expressed as follows:

$$\sigma = \sigma_{\max} - \frac{27\sigma_{\max}}{4}\left[\left(\frac{u}{u_f}\right)^2 - \left(\frac{u}{u_f}\right)^3\right].$$

Now, the optimum speed which minimizes acceleration noise can be obtained by differentiating the equation with respect to u and setting it as zero, as follows:

$$\frac{d\sigma}{du} = -2\alpha k_j u + 3\frac{\alpha k_j}{u_f} u^2 = 0$$

$$\Leftrightarrow \alpha k_j u\left(-2+3\frac{u}{u_f}\right)=0.$$

Thus, acceleration noise is minimized when $u=\frac{2}{3}u_f$, which is equal to u_m' only if $n = 1$.

REFERENCES

Babu, Y., and Pattnaik, S. (1997). "Acceleration Noise and Level of Service of Urban Roads - A Case Study." *Journal of Advanced Transportation*, 31(3), 325-342.

Barth, M. J., Johnston, E., and Tadi, R. R. (1996). "Using GPS Technology to Relate Macroscopic and Microscopic Traffic Parameters." *Transportation Research Record 1520*, 89-96.

Breiman, L., Friedman, J. H., A., O. R., and Stone, C. J. (1984). *Classification and Regression Trees*, Wadsworth, Inc., Belmont, California.

Capelle, D. G. (1966). "An Investigation of Acceleration Noise as a Measure of Freeway Level of Service," Texas A&M University, College Station, TX.

Chang, D. J., and Morlok, E. K. (2005). "Vehicle Speed Profiles to Minimize Work and Fuel Consumption." *Journal of Transportation Engineering*, 131(3), 173-182.

Choocharukul, K., Sinha, K. C., and Mannering, F. L. (2004). "User Perceptions and Engineering Definition of Highway Level of Service: An Exploratory Statistical Comparison." *Transportation Research Part A*, 38, 677-689.

Conover, W. J. (1980). *Practical Nonparametric Statistics*, John Wiley and Sons, New York.

Croft, F., and Clark, E. (1985). "Quantitative Measure of Levels of Service." *Transportation Research Record 1005*, 11-20.

Czerniak, R. J., and Reilly, J. P. (1998). "Applications of GPS for Surveying and Other Positioning Needs in Departments of Transportation." NCHRP Synthesis 258, Transportation Research Board, National Research Council, Washington, D.C.

D'Este, G. M., Zito, R., and Taylor, M. A. P. (1999). "Using GPS to Measure Traffic System Performance." *Computer-Aided Civil and Environmental Engineering*, 14, 255-265.

Drew, D. (1968). *Traffic Flow Theory and Control*, McGraw-Hill, Inc.

Drew, D., Dudek, C., and Keese, C. (1967). "Freeway Level of Service as Described by an Energy-Acceleration Noise Model." *Highway Research Record 162*, 30-85.

Drew, D., and Keese, C. (1965). "Freeway Level of Service as Influenced by Volume and Capacity Characteristics." *Highway Research Record 99*, 1-47.

Eisele, W. L., Turner, S. M., and Benz, R. J. (1996). "Using Acceleration Characteristics in Air Quality and Energy Consumption Analyses." *Technical*

Report 465100-1, Southwest Region University Transportation Center, Texas Transportation Institute, College Station, Texas.

FHWA. (2003). "Highway Statistics 2003."

Flannery, A., McLeod, D., and Pedersen, N. (2006). "Customer-Based Measures of Level of Service." *ITE Journal*, 76(5), 17-21.

Gibbons, J. D., and Chakraborti, S. (2003). *Nonparametric Statistical Inference*, Marcel Dekker, Inc., New York.

Grant, C. D. (1998). "Representative Vehicle Operating Mode Frequencies: Measurement and Prediction of Vehicle Specific Freeway Modal Activity," Georgia Institute of Technology, Atlanta, USA.

Greenshields, B. D. (1961). "The Quality of Traffic Flow." A Symposium on Quality and Theory of Traffic Flow, Bureau of Highway Traffic.

Haglund, M., and Aberg, L. (2002). "Stability in Driver's Speed Choice." *Transportation Research Part F*, 5, 177-188.

Hallmark, S., and Guensler, R. (1999). "Comparison of Speed-Acceleration Profiles from Field Data with NETSIM Output for Modal Air Quality Analysis of Signalized Intersections." *Transportation Research Record*, 1664, 40-46.

Hamad, K., and Kikuchi, S. (2002). "Developing a Measure of Traffic Congestion: A Fuzzy Inference Approach." *Transportation Research Record 1802*, 77-85.

Hastie, T., Tibshirani, R., and Friedman, J. (2001). *The Elements of Statistical Learning; Data Mining, Inerence, and Prediction*, Springer-Verlag, New York.

Herman, R., Montroll, E., Potts, R., and Rothery, R. (1959). "Traffic Dynamics: Analysis of Stability in Car Following." *Operations Research*, 7, 86-106.

Herman, R., and Rothery, R. (1962). "Microscopic and Macroscopic Aspects of Single Lane Traffic Flow." *Journal of the Operations Research Society of Japan*, 5(2), 74-93.

Hofmann-Wellenhof, B., Lichtenegger, H., and Collins, J. (1994). *GPS: Theory and Practice*, Springer-Verlag, New York.

Hostovsky, C., and Hall, F. L. (2003). "Freeway Quality of Service: Perceptions from Tractor-Trailer Drivers." *Transportation Research Record, Journal of the Transportation Research Board*, 1852, 19-25.

Hostovsky, C., Wakefield, S., and Hall, F. L. (2004). "Freeway User's Perceptions of Quality of Service: Comparison of Three Groups." *Transportation Research Record: Journal of the Transportation Research Board*, 1883, 150-157.

Humphreys, J. B. (1969). "Effect of Trucks on the Urban Freeway." *Highway Research Record*, 308, 62-79.

Johnson, R., and Wichern, D. (1992). *Applied Multivariate Statistical Analysis*, Prentice-Hall, Inc., New Jersey.

Jones, T., and Potts, R. (1962). "The Measurement of Acceleration Noise - A Traffic Parameter." *Operations Research*, 10(6), 745-763.

Jun, J., Guensler, R., and Ogle, J. (2006). "Smoothing Methods Designed to Minimize the Impact of GPS Random Error on Travel Distance, Speed, and Acceleration Profile Estimates." *Transportation Research Record, Journal of the Transportation Research Board*.

Kharoufeh, J. P., and Goulias, K. G. (2002). "Nonparametric Identification of Daily Activity Durations Using Kernel Density Estimators." *Transportation Research Part B*, 36, 59-82.

Kim, J.-T., Courage, K. G., Washburn, S. S., and Bonyani, G. (2003). "Framework for Investigation of Level-of-Service Criteria and Thresholds on Rural Freeways." *Transportation Research Record 1852*, 239-245.

Klir, G. J., and Yuan, B. (1995). *Fuzzy Sets and Fuzzy Logic: Theory and Applications*, Prentice Hall PTR, Upper Saddle River, New Jersey.

Lee, J., Guensler, R., and Hunter, M. (2006). "Evaluation of Video Detection System Data Quality." Unpublished Manuscript, Georgia Institute of Technology.

Lee, J., and Yu, J. C. (1973). "Internal Energy of Traffic Flows." *Highway Research Record*, 456, 40-49.

Longford, N. T. (1993). *Random Coefficient Models*, Oxford University Press, New York.

Mendel, J. M. (2001). *Uncertain Rule-Based Fuzzy Logic Systems: Introduction and New Directions*, Prentice Hall PTR, Upper Saddle River, New Jersey.

Neter, J., Kutner, M. H., Nachtsheim, C. J., and Wasserman, W. (1996). *Applied Linear Statistical Models*, McGraw-Hill, Boston, Massachusetts.

Ogle, J. (2005). "Quantitative Assessment of Driver Speeding Behavior Using Instrumented Vehicles," Georgia Institute of Technology, Atlanta, Georgia.

Ogle, J., Guensler, R., and Elango, V. (2005). "Commute Atlanta Value Pricing Program: Recruitment Methods and Travel Diary Response Rates." *Transportation Research Record 1931, Journal of the Transportation Research Board*, 28-37.

Ogle, J., Ko, J., and Guensler, R. (2006). "Travel Diary Underreporting in the Commute Atlanta Instrumented Vehicle Study." Manuscript.

Pecheux, K. K., Flannery, A., Wochinger, K., Rephlo, J., and Lappin, J. (2004). "Automobile Drivers' Perceptions of Service Quality on Urban Streets." *Transportation Research Record: Journal of the Transportation Research Board*, 1883, 167-175.

Pfefer, R. C. (1999). "Toward Reflecting Public Perception of Quality of Service in Planning, Designing, and Operating Highway Facilities." *Transportation Research Record 1685*, 81-89.

Platt, F. N. (1963). "A Proposed Index for the Level of Traffic Service." *Traffic Engineering*, 34(2), 21-26.

Rowan, N. J. (1967). "An Investigation of Acceleration Noise as a Measure of the Quality of Traffic Service on Major Streets," Texas A&M University, College Station, Texas.

Ryden, T. K. (1976). "Measuring Levels of Service of a City Street by Using Energy-Momentum Techniques." *Transportation Research Record*, 567, 37-44.

Taylor, M. A. P., Woolley, J. E., and Zito, R. (2000). "Integration of the Global Positioning System and Geographical Information Systems for Traffic Congestion Studies." *Transportation Research Part C*, 8, 257-285.

Teodorovic, D., and Vukadinovic, K. (1998). *Traffic Control and Transport Planning: A Fuzzy Sets and Neural Networks Approach*, Kluwer Academic Publishers, Norwell, Massachusetts.

Torres, J. F. (1969). "Acceleration Noise, Power Spectra, and Other Statistics Derived From Instrumented Vehicle Measurements Under Freeway Driving Conditions." *Highway Research Record 308*, 13-33.

TRB. (1975). *Traffic Flow Theory*, Transportation Research Board, National Research Council, Washington, D.C.

TRB. (2000). *Highway Capacity Manual*.

Underwood, R. T. (1968). "Acceleration Noise and Traffic Congestion." *Traffic Engineering and Control*, 10(3), 120-123.

Vaziri, M. (2002). "Development of Highway Congestion Index Using Fuzzy Set Models." *Transportation Research Record: 1802*, 16-22.

Washburn, S. S., Ramlackhan, K., and McLeod, D. (2004). "Quality-of-Service Perceptions by Rural Freeway Travelers." *Transportation Research Record: Journal of the Transportation Research Board*, 1883, 132-139.

Winzer, T. (1981). "Measurement of Acceleration Noise and Discussion of the Energy Model Developed by Drew." *Transportation Research Part A*, 15(6), 437-443.

Yoon, S., Li, H., Jun, J., Ogle, J., Guensler, R., and Rodgers, M. (2005). "A Methodology for Developing Transit Bus Speed-Acceleration Matrices to be used in Load-Based Mobile Source Emissions Models." *Transportation Research Record: Journal of the Transportation Research Board*.

Zadeh, L. A. (1965). "Fuzzy Sets." *Information and Control*, 8(3), 338-353.

Zito, R., D'Este, G. M., and Taylor, M. A. P. (1995). "Global Positioning Systems in the Time Domain: How useful a Tool for Intelligent Vehicle-Highway Systems." *Transportation Research Part C*, 3(4), 193-209.